KAUNAS UNIVERSITY OF TECHNOLOGY

MANTAS VENSLAUSKAS

INVESTIGATION AND APPLICATION OF THE HUMAN BLOOD FLOW IMPROVEMENT BY MECHANICAL VIBRATIONS

Doctoral Dissertation
Technological Sciences, Mechanical Engineering (09T)

2015, Kaunas

This dissertation was prepared at Kaunas University of Technology, Institute of Mechatronics, during the period 2011 – 2015.

Scientific Supervisor:

Prof. habil. dr. Vytautas OSTAŠEVIČIUS (Kaunas University of Technology, Technological Sciences, Mechanical Engineering – 09T).

Editor:

Tony Bexon.

ISBN 978-609-02-1170-0

CONTENTS

NOMENCLATURE

AHR	Average heart rate
BMI	Body mass index
BPM	Beats per minute
DVT	Deep vein thrombosis
ECG	Electrocardiogram
e	Eccentricity
E	Young's modulus
E'	Combined elasticity modulus
ePTFE	Polytetrafluoroethylene
f_i	Body force
F	Volume force
F_0	Force amplitude
FDA	Food and Drug Administration
FSI	Fluid-structure interaction
g	Contact gap distance variable
g	Gravitational acceleration
HGW	Glass-cloth laminate
I	Diagonal matrix
m	Mass of the eccentric
M	Bulk mass of the whole system
MHR	Maximum heart rate
n	Normal vector to FSI boundary
p	Static pressure
r	Distance from the motor shaft to the centre
R	Combined radius
RBC	Red blood cell
RPM	Revolutions per minute
t	Time interval
$T_{0:}$	Estimated contact pressure
u	Displacement field
v	Velocity
V	Poisson's ratio
WBV	Whole body vibration
x	Displacement of the particles
x_1 and x_2	System's displacements
Γ	External boundary
δ	Constant penalty factor
$\sigma_{ij,j}$	Stress component
σ_{ij}^{s}	Structural stress
σ_{ij}^{f}	Fluid stress
ε_{ij}	Strain
ζ	Head loss coefficient

η	Dynamic viscosity
λ and G	Lame constants
μ	Mass ratio
µPIV	Micro Particle Image Velocimetry
ρ	Mass density
$\Phi\ (x,y)$	The correlation function
ω_1	Natural frequency of the structure
ω_2	Natural frequency of the damper
ω	Angular velocity
Ω_f	Fluid domain
Ω_s	Structural domain

LIST OF FIGURES

LIST OF TABLES

INTRODUCTION

Research Relevance, Aim and Objectives

The World Health Organization adopted the declaration of "Health for all in the twenty-first century" where a target of "healthy aging" was laid out for the European region. It is foreseen that in Europe the population of people older than 65 years will increase to 70% by 2050, while those over 80 years will increase by 170% [1]. Besides, more than 10 % of the population is affected by such diseases as Diabetes mellitus or Arthritis that could lead to blood circulatory disorders. As a consequence, the present medical community requires non-invasive smart technologies and tools that could be applied when dealing with aging-related and blood circulatory disorder health problems. The increase in a person's age has a marked influence on the occurrence of disorders in the cardiovascular system. Therefore, development of means for treatment and prevention of such disorders is highly relevant nowadays. Pathological processes often disrupt the function of arterioles and capillaries, thus causing an increase in blood pressure or malfunctions in tissue feeding. Therefore, innovative research efforts in the field of vascular dynamics are particularly important at the moment.

Due to the lack of methodologies and means for the blood circulatory improvement in capillaries, it was decided to create a novel approach to perform low-frequency vibrational therapy for people with disabilities and for those suffering from diabetics, arthritis, hypertensions and other diseases with circulatory disorders. The main aim was to create the human-compatible prototype with a purpose of 'low-frequency vibrational therapy influence' investigation on significantly improving blood circulation. The novel approach is based on the vibration of limbs to compensate for the obstruction of blood circulation, especially in capillaries. According to the requirements and application field, the decision was made to develop two separate devices for the specific disorders and concentrating on the diseased part of the body. It has been decided to use rotating unbalanced masses and initiate beating phenomenon with the purpose to generate and transmit low-frequency vibrations. Beating frequencies are used in various areas of new technologies. Similar technology using two small size vibrating motors as a miniature vibro-tactile sensory substitution device are found for multi-fingered hand prosthetics [2] and two-micro-motor platforms design for actuating control of a novel sliding micro-robot [3]. The proposed application of beating frequencies is therefore innovative in the medical device area.

Statement of novelty

The following scientific novelties are presented in the thesis:

1. Experimental setup of an imitational blood circulation system; consisting of a peristaltic pump, vibration actuator and μPIV equipment, which enables researchers to analyse alterations of fluid (blood) parameters in the microchannel during the vibrational excitation at various frequencies and amplitudes.
2. Experimental and theoretical proof of low-frequency's vibrational excitation influence on blood flow improvement. Prescribed frequencies of

induced beating phenomenon in conjunction with sufficient displacement range significantly increase blood flow velocity and pressure in the microchannel and reduces maximum contact pressure between the erythrocyte and the capillary wall.

3. Unique prototypes of a vibrating bracelet and a vibrating machine for legs were designed and experimental proof of capturing thermal imagery of temperature increase in limbs after the vibrational excitation has been conducted.

Practical value

The new type of vibrational excitation approach to the human body is proposed, which is intended exclusively for the improvement of the blood flow; thus feeding the human body tissue for diabetics and people with disabilities, relieving the arthritis caused pain and lowering high blood pressure. Blood circulatory disorders could lead to the amputation of diseased limb and a lack of existing solutions has therefore been identified and fulfilling the market with unique means are proposed.

The numerical models of blood vessel, capillary and erythrocyte enables the reduction of the need for time-consuming and expensive invasive studies with biological tissues of the human body. The developed models could be modified depending on the application field, thus improving the design process and reducing costs.

The subject of research and methodology

The subject of research is the blood flow improvement in human limbs' with the effect of vibration exposure.

The research methodology is based on the analysis, purification and generalization of scientific sources of vibration exposure on the human body. The influence of low-frequency vibrations were investigated; monitoring blood pressure and velocity parameters, as well as maximum contact pressure, between the erythrocyte's and capillary's walls. The numerical analysis was conducted with the Comsol Multiphysics software 'Acoustic-Solid Interaction Frequency domain and Fluid-structure Interaction modules' while the adequacy of numerical models was investigated with the Micro-particle Image Velocimetry equipment and capturing thermal imagery of handbreadth and foot after the vibration exposure with the designed actuators.

Defended dissertation statements

The novel approach and devices of vibration exposure was proposed that improves blood flow in human limbs. The devices were designed considering diseased parts of the body affected by diabetes mellitus, arthritis and other circulatory disorders, thus eliminating conceivable resonance with internal organs and the negative effect to the spine.

The developed numerical models of blood vessel, capillary and erythrocyte simplifies the research of vibration exposure influence on different cardiovascular parameters, as well as material property changes as a result of various diseases.

The significant findings of numerical and experimental investigations provide the validity of the designed devices in the area of blood flow improvement using low-frequency vibrations.

Document structure

The thesis consists of an introduction, four sections, general conclusions and a list of literature and scientific publications on the topic of dissertation. The volume of the dissertation is 112 pages in total; 35 numbered formulas, 81 figures and 10 tables are used in the main body. The list of references contains 106 sources.

Future work

Future work will include clinical trials on diabetics and long-term investigations of low-frequency vibrational exposure on blood flow improvement, especially in the limbs' capillaries. The gathering of patients meeting the requirements for such clinical trials is a liable and time consuming process. Therefore, a questionnaire about physical condition is prepared and distributed around potential disease affected patients. Development of a sophisticated mathematical model of flowing with more than one erythrocyte in the micro-channel of capillary should be executed.

Research approbation and Publications

Theoretical and experimental studies were performed at Kaunas University of Technology, Institute of Mechatronics. Some of the research results were obtained and reclaimed implementing the research project "In-Smart" (Nr. VP1-3.1-ŠMM-10-V-02-012), funded by the EU Structural Funds Project Ministry of Education and Science, Lithuania.

The results of this dissertation have been published in 9 scientific papers: 3 in journals listed in ISI Master Journal List, 2 – in ISI proceedings and 4 – in conference proceedings.

The results have been presented at 7 conferences:

- „Tarpdalykiniai tyrimai fiziniuose ir technologijos moksluose – 2012“, Vilnius;
- International conference of "Vibroengineering" 2013, Druskininkai;
- „Tarpdalykiniai tyrimai fiziniuose ir technologijos moksluose – 2014“, Vilnius
- 19th International conference "Mechanika-2014", Kaunas
- "12th International Symposium Computer Methods in Biomechanics and Biomedical Engineering", 2014, Amsterdam, The Netherlands;
- 20th International scientific conference "Mechanika-2015", Kaunas.
- The 14th IFToMM World Congress, 2015, Taipei, Taiwan.

1. LITERATURE REVIEW

1.1. Blood circulatory disorders

According to the statistics, more than 50 percent of deaths are caused by heart and cardiovascular diseases in the European Union, which is also prevalent in Lithuania [4]. The main function of the cardiovascular system is to feed tissue by supplying oxygen and nutrients as well as removing carbon dioxide and metabolites. These processes can only be in the capillaries system. The capillaries are the smallest tissue blood channels with a diameter of about 5-8 μm. Capillaries are one of the most important parts of the cardiovascular system. These small micro-vessels are widely branching out throughout the human body, thus creating a capillaries network. The metabolic processes occur between the capillaries and contact tissue. Pathological processes often disturbs the function of the arterioles and capillaries, thus cause high blood pressure and nutrition disorders.

As mentioned above, the human body's circulation system is responsible for sending blood, oxygen and nutrients throughout the body. The reduction of blood flow to a specific part of the human body may cause the symptoms of poor circulation. Human extremities, such as legs and arms, are affected the most by poor circulation. Insufficient circulation is the result from other health issues and is not a condition in itself. The most common reasons of circulatory disorders are obesity, diabetes mellitus, arthritis, disability, heart conditions and arterial issues. The diabetes mellitus, arthritis and hypertension alone affects hundreds of millions of people worldwide. Diabetes mellitus can be named as one of the most common pathology and there are a lack of means for solving problems caused by this disease.

Diabetes mellitus

Blood sugar level is not the only thing affected by diabetes mellitus. The disease causes poor blood circulation that leads to leg cramping and pain in calves, thighs or buttocks. Diabetes mellitus dramatically increase the risk of heart and blood vessel problems, as well as atherosclerosis and high blood pressure. 25 years ago there were only 30 million diabetics globally. Now this number has risen to 366 million. The International Diabetes Mellitus Federation predicts that in 2030 there will be 552 million of these patients [5]. The number of diabetics in Lithuania is equally increasing, as in the rest of the world. Supposedly, there is about 5 % (150 000) of the Lithuanian population suffering from Diabetes mellitus. 3500 Lithuanians die (10 per day) from this illness annually and 29.1 million suffer from diabetes mellitus in the US [6]. According to statistics, 600,000 diabetics with limb ulcers are diagnosed every year, furthermore, about 90,000 cases of limb amputations are performed worldwide. The essential cause of diabetic feet – insufficient blood supply. People with diabetes mellitus may bear many different problems with their feet. Even ordinary problems can get worse and lead to serious complications. Poor blood flow or shape changes of the feet or toes may also cause problems. People might not notice a foot injury until the skin breaks down and becomes infected. Walking on an ulcer can make it get larger and force the infection deeper into the foot. Poor blood flow can make the foot

less able to fight infection and to heal. Diabetes mellitus causes blood vessels of the foot and leg to narrow and harden. In this case the role of capillaries are crucial.

Early and thorough limb examination of diabetic patients, permanent blood stimulation and effective control of the problem can help protect the patient from further complications. This encourages the development of modern and innovative disease suppression tools to reduce patient disability, medical costs and to increase the quality of life. The latest studies indicate that low-frequency mechanical vibrations could be used with the purpose of a faster healing of a diabetic foot ulcer [7].

Arthritis

Nearly 50 million people in the U.S. report having some form of arthritis [8]. 100 million in the EU are also suffering from arthritis or other rheumatic diseases [9]. Permanent daily pain and functional disorders caused by a rheumatic disease dramatically reduces the quality of life. Arthritis is the main reason of permanent disabilities worldwide and the second main cause in Lithuania. There are some 250 000 Lithuanians suffering from arthritis according to current calculations. In most cases, doctors don't know what causes arthritis. Affected by arthritis, the immune system destroys healthy cells. The first symptoms appear in the age bracket 30 to 50. The majority of people suffering from arthritis are working-age women. The most important factor in the development of arthritis is poor circulation of the microscopic blood vessels that carry oxygen and other nutrients to the joints. Insufficient blood flow causes pain in the small joints of the hands, including the wrists and the base of the fingers. Furthermore, other parts of the body, like elbows, shoulders, ankles, hips, feet and knees, are also affected. Today, medications are the main means of relieving the symptoms. Exercising is strongly recommended as a way of self-treatment because of a natural facilities to enhance blood circulation. First, it should be the easy exercises and then trying medium strength training. The load should be selected regarding the condition of the disease. Generally, treatment methods should be defined individually. Just a very few self-treatment tools could be found in the literature. Lack of proper means motivates researchers to make and offer novel methodologies. Vibrating machines are becoming more popular by adopting them for arthritis but the main purpose of them is to strengthen muscles and joints with less stress on the joints than regular strength training. By using different vibrational frequencies, supply of vital nutrients can be significantly improved. For this reason, further research is necessary.

Hypertension

Arterial hypertension (high blood pressure) is widely spread all over the world. The latest studies show that arterial hypertension is diagnosed in 1 in 3 Lithuanians. High blood pressure prevalence is one of the largest in the European Union. Every second person (25 – 64 years old) suffers from hypertension in the EU. About 70 million American adults have high blood pressure – that is 1 in 3 adults [10]. Permanent or temporary higher blood pressure is diagnosed at 5 % of the population of those younger than 15 years old. Untreated arterial hypertension can violate various

blood vessels, heart, kidneys and the central nerve system in just a few years. The extent of the disease is significant but there are no means of effective control.

If the permanently monitored Systolic blood pressure is between 120 and 139 mmHg and Diastolic between 80 and 89 mmHg than this stage is called Prehypertension. If these numbers are higher, the diagnosis is Hypertension. In the first stage of Hypertension (Systolic pressure up to 159 mmHg and Diastolic up to 99 mmHg) and Prehypertension it is recommended to start exercising and make a healthier lifestyle. Usually, doctors take more care about systolic blood pressure because of its direct relation with cardiovascular diseases. In most people, systolic blood pressure increases with age. Non-treatment of arterial hypertension can affect the vascular system, heart, kidneys and the central nervous system in just a few years. It is widely accepted that the early phase of primary hypertension is characterized by elevated cardiac output, whereas in later stages the increased blood pressure is due to increased peripheral resistance. Most people are only aware of hypertension only after a suffering heart attack or stroke. The majority of patients with hypertension do not know what steps to take to lower blood pressure. Methodology of blood circulation enhancement in the micro-vascular system can provide the development of non-medication means.

Raynaud's Disease

People with chronic cold hands and feet may have a condition called Raynaud‘s disease [11]. The small arteries in the hands and toes narrow as a result of this disease. This causes difficulties for blood moving through the body and leads to symptoms of poor circulation.

The primary type of Raynaud's disease tends to be less serve than secondary Raynaud's. With primary or secondary Raynaud's, cold temperatures or stress, can trigger "Raynaud's attacks." During an attack, little or no blood flows to the affected body parts.

About 5 percent of the U.S. population has Raynaud's disease [11]. For most people, primary Raynaud's is more of a bother than a serious illness. Secondary Raynaud's is harder to manage and it is important to treat the underlying disease or what is causing the condition.

Peripheral Artery Disease

The Pheripheral Artery Disease causes the narrowing of the blood vessels and arteries and can lead to poor circulation in the legs, therefore decreased blood flow in feet can result in pain. Over time, numbness, tingling, nerve damage and tissue damage can occur. The Pheripheral Artery Disease is most common in adults over age 50.

When people have a blockage or narrowing of the arteries in the legs, the circulation is reduced. Tissue in the leg will die because of the insufficiency of oxygen and nutrients. This can lead to infection and gangrene, which could be very dangerous and life-threatening. Amputation is always a last resort.

Disabilities

Walking and running increases blood flow out of and into the legs. People sitting in a wheelchair or having other mobility problems cannot stimulate blood circulation naturally. Insufficient blood volume could lead to various problems, like cold feet, feeling numb, ulcers or even amputation. Electro muscle stimulators could be used to increase blood circulation in the legs. Electrical impulses transmitted via electrodes, make the muscles contract, thereby blood circulation increases. However, this methodology is controversial and long-term studies need to be done. In most cases, therapeutics are used to recommend natural movement imitation instead of electrical muscle stimulation methodology. The practice of using walking imitators are still more common. Most of the therapy tools could only be accessed in clinics. The lack of home-adopted tools make many difficulties for people with disabilities. Only economically strong countries have a good infrastructure for people with disabilities to migrate into cities and assist in gaining access to therapeutic tools. Therefore, adopting vibrational methodologies on blood circulation would simplify and enable a self-therapeutic process.

Wound healing

The healing process depends on the blood circulation to the skin. Sufficient blood flow ensures delivery of oxygen and nutrients that are crucial to the healing process. The findings in the study with diabetic mice shows that low-intensity vibrational training may be a novel therapeutic method for healing diabetic wounds [12]. The effect of vibration on the skin microcirculation was observed in another study with mice. It was found that skin blood flow increases when effecting it with vibrational excitation of 47 Hz [13].

The problems mentioned above causes blood circulation disorders. The lack of circulation can cause coldness and soluble feelings in hands and legs. Disabled people, diabetics or those suffering from arthritis and even athletes have soluble limbs. The final outcome could even be an amputation of the extremities.

1.2. Cardiovascular system - capillaries and arterioles

There are three major types of blood vessels: veins, arteries, and capillaries. The blood circulation starts from the heart and goes to arteries, arterioles, capillaries then flows back through venules and veins. Arteries carry blood away from the heart, forming smaller divisions by increasing the distance from heart. The smaller branches of arteries are called arterioles. The blood flows through arterioles to the capillaries, which are the only vessels in contact with tissue cells. The blood pressure in the entrance of the capillary bed is about 40 mmHg. At the exit, blood pressure decreases and is about 20 mmHg or even less. Capillaries are extremely permeable and fragile, thus low pressure is required. The most important function of capillaries are to directly serve cellular needs. The smallest vessels deliver gases, nutrients and hormones. Capillaries enable the body to make blood exchange through gossamer-thin walls and these functions separates them from arteries and veins, which function as conduits. Capillaries are composed only of endothelium. The walls are very thin and are stabilized by spider shaped smooth muscle-like cells. The diameter of a capillary is

large enough for red blood cell to move through. The only tissue exceptions that are not supplied by the capillaries are tendons, ligaments, cornea and the lens of the eye. Because of their exclusive facilities and importance, capillaries will be the major attention in this paper.

There are three main structural types of capillaries:

- Continuous capillaries;
- Fenestrated capillaries;
- Sinusoidal capillaries.

The continuous capillaries are the most common and the highest concentration could be found in skin and muscles. Naturally, the blood flow through the capillaries are mainly regulated by vascomotor nerve fibers and local chemical conditions. There are two routes of possible blood flow through capillaries. When pre-capillary sphincters are open; blood flows through the true capillaries. When pre-capillary sphincters are closed; then blood flows through shunt and circumvents tissue cells without exchanging nutrients. This is how the flow through capillaries are described by the cardiovascular theory. But in some cases, there could be different sources of dysfunction.

Red blood cells (RBC) can be significantly affected by genetic or some pathological conditions. The healthy RBCs are disc-shaped and have a flexible membrane. High surface-to-volume ratio lightens reversible elastic deformation, which is crucial, by continuously passing the micron diameter capillaries and transporting nutrients and oxygen. Pathological conditions can considerably influence changes of form or membrane properties of the disc-shaped RBC. In some cases, these alterations causes circulation obstruction. This could lead to necrosis and organ damage [14].

As an example, the influence of diabetes mellitus is described further. Changes in rheological properties affect mechanical properties like; micro-viscosity, aggregation and adhesiveness. These alterations lead to dysfunctioning of the membrane structure and composition [15, 16]. The increased red blood cell rigidity has been observed in a number of previous studies. In a study of diabetic patients with renal insufficiency, reduced RBC deformability was found [17]. Findings from another study showed that red blood cell rigidity dramatically increase in hypertension and diabetes mellitus [18]. Further analysis on RBC's deformability is needed and a lack of similar studies has been observed.

1.3. Literature review of vibration therapy influence on the cardiovascular system

Human vibration therapy dates back to ancient Greece. Vibrational therapy is known for its benefits to improve muscle strength, power and flexibility, as well as coordination or even the cardiovascular system. It is known that vibration exercises has an effect of preventing parasites and other germs from invading the body and at the same time helping to activate, to a suitable degree, the various organs of the body [19]. There has been much research of the vibration effect to the human's biological processes.

Katsuzo Nishi [20] introduced the Nishi-Shiki health system in 1927. Nishi-Shiki provides a number of exercises for the treatment of circulatory disorders. It was based on his own studies and practice of what would amount to some 360 types of folk cures and health methods, both ancient and contemporary - Oriental and Occidental. His methodologies are based on his own studies and theories of the dynamics of the human body, with reference to mechanical engineering science. His theories are characterized by the idea that a humans′ internal organs are basically the same as those that evolved for the mammalian, and a human two-legged life style causes certain structural strains on the human bone structure, which then causes obstruction problems of the food flow through the intestines. These methods are characterized by the idea that a humans' internal organs are doubled and the capillaries are the human's second heart. Nishi stated that the capillaries provide the true driving force of the circulatory system. To compensate for the obstruction of circulation in a human's limbs; he proposed the capillarity exercise.

In vascular beds that exhibit arteriovenous asymmetry, increased flow may trigger an increased flow resistance by a mechanism involving the tendency of vascular segments to reduce their luminal diameters in response to increased transmural pressure. Blood vessels have an ability to control blood flow velocity by shrinking or expanding, because of their elastic properties. When the pressure is constant, the fluid volume flow rate is reduced as a result of increased flow resistance. This permanent reaction can be characterized as 'structural auto regulation' [21]. In paper [22] new models of the micro dosing elements are presented; to investigate blood circulation in the capillaries.

Positive vibrational therapy effect on heart rate values and blood circulatory system is noted in a number of previous studies [23, 24]. It is confirmed that blood flows into the capillaries at high speed and the stored energy is converted into heat, thus significantly reducing the blood pressure. The influence of induced whole body vibration (WBV) was investigated on arterial stiffness. According to that paper, brachial-ankle pulse wave velocity decreased 20 and 40 min after the WBV trial and recovered to baseline 60 min after the trial. These results suggest that WBV acutely decreases arterial stiffness [25]. Investigation on vibration training on the cardiovascular system has showed that capillaries are opened in order to keep the necessary level of cardiac output needed for the body [26]. Earlier studies have showed that whole body vibrations affect increase artery blood flow, heart rate and other parameters [27, 28].

Research to date provides evidence that a rarefaction of capillaries is known to occur in many tissues in patients with essential hypertension [29, 30, 31, 32, 33]. The Cohn study indicates that hypertension may be a consequence of a reduced number of capillaries and arterioles [34]. Another study, made by Cheng et al. 2008, was made aiming to determine if capillary rarefaction is detectable in people with mild systolic blood pressure elevation. The findings show that the measured functional capillary rarefaction were notably lower in both high blood pressure groups compared to normotensives [35]. Vibration therapy was proved as an appropriate approach for the prevention of joint, muscular, ligament and tendon injuries. Furthermore, a 5-minute cycle ergometer warm-up elicits results comparable to a vibration warm-up.

The purpose of the other study was to investigate the influence of whole-body vibration on blood flow velocity and muscular activity after different vibration protocols in Friedreich's ataxia patients. Ten patients received whole body vibration treatments with random combinations of frequency and protocol. Femoral artery blood flow velocity, vastus lateralis and vastus medialis electromyography, and rate of perceived exertion were registered. Peak blood velocity was increased. Electromyography amplitude was increased and frequencies decreased during the application of whole body vibration. The results suggest that whole body vibration is an effective method to increase blood flow in patients with Friedreich's ataxia [36].

Another study partly aimed to determine the effects of vibration on leg blood flow after intense exercise. Twenty-three participants performed exercise tests followed by a recovery period using whole-body vibration or a passive control in the seated position, after the blood flow was assessed. Results showed that the whole body vibration pulsatility index decreased in the popliteal artery following maximal exercise and was effective in increasing performance in later exercise tests [36, 37].

The effect of whole-body vibration on leg blood flow has been investigated on young adult males. The subjects completed a set of random vibration and nonvibration exercise bouts whilst squatting on a vibrating plate. Blood pressure of the common femoral artery and blood cell velocity were measured in a standing or rest condition prior to the bouts, then during and after each bout. This research made by Lythgo et al. [38] shows that leg blood flow systematically increases in the vibration bouts. Osawa et al. [28] has identified that the whole body vibration therapy influences increasing arterial blood flow and other cardiovascular parameters. The study with twenty healthy adults [39] was performed on the vibrating platform imitating mechanical vibrations of 26 Hz. The mean blood flow velocity in the popliteal artery increased from 6.5 to 13.0 cm x s(-1). Baum et al.'s [40] studies on type II diabetes mellitus patients performing vibration exercises suggested that vibration exercise may be an effective and low time consuming tool to enhance glycaemic control. The studies performed at the Loma Linda University [41] indicated the significant increase in skin blood flow when performing five minute vibrations of 30 Hz or 50 Hz. It was mentioned that future research should be done to determine if this method is eligible with diabetes mellitus having low circulation. Another study at the Loma Linda University [42] showed the increased skin blood flow after whole body vibration exercise at post intervention time intervals. However, the lack of investigations analysing fluid parameter changes by affecting it by external vibrations and the possibility to adopt the vibration method on diabetics were noted.

The influence of high frequency vibrations generated by cylindrical piezo-actuator to the flow of liquid substances in a micro-channel is investigated in the work of Palevicius et al. (2004) [22]. Hybrid experimental-numerical analysis techniques were used for the investigation of micro spray systems. Laminar flow in straight channel analysis was made by Silva et al. (2009) [43] and Puccetti et al. (2014) [44]. The results of the studies have been compared to theoretical calculations and indicated a 4 % difference between experimental and theoretical results. The accuracy of the μPIV method was also determined by Wang et al. (2009) [45], who investigated different length sides of four square micro-channels with different Reynolds numbers

(Re). Similar research of rectangular channels was made by Devasenathipathy et al. (2003) [46] and the acquired results matched theoretical calculations. μPIV measurements close to the micro-channel wall with attached artificial thrombus were made by Tolouei et al. (2009) [47] and the results of a similar study of Completo et al. (2014) [48] had showed that the μPIV method could be used for the assessment of blood flow and thrombus geometry influence near the walls. μPIV technology is beneficial on the experiments investigating fluid velocity parameters' response to low frequency vibrations.

1.4. Technological means to improve blood circulation

Therapeutic massage is one of the best clues to improve blood circulation in the human body. The method is proved and there is no questions about its positive effect. Furthermore, massage replacing means can be found in literature. Various types of devices using thermal, mechanical and electrical or ultrasound technologies has been developed as prototypes or final products. The diversity of named technologies' applicability is even wider. Thermal therapy is more convenient by using it for relaxation or for athletes' recovery/warm-up. The applicability of electrical impulses and ultrasound technologies more frequently occurs in the surgery or rehabilitation field. Mechanical load or vibrational therapy could be named as the most comparable method to the therapeutic massage. The major part of products are designed for athletes with the purpose of improving muscle performance. It is worth mentioning that previously stated scientific findings prove the unquestionable effect of vibrational exposure on human body. However, previously listed diseases are united by blood circulation disorders but only the minority of means are designed to solve this problem. The products in the market or described in patents that provides similar methodologies and solving the previously described problems were overviewed. The competition can be separated in two main types:

- Vertical (functional) competition – competing between the same needs but different type of items.
- Horizontal (type) competition – competing between the same needs and same type of items.

Both types of products, technologies or methodologies were analysed and the most relevant are described below.

Whole body vibration machines

Probably the most popular and thoroughly investigated application of vibrational therapy are for health or improved performance purposes. The whole body vibration machines (Fig. 1) are mostly adopted for athletes with the purpose of gaining more muscle mass, strengthen bones and joints and performing warm-up before a workout. Only the newest models are partly adopted for people in a wheelchair. Although the manufacturers' state that blood circulation improvements is not the primary goal.

There are a number of similar products on the market, but the reviews only encompass general purposes and stated benefits. The majority of the whole body vibration machines [49, 50, 51] use mechanical oscillatory movement. This provides

for the performance of static or dynamic exercises depending on the type of machine. The vibration platform generated oscillations, transfers the energy directly to the human body. The majority of whole body vibration machines provide sinusoidal shaped oscillations that are described by their frequency, amplitude and phase angle [52]. Parameters of whole-body vibration modalities are an essential part of a patent. Patent claims for vibrational platforms include direction, amplitude, frequency, and vibration acceleration (patents 20100049105; 20090269728; 20090076421; 20080009776; 20070290632; 20070225622; 20070219052; 20050251068) [53].

The platforms are characterised by acceleration levels and by the way in which they apply vibration. Lower than 1g accelerations are considered as low intensity while more than 1g – high intensity. The frequency range of most platforms range from 12 to 40 Hz and the amplitude ranges from 0.7 to 5 mm.

Fig. 1. Whole-body vibrational training machine [49]

The whole-body vibration training machine is a well-known product in the fitness equipment field, with wide applicability, starting from enhancing muscle performance, bone density and blood circulation for healthy athletes. The technology has been scientifically proved and products from different manufacturers are spread worldwide, although it has some disadvantages. The whole body and all internal organs are affected by external vibrations, thus, this could lead to spine problems such as the emergence of a hernia. The long term positive effect is not proved scientifically. The whole body vibrational devices have not been approved for medical purposes, as the applicability is limited due to the construction and working regimes of the technology used to generate vibrations.

Intellinetix vibrating gloves

The purpose of using vibrating gloves (Fig. 2) is to reduce pain in fingers or hands that is caused by arthritis or other chronic conditions. The Intellinetix gloves [54] increase blood circulation and warms aching joints. The product is patent-pending (in the U.S.), although no information on the FDA website about this product was found.

The gloves provide gentle vibrations using small vibrating motors. The motors are fixed near the fingers and wrist. It can be assumed that these motors are working in higher than 20-30 Hz frequency range.

Fig. 2. Intellinetix vibrating gloves [54]

The strength of Intellinetix vibrating gloves is that this product is patented and sellable worldwide. From the functional side of view it is advantageous because of the compatibility with a pacemaker and its small size makes it easily transportable. However, the gloves have limited applicability and solves only arthritis caused problems by enhancing blood circulation in the hand and warming up the wrist.

Legs and hands massager

OSIM uPhoria Foot & Calf Massager [55] stimulates meridian points along the legs. The device (Fig. 3) uses vibrational and warmth technologies together or separately. The manufacturer states that the device is a deep-tissue massager that helps to relieve soreness and aches. It is based on the principles of reflexology massage.

Fig. 3. OSIM uPhoria Foot & Calf Massager [55]

The therapeutic Oster – Stim-U-Lax Body massager [56] uses single speed and thousands of vibrations per minute that are transmitted directly to the hand. As the

manufacturer declares, the 15-watt motor rotates six ball bearings laterally and vertically. The intensity is controlled by the user by changing the pressure. The device (Fig. 4) power source is AC supply and the input voltage is 120 V.

Fig. 4. Oster – Stim-U-Lax Body Massager [56]

These devices have the advantages of traditional massage and can be named as massage replacements, however the primary purpose of these devices is as a relaxation tool, therefore the blood circulation enhancement is just an auxiliary purpose.

Neurostimulation devices

Depending on the application field, the methodology may be different on the various devices. The Geko device [57] (Fig. 5) emits a 27mA current to the back of the knee. Electrical impulses make the calf muscle contract and stimulates the blood flow. The device stimulates the peroneal nerve that is very close to the surface of the skin. It is stated that the Geko device increases blood flow by a factor of four for someone who is sitting down. Furthermore the same technology is being used for athletes to aid muscle recovery.

Fig. 5. Geko neuro-stimulation device [57]

The Geko device's small size means that could be easily used anywhere. Wide applicability and a huge distributor's network makes it easily accessible, however, it could not be used with a pacemaker and the positive effects are contradictory.

VibeTech

The VibeTech is the only device that combines strength training and vibrational therapy to commit physical and occupational therapy. The VibeTech device [58] is designed for people with impaired physical mobility to improve muscle strength, balance and to restore neural sensation.

Fig. 6. VibeTech device [58]

The device is clinician friendly and helps to solve neurological disorders, reduce pain, enhance blood circulation and is registered at the FDA. The developers are a NASA spinoff. Nevertheless, the rehabilitation oriented device is made only for purposes of mobility improvement and neuromuscular therapy.

Patent analysis of the vibrational technology usage for massage or blood circulation stimulation purposes

Vibrator massager using beat frequency (US 4570616 A) **[59]**

The patented device for therapeutic vibration purpose consists of two motors and rotating discs having eccentric weights. The discs have non-equal diameters and are mutually connected. A vibrational device with this technology could be used in a cushion of pillow. The appliance provides a beating frequency for conveyance of body massage vibrations. In the content of the patent, a 3000 rpm and 3060 rpm respectively rotation speed was stated, which generates a beat of 1 cycle per second. It is noted that beating frequencies of between 0.5 and 2 cycles per second have been found to be the most appropriate and beneficial in vibrating devices, used for the massage of feet. Furthermore, it is claimed that the described device consists of contacted disks in order to enhance the generated force. The contact can be frictional or geared. The other possibilities are represented in the patent application.

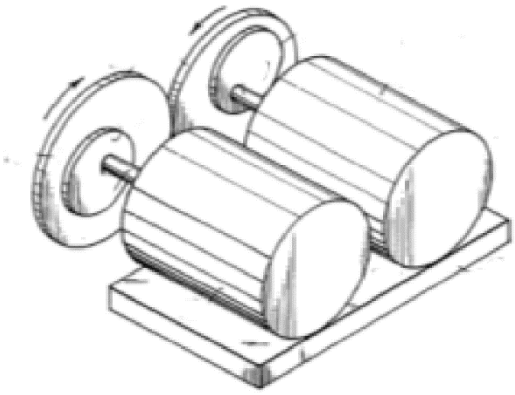

Fig. 7. US 4570616 A patent object [59]

Method and apparatus for improving local blood and lymph circulation using low and high frequency vibration sweeps (US 7909785 B2) **[60]**

Method and apparatus are patented for improving blood circulation by placing one or more transducers on the patient's body. The method uses lower-frequency and higher-frequency sweeps that are converted to microvibrations. The patented object provides massage to the muscle and improved blood circulation to the larger and smaller blood vessels and capillaries.

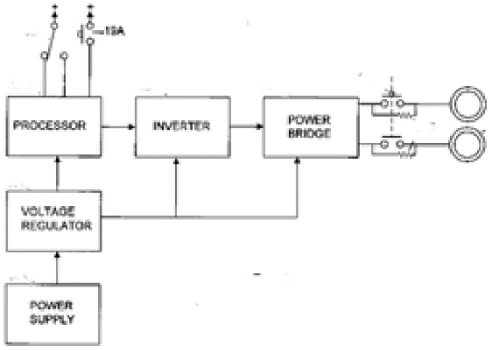

Fig. 8. US 7909785 B2 patent object [60]

It is stated that the amplitude of mechanical vibrations ranges of 5 to 40 microns. The lower-frequency sweep consists of frequencies below 1000 Hz, while the higher-frequency sweep consists of frequencies above 1000 Hz for stimulating blood circulation in larger and smaller blood vessels respectively.

Foot sole massaging device (US 5910123 A) **[61]**

The purpose of the patented device is to stimulate blood circulation of the foot sole. The massaging device uses a vibration plate to vibrate horizontally and produces a stimulation on the knobbed solerests.

Fig. 9. US 5910123 A patent object [61]

The patented device is not equipped to generate a vibration of the most suitable frequency for effective stimulation. The vibration frequency can be easily regulated remotely by a controlling unit.

***Randomic vibration for treatment of blood flow disorders (US 20090069728 A1)* [62]**

The patent covers a therapeutic device and method for treatment of blood circulatory disorders using a non-invasive application of low frequency vibration. In a preferred embodiment, the patented objects could be applied as an adjunct to systemically intravenously administered thrombolytic drug therapy.

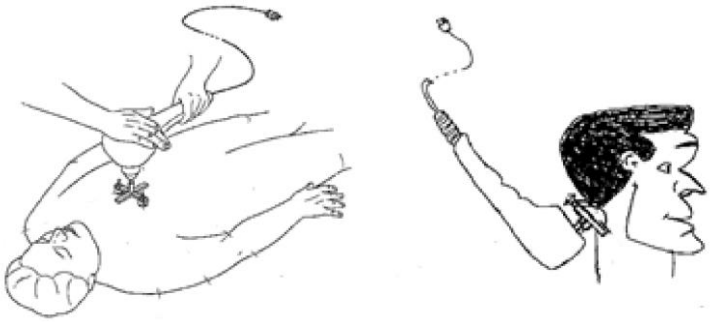

Fig. 10. US 20090069728 A1 patent object [62]

The inventions consist of statements that low frequency mechanical vibrations are preferable for using for treatment to thrombolytic or other clot disruptive and other blood circulatory disorders. The disclosed apparatus and method, using low frequency vibrations, enhances mixing of a clot disruptive therapeutic agent into a low flow artery. It is stated that low frequency vibration has a clot disruptive and vasodilatory properties. A similar device and apparatus is patented for different purposes by the same inventor (Low frequency vibration assisted blood perfusion emergency system US 7517328 B2).

***Method for Improving Blood Circulation (US 20080309132 A1)* [63]**

The disclosed method for improving blood circulation of a seated or lying person using at least one device to generate vibrations locally in a specific areas of the body. The generated frequency ranging of 5 to 30 Hz cycle lasts up to a minute. According to the statements, the method has an amplitude of 0.5 to 2 mm.

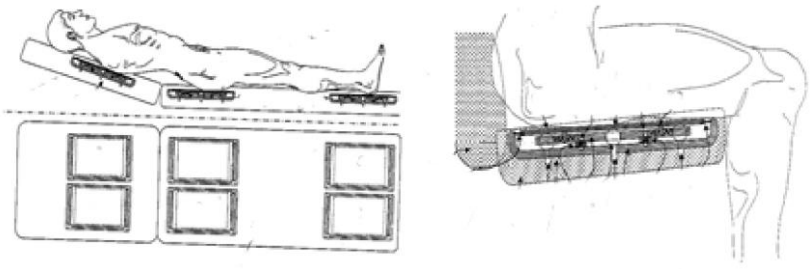

Fig. 11. US 20080309132 A1 patent object [63]

***Leg ulcer, Lymphoedema and DVT vibratory treatment device (WO 2002065973 A1)* [64]**

Three-dimensional vibrations are applied for the purpose of treatment of an ulcer, lymphoedema and DVT. Mechanical vibrations of between 15 and 75 Hz, and with an amplitude of between 0.1 and 0.5 mm are used. A pad transmits vibrations directly to the limb which it is pressed against.

1.5. Limitations and side effect of vibrations to the human body

The human body can be compared with a mechanical structure and it is well known that it has resonance frequencies. The resonance may vary depending on the type of body and with posture. Transmissibility and impedance are the mechanical responses of the body that defines vibrational influence. The transmissibility is mostly reliant on vibration frequency, axis and posture, in range of 3 to 10 Hz. The mechanical impedance shows the effort needed to move the human body and vertical impedance usually shows resonance at about 5 Hz.

The discomfort is clearly defined by ISO standards and it depends on the frequency, axis, the point of contact with the body and the duration. During studies with animals, borders of significant physiological changes were defined where the lower border is around 0.7 m/s^2 r.m.s. between 1 and 10 Hz and up to 30 m/s^2 r.m.s. at 100 Hz.

The elevated risk of spinal health risk is observed during long-term and intense whole body vibration. Degenerative change of the vertebrae and disks are the most frequent disorders [65]. These findings direct to the development of apparatus and methodology of locally transmitted vibrations.

The “vibration diseases” are characterized by a complex of symptoms and pathological changes of the central nervous, musculo-skeletal and circulatory systems [66]. These symptoms have been diagnosed in workers standing on machines that were exposed to whole-body vibration frequencies above 40 Hz. These frequencies are limited by the ISO 2631 standard. In addition, the findings on long-term low

frequency vibrational exposure studies show the same symptoms and pathological changes. The exposure limits of frequencies and acceleration values are defined by ISO 2631 and given below.

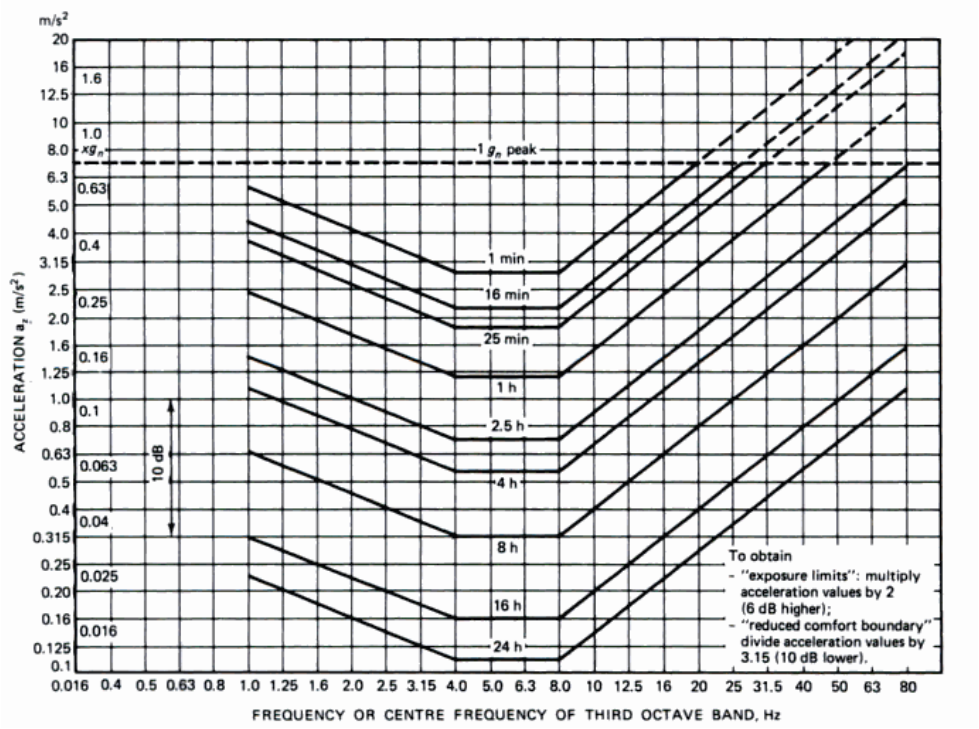

Fig. 12. ISO 2631 vibrational exposure limits [67]

ISO has defined vibration limits for comfort, performance proficiency and safety based on the known occupational hazards, and ISO 2631-1 defined high intensity vibrations (those that produce more than 1 g force) as hazardous; regardless of frequency [67]. ISO 2631-5 define methods of evaluation of mechanical vibration and shock to the whole-body. ISO 5349-1 define the measurement and evaluation of human exposure to hand-transmitted vibration. The standard must be reviewed considering that the methodology of the enhancement of blood circulation is based on mechanical vibrations to the human limbs. ISO 5805 defines human exposure to mechanical vibration. The limb vibrator for therapeutic purposes is described as a segmental vibration machine for applying vibration locally to a human limb for trial or therapeutic purposes. ISO 13090-1 describes safety guidance for experiments with people on whole-body vibrational excitation. The standard provides guidelines of the experiments with humans exposed to mechanical vibration. The purpose of ISO 13090 is to minimize the risk of injury or impaired health. Furthermore, the ISO 14835-1 standard defines the methodology of tests for the evaluation of peripheral vascular function, measuring finger skin temperature. It is stated that the finger skin temperature depends on the blood circulation and could be used as a factor defining blood perfusion at capillaries and arteries. This standard defines the methodology of

cold provocation tests but it is clearly stated that mechanical or physiological effects may change finger skin temperature thus enhancing blood flow.

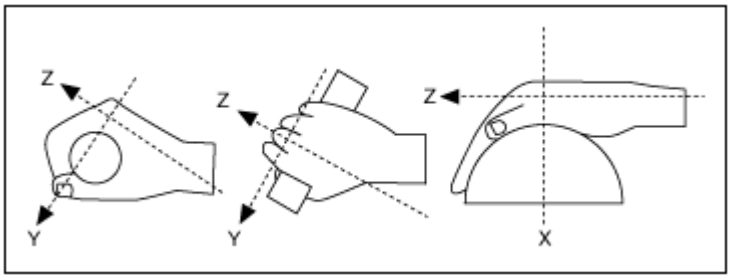

Fig. 13. The coordinate system used to assess hand-arm vibrations (ISO 5348:1986) [67]

1.6. Thesis objectives

Vibrational exposure methodology is unique among the products on the market and with reference to the overview of scientific literature. The approach of vibrational excitation has had to be implemented by developing an innovative system with the purpose to enhance blood circulation in the microchannel. The aim and objectives of this work have been determined according to the results of literature and existing technology reviews.

The aim of this research is to develop and investigate the influence of mechanical vibrations on blood circulation with low-frequency vibrational expose prototypes for human limbs.

In order to reach this aim, the following objectives were determined:

- I. Develop mathematical models of blood vessel connected to the capillary, including red blood cells, define its material properties and identify values of Eigenfrequencies'.
- II. Simulation of vibrational excitation and identification of the influence on the blood velocity changes and red blood cells movement from the arteriole to the capillary.
- III. Develop experimental setup of imitational blood circulation comprising of artificial blood vessel, peristaltic pump, vibrating element, displacement and pressure sensors and measurement equipment and conduct experiments by initiating a beating phenomenon and monitoring blood pressure changes inside the vessel.
- IV. Adapt experimental setup by the Micro-Particle Image Velocimetry (μPIV) system and conduct research by monitoring blood velocity changes in the microchannel.
- V. Design and develop a prototype of vibrating bracelet and legs actuator, identify Eigenfrequencies' of legs' vibration machine depending on different human weight and confirm adequacy of the created theory models to physical ones.
- VI. Verify the influence of vibrational excitation on the improvement of blood circulation in limbs by evaluating temperature measurements.

1.7. Section conclusions

This section presented a review of recent publications, technological means, as well as a detailed description of the blood circulatory system; particularly concentrating on capillaries and vibrational exposure as an improvement means of circulatory disorders. In general, this section introduced the usage of vibrational exposure on the improvement of the cardiovascular system related to recent research achievements, commonly met issues and steady theoretical ground to understand numerical and experimental research presented in the subsequent sections of the thesis.

The following conclusions were drawn from the completed analysis:

- The analysis of disease influenced blood circulatory disorders showed the need for vibrational exposure means that could induce vibrations to the hands and legs separately by eliminating the effect to the internal organs of the human body.
- In terms of literature review, low-frequency analysis on the blood flow was considered for further research. Unique imitational stand of blood circulatory was decided to be developed, including μPIV measurement means. Numerical models of blood vessel, microchannel capillary and red blood cell were decided to be designed in the case of simplifying experimental studies and deeper analysis of micro-particles.
- Prototypes of low-frequency vibrational exposure were decided to be designed considering the limitation of vibrations to the human body. According to the review of existing technological solutions, the novel approach of locally induced vibrations was suggested for people who are suffering from arthritis, diabetes mellitus and other circulatory disorders.

2. THEORETICAL INVESTIGATIONS OF THE VIBRATION INFLUENCE ON BLOOD VELOCITY IN THE CAPILLARY

Blood circulatory disorders can lead to a various range of problems, starting from cold limbs and ending with an amputation or even worse. Diagnosis of initial causes of circulatory disorders are crucial, but mostly only in-vitro methods are available. Mathematical modelling of the cardiovascular system can be performed only with up-to-date software, comprising of specified built-in modules. In most cases, Comsol Multiphysics, Matlab and Ansys software can be appropriate tools for calculations of the cardiovascular system or its processes. Non-invasive analysis methods are necessary and a priority, especially when they are used in exchange of the in-vitro research. The red blood cell is widely analysed as a mechanical structure. However, there is a lack of studies where RBC's natural frequencies are analysed. Moreover, there is no methodology of how to improve RBC's movement through the capillary when its material properties are affected by such diseases like diabetes mellitus or arthritis, which increases the rigidity of erythrocyte and thus lead to the erythrocyte deformability problems in order to flow through the capillary. The theoretical analysis with high-end software tools can help to define the roots of the problem and invent methods of non-invasive treatment. The mechanical vibrations have to be analysed as an approach of a RBC's deformability increasing tool. Furthermore, the number of overviewed studies describes the influence of vibrational therapy on the blood circulation enhancement. The findings show an increased blood velocity during and after the vibrational therapy. However, none of the studies were conducted to find the most appropriate vibrational excitation frequencies. Due to the scarcity of studies of the blood flow velocity changes during the vibrational excitation, it is necessary to investigate this phenomenon by using Comsol Multiphysics software and a mathematical blood vessel model. The mathematical model enables the conduct of studies with blood vessels by shifting mechanical and dynamical parameters, as well as the material properties by applying different environmental studies.

In order to study the erythrocyte's deformability, two separate mathematical models were analysed. The first model of the erythrocyte consisted of two different materials – membrane and lipids. For the second model, the erythrocyte was placed in the blood liquid material the Eigenfrequency values and the deformability modes were identified. The model has been designed by using SolidWorks software, which was imported in to the Comsol Multiphysics environment. Finally, the RBC's mathematical model was introduced into the arteriole and its movement through the capillary was examined.

In order to design the limbs actuator, Comsol Multiphysics studies were conducted to analyse natural frequencies of the vibrating glass-epoxy cantilever. The importance of selection of the "personal frequencies" was obtained in order to gain the highest influence on the blood velocity changes.

2.1. Evaluation of fluid flow response in micro-channel to vibrational excitation

As capillary's displacement coincides with the surrounding soft human tissue movement, it has been decided to measure fluid velocity inside the capillary induced

by external low-frequencies vibrations. A virtual 2D model with the settings of the vibrating microchannel of the capillary has been designed to simplify the testing of the influence of different parameters'. The aim of the virtual microchannel model was to substitute and to reduce the demand of experimental setup for further studies. The virtual model enables time to be saved and costs reduced due to the variability of different parameters that can be changed easily.

Comsol Multiphysics software has been used to perform operations with coupled systems of partial differential equations. At each computational step, the fluid flow field and the structure have been evolved as a coupled system. The flow and structure interaction forces were immediately accounted and their resultant motions enforced in each step. Before designing the model, the research studies of microchannels analysis [68, 69] were overviewed, as well as the built-in blood vessel model being deeply analysed.

The first, simplified 2D model (Fig. 14 (a, b)) was created to investigate alterations of fluid properties affecting it on various vibrational actions. The channel model of 1 mm length and 8 μm diameter was built with reference to the vascular graft tubes that are planned to be used for the experimental setup. Part of the channel of 0.15 mm length was placed in the human tissue properties imitating model. The microchannel was fulfilled by the liquid containing blood material properties. The density of 1060 kg/m^3 and the dynamic viscosity of 0.005 Ns/m^2 has been defined. The fluid-structure interaction (FSI) study has been selected as the most compatible according to the model and its parts. Usability of this particular study is recommended when modelling the interaction of deformable structure with flowing fluid. Some FSI applications include cell bio-mechanics modules as cell deformation, fluid dynamics, ciliary beating, etc. This type of study enables researchers to observe fundamental physics on the sophisticated numerical calculations between fluids and solids.

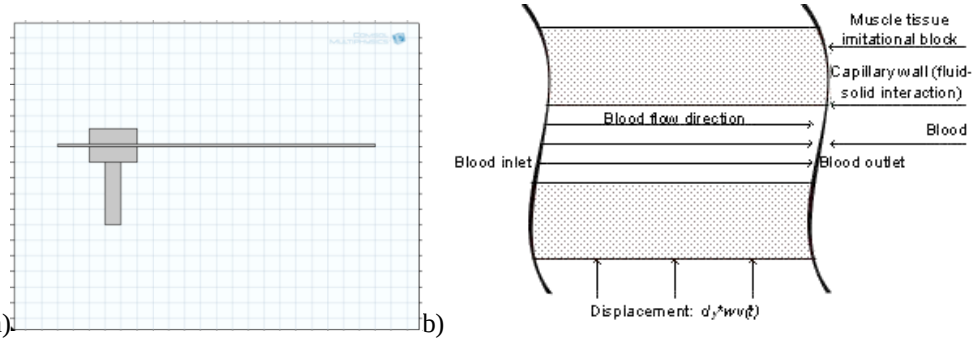

Fig. 14. 2D (a) COMSOL Multiphysics software models of fluid filled microchannel placed in human tissue; (b) schematic drawing.

The fluid-structure interaction problem can be defined by Ω, including structural domain Ω_s and the fluid domain Ω_f, with an external boundary Γ. The fluid-structure interaction is defined by $\Gamma_s = \Omega_s \cap \Omega_f$. Fluid and structure dynamics can be defined as a result of the D'Alembert's principle [70]:

$$\rho v_i - \sigma_{iJ,J}^{\cdot} + f_i = 0 \qquad (2.1.1)$$

where f_i is the body force, ρ is the mass density and $\sigma_{ij,j}$ represents the stress component. In the Structural domain, the equation is defined as

$$\rho^s \dot{v}^s_{ij,j} + f^s_i = 0, \text{ in } \overline{\Omega}_s \tag{2.1.2}$$

where the superscript, *s*, labels the amount linked with the structure. The velocity, v^s_i is the material (or total) time derivative of the displacement field u^s_i, i.e., $v^s_i = \dot{u^s_i}$. Equation (2.1.2) is usually used to describe the Lagrangian theorem. The first term of the equation (2.1.2) is linked with inertia and the second one – with internal stresses. In the case of describing the material as linear elastic, the structural stress will be described by Hooke's law; i.e.,

$$\sigma^s_{ij} = \lambda\delta_{ij}\varepsilon_{ll} + 2G\varepsilon_{ij} \tag{2.1.3}$$

where the structural stress σ^s_{ij} is a function of the strains, ε_{ij} and the Lame constants λ and *G*, which are determined by

$$\varepsilon_{ij} = \frac{1}{2}\left(u_{i,j} + u_{j,i}\right), \tag{2.1.4}$$

$$G = \frac{E}{2(1+v)}, \tag{2.1.5}$$

$$\lambda = \frac{Ev}{(1+v)(1-2v)} \tag{2.1.6}$$

where *E* is the Young's modulus and *v* is the Poisson's ratio. In the fluid domain, the equation is written as

$$\rho^f \dot{v^f_i} - \sigma^f_{i,J,J} + f^f_i = 0, \text{ in } \overline{\Omega}_f \tag{2.1.7}$$

which is usually standing for the Eulerian description. In the inertia term, equation is given by

$$\dot{v^f_i} = \frac{dv^f_i}{dt} = \frac{\partial v^f_i}{\partial t} + v^f_j v^f_{i,J} \tag{2.1.8}$$

In the case of incompressible Newtonian fluid model, the fluid stress σ^f_{ij} is given by

$$\sigma^f_{ij} = -p\delta_{ij} + \tau_{ij} \tag{2.1.9}$$

where

$$\tau_{ij} = 2\mu\left(e_{ij} - \frac{\delta_{ij}e_{kk}}{3}\right) \tag{2.1.10}$$

$$e_{ij} = \left(v^f_{j,i} + v^f_{i,j}\right), \tag{2.1.11}$$

The p is the static pressure used to enforce the incompressibility condition, $v^f_{i,i} = 0$.

The no-slip state on the fluid-structure interaction Γ_s is maintained by defining Dirichlet and Neumann conditions as:

$$v^s_i = v^f_i, \text{ on } \Gamma_s \tag{2.1.12}$$

$$\sigma^s_{ij}n_i = \sigma^f_{ij}n_i, \text{ on } \Gamma_s \tag{2.1.13}$$

The equation (2.1.13) is in fact the differentiation of the displacement condition that both fields share the same interface,

$$x_i^s = x_i^f, \text{ on } \Gamma_s \tag{2.1.14}$$

In some cases, the equation (2.1.14) is being used instead of (2.1.12).

The displacement of 0.1 ÷ 8 mm on the Y-axis and sine waveform function to imitate oscillations varying from 1 to 6 Hz have been determined for the human tissue imitational model. Different angular frequency values of sine waveform enabled the variability of oscillations of the material, imitating the human tissue mechanical properties. The fluid material with reference to the experimental setup was imposed. The prescribed mesh displacement of the fluid material of 0 mm on the X-axis for the inlet and the outlet of the microchannel have been set. The prescribed mesh displacement of 0 mm on the Y-axis was imposed for longitudinal microchannel boundaries excluding fluid-solid interface boundaries. In further studies, Moving-mesh physics has been used. This type of study enables researchers to track the deformation of the fluid mesh. The boundaries of contacting solid and fluid area were prescribed in this study. The two-way coupling conditions can be defined from the equations below:

$$v_{Fluid} = v_{Solid} \tag{2.1.15}$$

$$v_{Solid} = \frac{\partial u_{Solid}}{\partial t} \tag{2.1.16}$$

$$(\sigma \cdot n)_{Fluid} = (\sigma \cdot n)_{Solid} \tag{2.1.17}$$

where *v* is the velocity vector, *u* is the displacement vector, *σ* is the stress tensor, and *n* is the normal vector to the FSI boundary.

The roller movement restriction of the oscillating part of the model was chosen. The material properties of the oscillating part of the model were set with reference to the human body tissue parameters. Vibrational movement of the oscillating part has been described by the sine waveform function where angular frequency, amplitude and phase were variable parameters. Sine wave function has been considered as the most compatible to define the prescribed oscillations (Equation (2.1.18)). A 3D model with the same properties was designed for more precise calculations (Fig. 14 (b)).

$$f(t) = A\sin(\omega t + \varphi) \tag{2.1.18}$$

Incompressible Newtonian fluid flow physical model and Laminar Navier-Stokes equations were used to define blood fluid physics.

$$\rho\frac{\partial \mathrm{u}}{\partial t} + \rho\mathrm{u}\cdot\nabla\mathrm{u} - \nabla\cdot(-p\mathrm{I} + \eta\left(\nabla\mathrm{u} + (\nabla\mathrm{u})^{\mathrm{T}}\right) = \mathrm{F} \tag{2.1.19}$$

$$\nabla\cdot\mathrm{u} = 0 \tag{2.1.20}$$

where ρ is the density, $\mathbf{u} = (u, v)$ is the fluid velocity, p is the pressure, $\mathbf{I}$ is the unit diagonal matrix, η is the dynamic viscosity and $\mathbf{F}$ is the volume force.

This helps to define the load with a prominent pressure distribution. Open fluid boundaries were defined. The inlet boundary has been selected by prescribing normal inflow fluid velocity of 0.00065 m/s.

The biological tissue related domains are included into the mechanical analysis of the study. This type of study is advanced because of the behaviour of the materials.

Dramatically large strains, nonlinear stress-strain connection and the incompressibility property of hyper-elastic material are the main issues that must be considered when properties of biological materials are involved. It is essential to properly define stress and strain measures. The assumptions of infinitesimal displacements are not acceptable. The geometrical nonlinearity could be prescribed when the strains are larger than a few percent and the loading of the body depends on the deformation. In the case of dealing with these issues, the Nonlinear Structural Material Module has been used. In the case of small displacements and strains, the linear elastic material model can be used. According to these assumptions, muscle material properties of 1200 kg/m^3 density, coefficient μ of $6.20*10^6$ N/m^2, bulk modulus of 20μ, Poisson's ratio ν of 0.45 and elastic modulus of $1.16*10^6$ N/m^2 have been prescribed. The time domain and stationary studies can be selected for an analysis of fluid dynamics. The further boundary conditions of the model are described below.

A no-slip boundary condition was designated on all walls. The displacement of the Y-axis (at 2D model) and the displacement of the X-axis (at 3D model) with the waveform function to imitate oscillations were used. Time dependent study duration of 10 seconds with the step of 0.1 second was specified for all the calculations. The structure imitating capillary covering human tissue was a flexible material with the following parameters: density of 30 kg/m^3, Young's modulus of 25 MPa and Poisson's ratio of 0.5 [69, 71].

On the COMSOL Multiphysics model; the cross-section changes of the velocity values were investigated after effecting the fluid on different frequencies' values. The changes of fluid velocity were monitored at the middle of the microchannel. The results were obtained by using the model of a microchannel of 8 μm diameter. The peak fluid velocity of the oscillating model on 4.3 Hz vibrations was 2.74 mm/s, while the maximum value of all the gathered data reached 3.23 mm/s (Fig. 15). The average blood flow velocity during the oscillations of 4.3 Hz frequency was 0.98 mm/s. The initial velocity increased by 66.3 %. The results show the raised average and peak velocity values on each mean of the given low frequencies. It was also observed that at some moments the direction of the fluid velocity was negative. In some cases the turbulent flow marks could be seen. This depends on the amplitude of the oscillating part and the frequency value. This phenomenon can be observed in Fig. 16 (a) and (b) when the velocity curve form at certain time moments is close to horizontal.

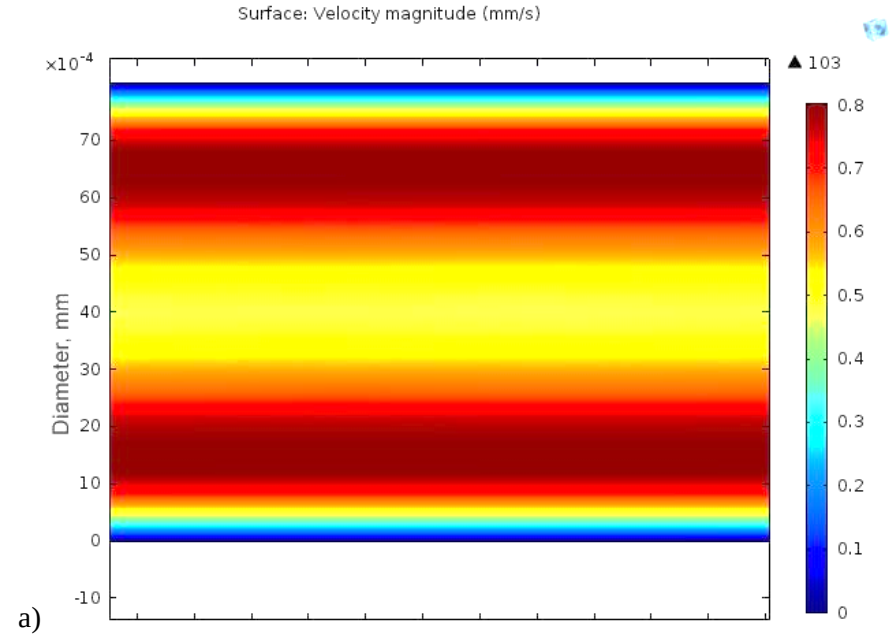

a)

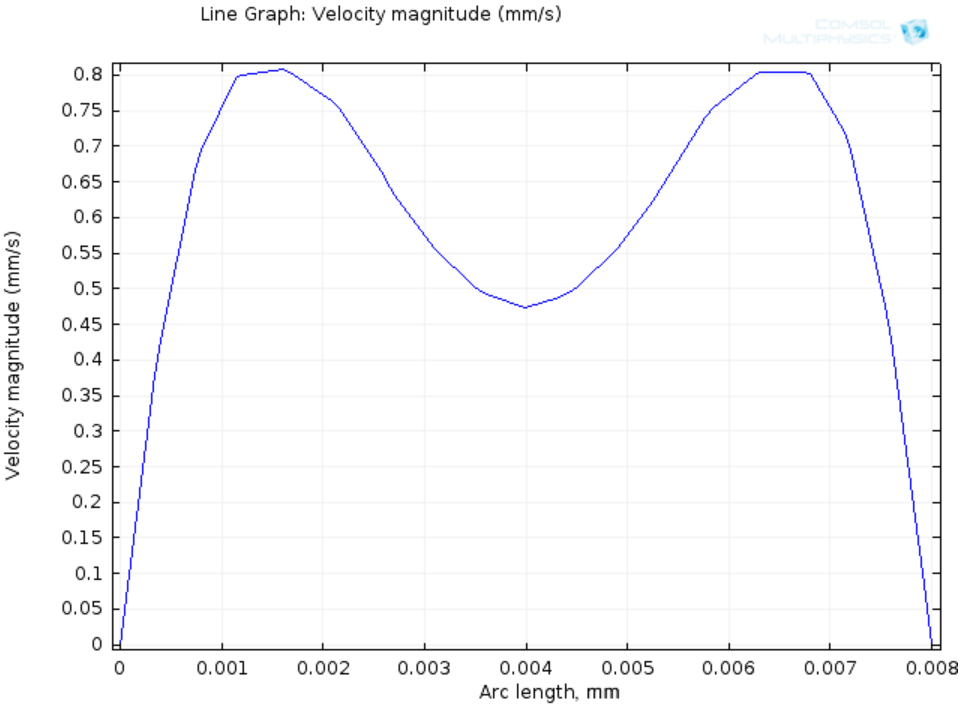

b)

Fig. 15. Fluid velocity spectrogram (a) and field (b) during 4.3 Hz vibration exposure.

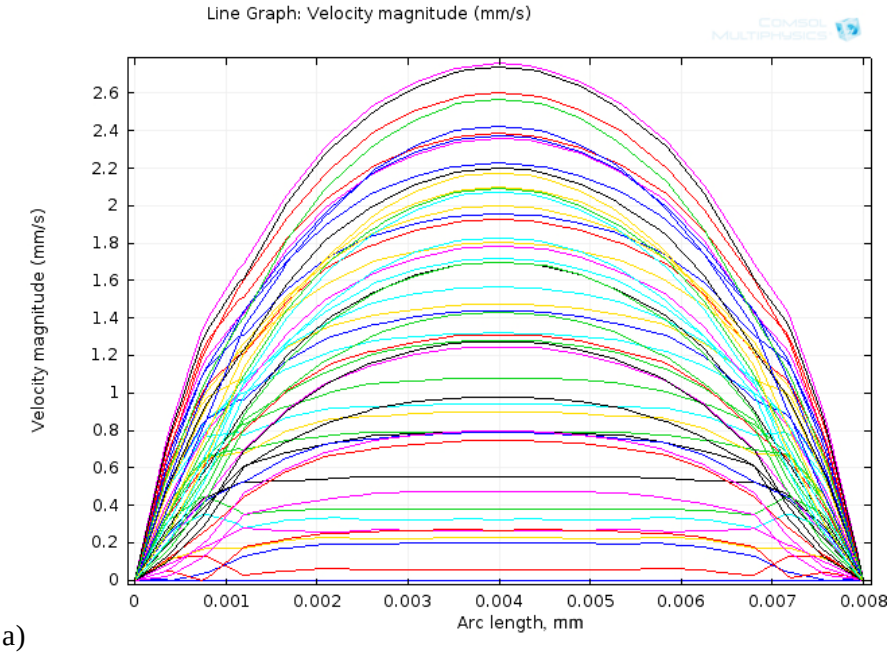

a)

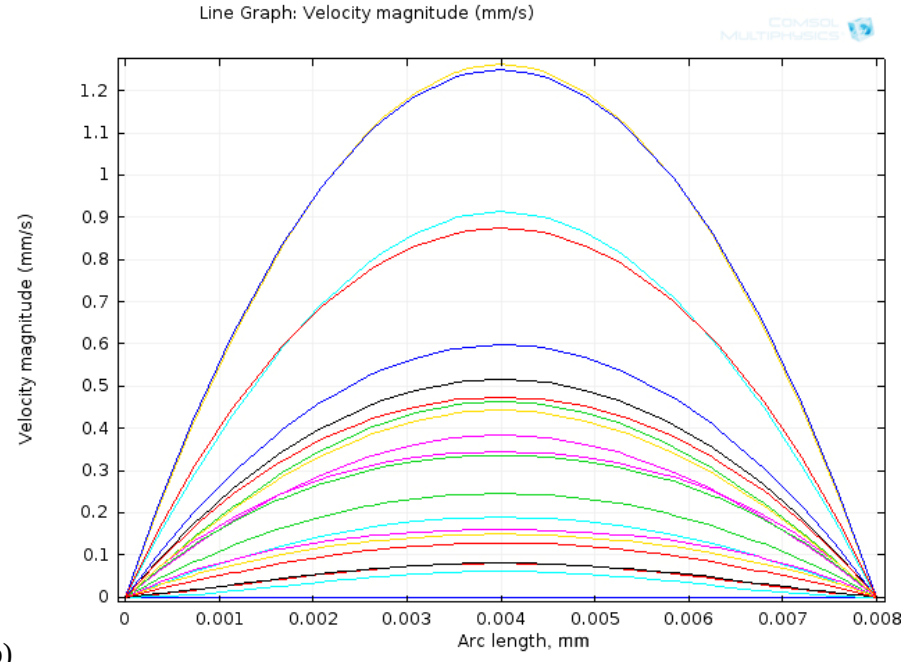

b)

Fig. 16. Fluid velocity fields during the vibration exposure of 4.3 Hz (a) and (b) 5.8 Hz frequencies and the amplitude of 6 mm.

Different microchannel diameters require different frequency and amplitude values in order to reach the same result of velocity changes and turbulent flow marks. These results were detected in the enhancing microchannel diameter up to 8 mm.

Therefore it is necessary to identify the purpose where the improvement of blood flow velocity would be the most effective and adapt the model to these findings.

The COMSOL Multiphysics was the proper choice for the simulation of the liquid flow in micro-channel imitating capillaries. The study made by Lythgo et al. [38] notes an increase of blood cell velocity of the femoral artery by 33 % on 10–30 Hz. Moreover, based on the findings of this study, it was mentioned that a vibration amplitude of 2.5 mm coupled with vibration frequencies in the order 5 – 20 Hz produced significant increases in leg blood flow. Our study obtained results that indicated the increase of momentum fluid flow velocity of more than 4 times on 4.3 Hz oscillations and 6 mm displacement. It could be argued that proper vibrations enhance blood circulation on separate vessels of human limbs and could be used as a method to enhance blood flow on diabetic limbs. No significant change in the fluid velocity were recorded on higher frequencies of 49 Hz with low displacement amplitude of <1 mm. The velocity field diagrams and spectrograms were comparable for oscillating micro-channels on the same frequencies and displacement values in both the experimental and computer modelling results. Similar results therefore leads researchers to use virtual model instead of experimental investigations in future studies. It was defined that the different micro-channels' diameters require different vibration values to enhance fluid flow rate. It is essential to choose proper frequencies on stimulating human limb capillaries. A computer modelling platform enables researchers to make investigations on shifting parameters with a less time consuming method. The human tissue analysis method [72] will be implemented with the purpose of individual excitation frequency identification.

Ability to increase blood flow velocity could be essential in solving blood circulation problems caused by diabetes mellitus. Momentum and average velocity increases were noted at the tube affected by the external vibrations. Studies made by Huang et al. [73] shows a significant decrease in red blood cell velocity in capillaries in diabetic mice. Considering that further investigations of the flowing erythrocyte in the vibrating arteriole and capillary are foreseen to be carry out. Different material properties of erythrocyte will be used with reference to biochemical changes in the membrane structure in type 2 diabetes mellitus [74] and unaffected erythrocyte.

Previous vibrational training influence studies were performed using vibrating plates with amplitudes ranging from 2 to 6 mm and frequencies ranging from 20 to 50 Hz [26, 28, 38, 39, 40, 41 & 42]. In most cases it is noticed that further studies on amplitude selection influence should be done. Martinez-Pardo et al. [75] had made a study investigating high and low amplitude effects on the development of strength, mechanical power of the lower limb, and body composition. They have found that high amplitude (4 mm) of whole body vibrational training a useful tool when looking for improved fitness and a full workout. Our study shows an increase in fluid flow velocity on major amplitudes as well, starting from 3.4 mm amplitude up to 8 mm. During the experiment, the highest velocity changes were obtained on measurements of 4.3 Hz and 6 mm, 5 Hz and 5.4 mm, 5.4 Hz and 8 mm, 4.8 Hz and 3.4 mm, 5.8 Hz and 6 mm. The studies, by using higher frequencies than 20 Hz coupling with low displacement amplitude (up to 1 mm), showed the results with non-significant

velocity changes. Based on these findings, further analysis was not conducted on higher frequencies.

2.2. Evaluation of red blood cell's natural frequencies

The red blood cell or erythrocytes is a biconcave shape cell and its mechanical properties mostly depends on membrane mechanical properties. Erythrocyte contains a constant volume of cytosol which is protected by the membrane. The high deformability of the membrane allows the RBC to float through the capillary, which has smaller diameter. The mean value of diameter of a healthy patient's erythrocyte is 7.34 μm and thickness ranges from 1.4 to 2.4 μm. The thickness of membrane is 200 nm [76]. The most reviewed studies analyse erythrocyte as a structure consisting of RBC membrane and cytosol liquid. In our case, a similar model has been designed and analysed.

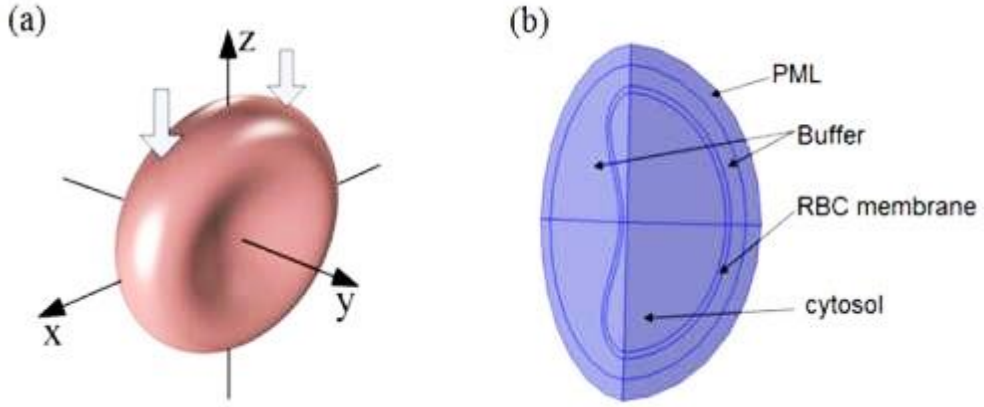

Fig. 17. Erythrocyte mechanical model (a) and composition (b) [82]

There are various studies where RBC's deformability is analysed [77, 78, 79, 80, 81] but the mechanical behaviour of the membrane is not clearly defined. Thus, the material properties of RBC's membrane can be found defined as Linear or Hyperelastic in a number of papers. Furthermore, different material models, like Neo-Hookean or Yeoh, are used. However, the majority of material properties are almost the same in most studies. The erythrocyte mechanical model has been designed by using SolidWorks software and then imported to COMSOL Multiphysics software (Fig. 18). The diameter of the model is 8.7 μm and the thickness is equal to 2.2 μm when the thickness of the membrane is 200 nm. λ and μ are the Lamé constants that describes the elasticity of the isotropic composite membrane. Generally, these parameters describe the viscoelastic response of the composite membrane to in-plane deformation [82]. The membrane is considered as a Hyperelastic material, Lamé coefficients have been defined regarding previous studies and is prescribed equally to 10^3 N/m^2 [83], in addition, both Lamé constants have been considered as equal ($\mu=\lambda$) [84]. Membrane as linear elastic material has been analysed because there are no findings that could clearly define its material properties and behaviour. The material properties of the membrane are listed in Table 1. Initial pressure of 5333 Pa has been prescribed pursuant to the blood pressure in the capillary (40 mm Hg). According to

various papers, the density of cytosol liquid is equal at 1200 kg/m^3 and the viscosity at 0.006 Pa s. In some papers, it is considered as eight times higher compared to water viscosity [85]. Thus, the water material has been defined and the parameter of Dynamic viscosity has been multiplied by eight. In the case of the study where RBC was placed into the liquid, the blood material properties have been defined for a surrounding liquid.

Table 1. Erythrocyte (RBC) membrane's material properties [86, 87]

Parameter	Value
Density	1100 kg/m^3
Poisson ratio	0.49 – 0.499
Young's modulus	4500 Pa

A number of different types of calculations have been used. First, Solid mechanics physics has been used for the analysis of the RBC's membrane natural frequencies. This type of study excludes the influence of fluid that reduces the natural frequencies of a solid body. Therefore, the Acoustic-Solid Interaction Frequency domain module has been used for the Eigenfrequency analysis of the fluid consistent model where cytosolic liquid has been taken into consideration. The desired number of eigenfrequencies calculations initially were set to 30, but according to the results this number was reduced to 20 for further calculations. After all, the RBC has been placed into the blood liquid to identify the changes of Eigenfrequency values depending on the medium. The cytosolic fluid has been considered as viscous fluid and the Bulk viscosity had to be prescribed. In the literature, it is noted that it may vary from 0.1 to 0.8 Pa s. The mean value of 0.4 Pa s has been prescribed. Blood's (37^o C) Bulk viscosity parameter was taken equal to 3.4 * 10^{-3} Pa s at the environmental temperature of 36.6^o C. The physics-controlled mesh of extremely fine grid has been selected.

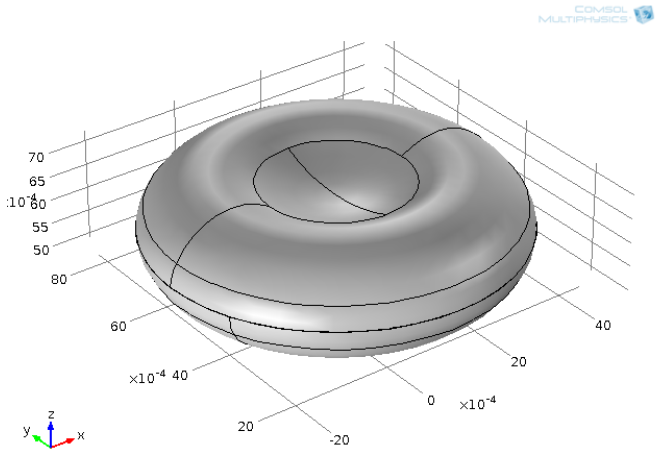

Fig. 18. Erythrocyte (red blood cell) model

The number of studies where RBC's rigidity were investigated provide findings of increasing rigidity of erythrocyte membrane in the case of diabetes mellitus or other

diseases. The consensus is unequivocal that the Young's modulus increases on diabetics. Thus converts the erythrocyte, as hardly deformable material, especially in the case of entering a capillary. The deformability is significantly lower as Young's modulus is much higher in diabetics compared with healthy patients [88]. In one study, an atomic force microscope has been used to investigate changes of Young's modulus on blood samples affected by diabetes mellitus. The results show that Young's modulus can increase greater than 3 times in diabetics patients compared with healthy ones [89]. The healthy patient erythrocyte is able to enter the microchannel of 3 µm considering that its non-deformed diameter is 7.5 µm (Fig. 19). Understanding the behaviour of the RBC's shape deformability (Fig. 19 c)) it was decided to investigate its natural frequencies and define displacements of the cell's membrane that would enable RBC to enter the capillary more fluently.

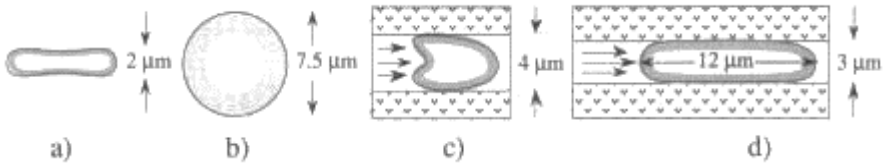

Fig. 19. Erythrocyte deformability [90]: a) RBC top projection (thickness); b) non-deformed RBC, front projection (diameter); c) partly deformed RBC (parachute form); d) fully deformed RBC in the narrowest capillary channel

First, the Eigenfrequency analysis has been performed on RBC's membrane, excluding the cytosolic liquid and the environmental parameters. The purpose of this study was to identify the deformability of the membrane, depending on the natural frequencies. It is known that the erythrocyte enters the capillary by bending and changing its disc form. The natural frequencies of the same or similar shape has been an objective of the Eigenfrequency analysis.

The results of the erythrocyte's membrane natural frequencies has been analysed. Shapes of deformed membrane could be compared to one at the moment of entering the capillary. These shapes have been identified on the frequency value of 2.01×10^5 Hz (Fig. 20 left) and 1.11×10^5 Hz (Fig. 20 right). No appropriate shape deformations were identified on lower frequency range values (up to 50 Hz).

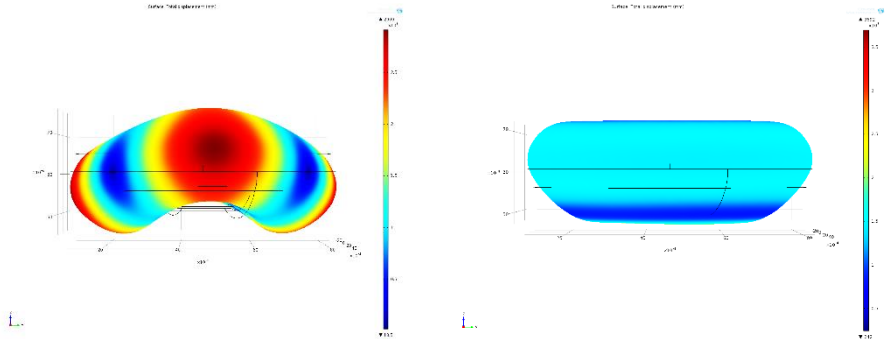

Fig. 20. Shapes of deformed erythrocyte at 2.01×10^5 Hz (left) and 1.11×10^5 Hz (right)

Further analysis has been conducted by using the Acoustic-Solid Interaction Frequency domain study. The model of this study contained cytosolic liquid, thereby the obtained results of frequencies and deformations of the membrane were different. First, the healthy patient's RBC has been analysed and the highest displacements of actual areas were obtained on 1.47 Hz.

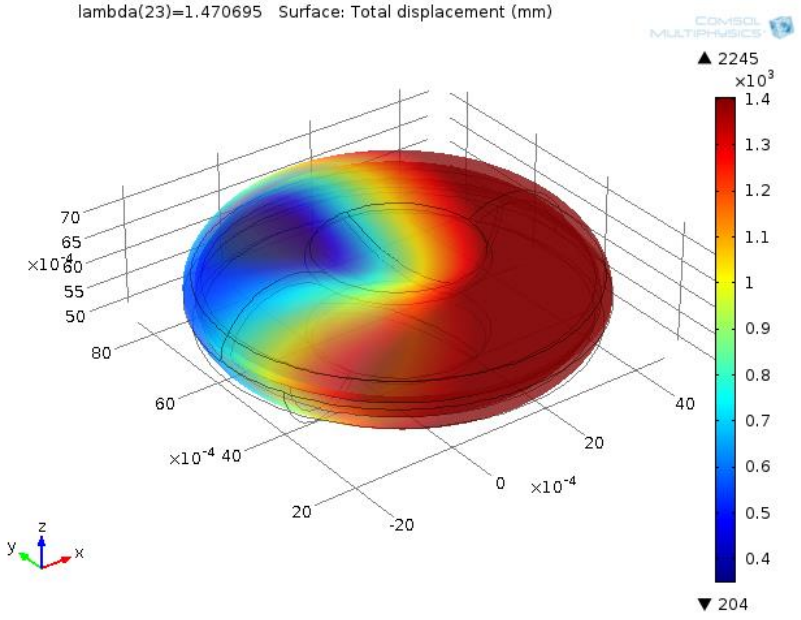

Fig. 21. Deformations of healthy patient erythrocyte at 1.47 Hz

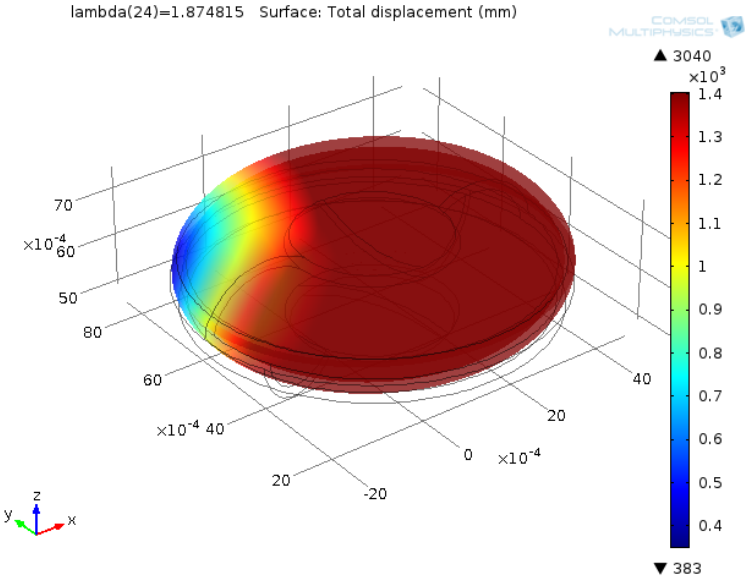

Fig. 22. Deformations of non-healthy patient erythrocyte with 3 times higher Young's modulus at 1.87 Hz

The higher values of the Young's modulus parameter increase the natural frequencies values. It can be obtained that the red blood cell may be deformed more fluently by affecting it with an external vibrational excitations of low frequencies. However, these results had to be compared with the immersed model that is more adequate to the natural environment. When the mechanical structures are immersed in a fluid, their natural frequencies are reduced. The fluid, as a source of damping, induces changes of the mode shapes, thus it was crucial to conduct this type of study. The problem was defined as a coupled acoustic-structure eigenvalue analysis and the damping was accounted due to the fluid viscosity by including a viscous loss term.

The model of erythrocyte comprising cytosolic liquid and immersed in blood has been designed (Fig. 23). A cylinder shape, imitating part of blood vessel, has been designed in which the erythrocyte model has been immersed.

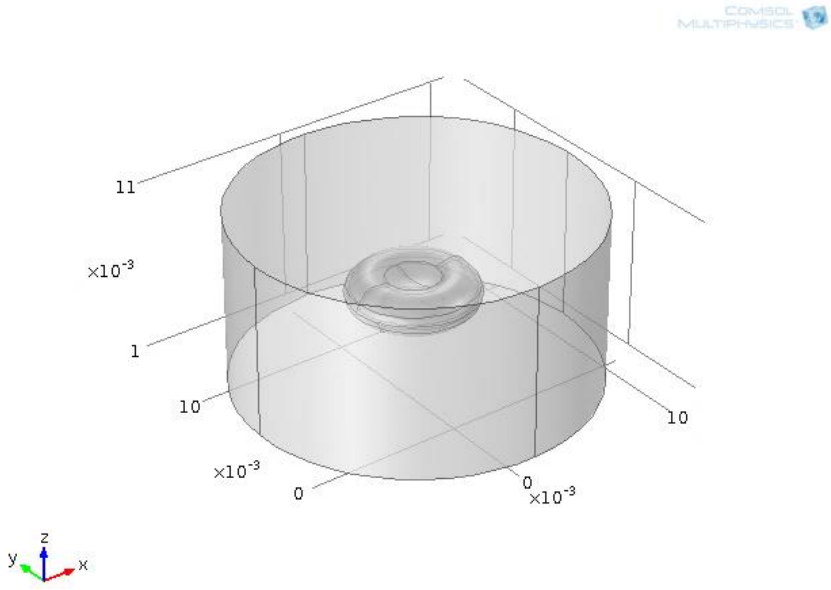

Fig. 23. Erythrocyte immersed in blood liquid

First, the analysis of natural frequencies has been conducted to a healthy patient erythrocyte. Next, the Eigenfrequency study was performed for a prescribed model with three times higher Young's modulus of 13500 N/m^2 [88]. The natural frequencies of 2.34 Hz (Fig. 24) were defined for a healthy patient erythrocyte as the most appropriate, by deforming RBC for a more fluent entrance to the capillary. The Eigenfrequency of 4.02 Hz (Fig. 25) of damaged erythrocyte with membrane material of a three times higher Young's modulus has been obtained. The natural frequencies of the disease affected patient erythrocyte vary from 0.4 Hz to 48 Hz according to calculations by changing the Young's modulus and Poisson's ratio.

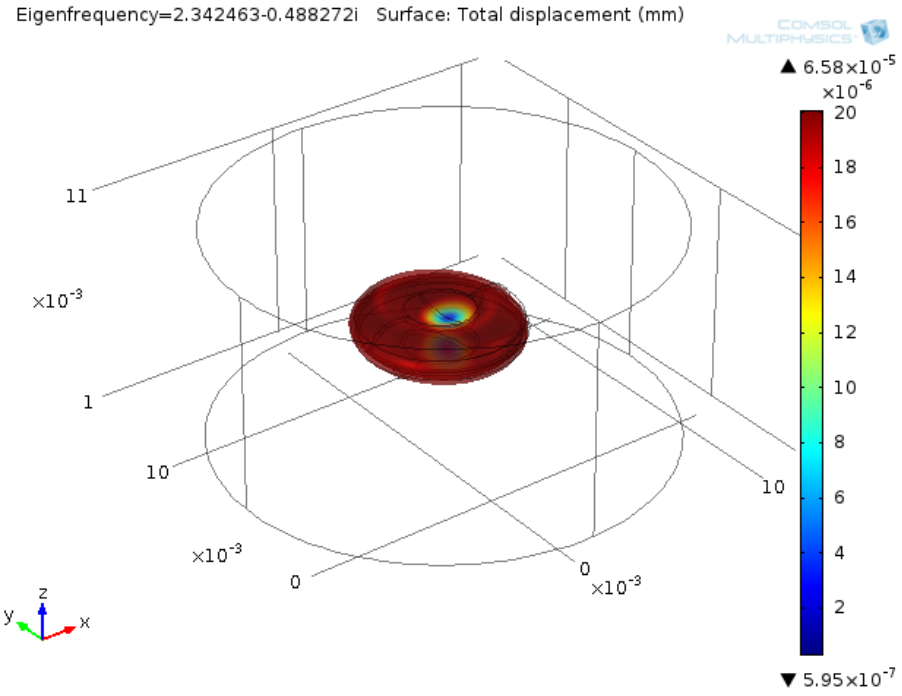

Fig. 24. RBC's displacement at Eigenfrequencies of 2.34 Hz

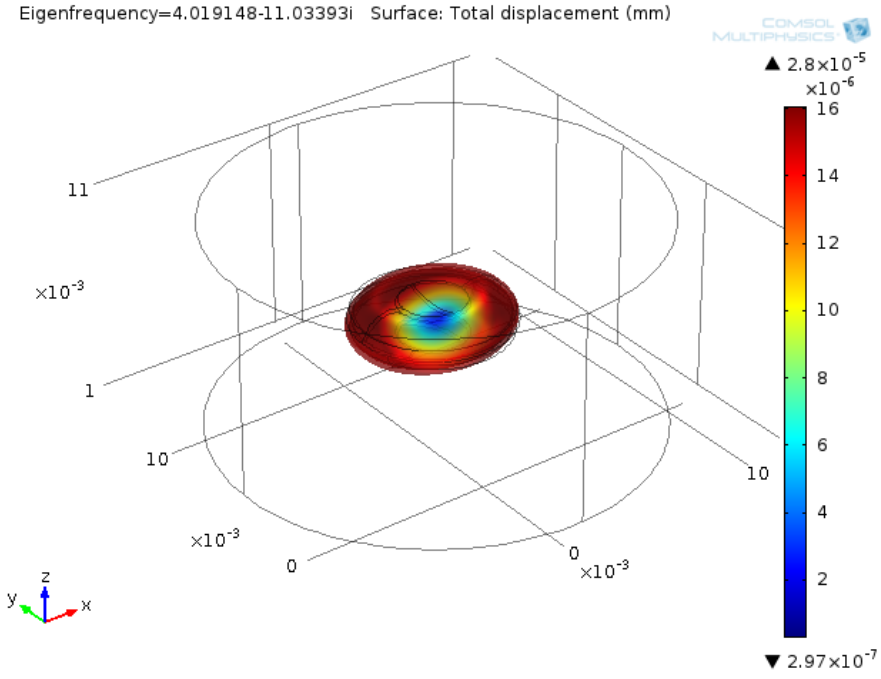

Fig. 25. RBC's displacement at Eigenfrequencies of 4.02 Hz

The results of the Eigenfrequency study have showed the RBC's areas of deformation at the lower frequency ranges. Basically the outer area of the membrane is mostly affected. This phenomenon could be compared to the natural deformations of RBC's by entering the capillary. The increase of deformability of the erythrocyte during the vibrational excitation on low-frequencies could be an effective way of rehabilitation for various diseases. Vibrational exposure is suggested as an approach of reduced friction in dynamics of the RBC's movement through the capillary. Therefore, further related investigations have been conducted.

2.3. Evaluation of RBC's deformability and maximum contact pressure alterations on the effect of vibrational oscillations

The red blood cell's flow by entering capillary has been analysed. Static and dynamic analysis has been conducted. A 2D model of immersed erythrocyte has been designed and a fluid-structure interaction study was performed. The RBC's membrane material property of Young's modulus has been changed during the different stages of investigation. A healthy patient erythrocyte of 4500 N/m^2 and a three times higher of 13500 N/m^2 for disease affected RBC has been used. In most papers, the erythrocyte's membrane is defined as hyperelastic material while in others as a linear elastic one. Studies of both different types of material of RBC's membrane has been conducted. To initiate RBC's deformability on the tapering channel, the contact pair parameter has been defined between the membrane's outer boundaries and capillary's walls. Inlet and outlet fluid boundaries were defined on the right and left sides of the model respectively. Yeoh mesh smoothing type and fluid as an incompressible flow was prescribed for this type of study. The erythrocyte's movement through the channel was defined by the function of prescribed displacement and using a displacement parameter to identify the steps of the stationary study. The erythrocyte model has been immersed in the model of fluid with material properties of blood. Initial experiments were made without oscillating the whole model. The maximum contact pressure parameter was observed on the contact pair erythrocyte membrane-capillary wall surface. Contact pressure analytically can be defined as a function on the x axis by the equation [91]:

$$P = \sqrt{\frac{F_n E'}{2\pi R'} \times \left(1 - \left(\frac{x}{a}\right)^2\right)} \tag{2.3.1}$$

$$a = \sqrt{\frac{8F_n R'}{\pi E'}} \tag{2.3.2}$$

Where F_n is the applied load per unit length, E' is the combined elasticity modulus, and R is the combined radius. The equations of combined Young's modulus and radius are listed below:

$$E' = \frac{2E_1E_2}{E_2(1-v_1^2) + E_1(1-v_2^2)}, \tag{2.3.3}$$

$$R' = \lim_{R_2 \to \infty} \frac{R_1R_2}{R_1R_2} = R_1 \tag{2.3.4}$$

Young's modulus of erythrocyte's membrane and capillary wall are defined by E_1 and E_2 respectively and R_1 is the radius of the erythrocyte upper part. The Penalty contact method has been used to assess the applied load at the contact boundary. This parameter can be expressed by using the local value of the contact gap distance variable g, constant penalty factor δ and an estimated contact pressure T_0:

$$T_n = \begin{cases} T_0 - Eh_{min}\delta g & if\ (g \le 0) \\ T_{0^e}^{-\frac{Eh_{min}\delta g}{T_0}} & otherwise \end{cases} \quad (2.3.5)$$

If the interference ($g<0$) occurs, the applied load is linearly increased using a penalty stiffness, the minimum element size on the contact pair boundary and a penalty factor δ. Using this method is not necessary to define an extra variable for the contact pressure.

The experiments with prescribed oscillating movement of the liner elastic part of the model had been conducted. Displacement of the oscillating part had been defined in the range of 5 mm to 2 cm with 5 mm steps. The main results are listed below (Fig. 26, Fig. 27, Fig. 28, Fig. 29 & Fig. 30).

The deformability of healthy patient erythrocyte during the stage of entrance to the capillary has been investigated. The maximum contact pressure on the surface of the RBC was observed. In Fig. 26, the entrance of healthy patient erythrocyte is shown with the value of a maximum contact pressure of 29.8 N/m^2. After increasing the stiffness of the RBC by three times, the maximum contact pressure increased by three times also, up to 89.4 N/m^2 (Fig. 27).

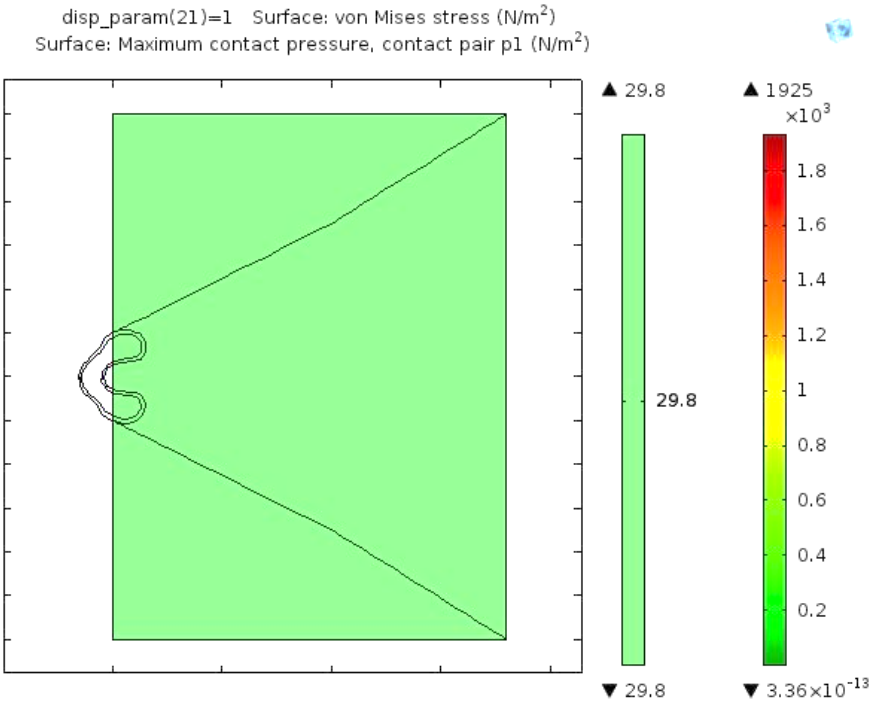

Fig. 26. Healthy patient RBC without vibrational oscillations

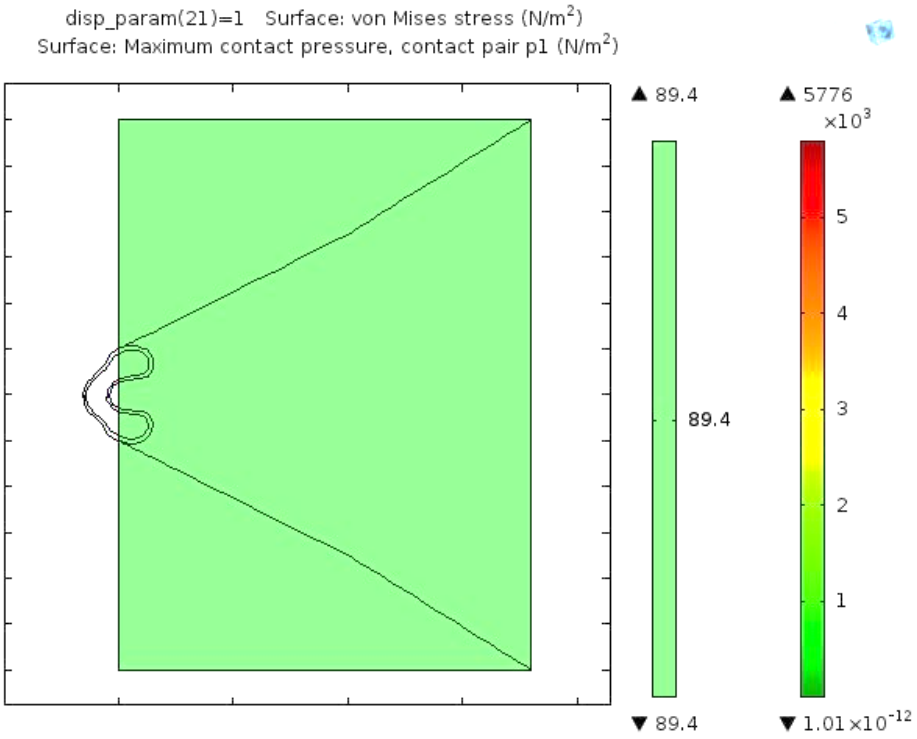

Fig. 27. Disease affected patient RBC without vibrational oscillations

The same parameters were investigated during the disease affected patient RBC's flow, by inducing vibrational oscillations to the model. First, the vibrations of 3 Hz frequencies and 5 mm displacement were prescribed. The maximum contact pressure has increased up to 95.9 N/m^2 (Fig. 28) at the same moment of entrance. The displacement has been increased by 5 mm. The mean of contact pressure increased up to 96.2 N/m^2.

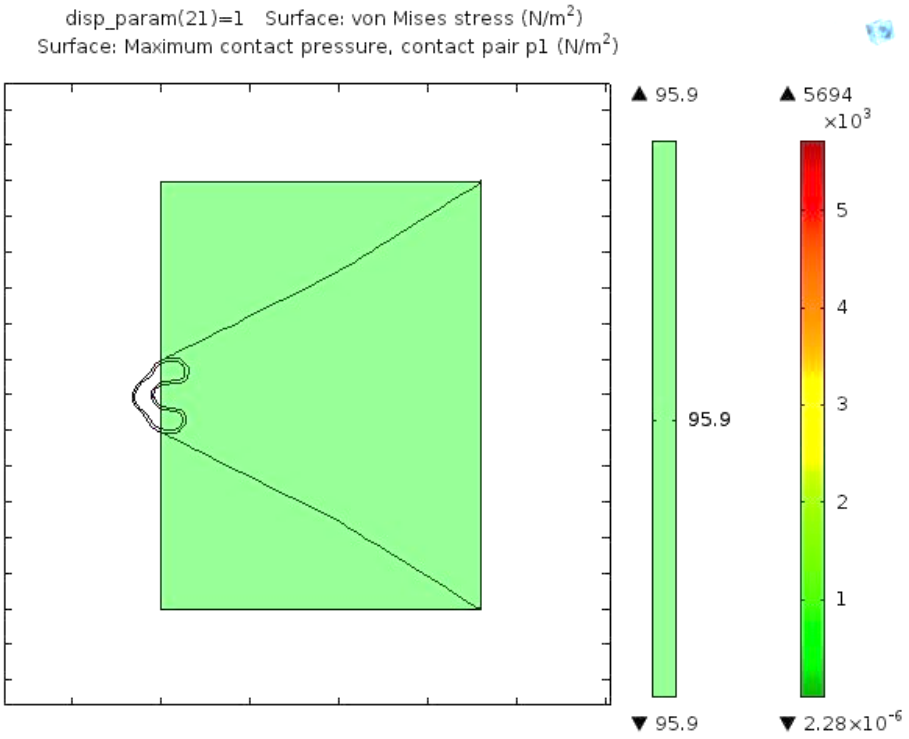

Fig. 28. Disease affected patient RBC on vibrational exposure of 3 Hz with 5 mm displacement

After increasing the displacement up to 15 mm, the monitored value had decreased and was equal to 87.3 N/m^2. This mean is lower compared to the non-vibrating model. Furthermore, enhanced displacement of the moving model by 20 mm had the lowest value of maximum contact pressure of 64.1 N/m^2 ,which is nearly twice higher compared to the healthy patient erythrocyte and 28.2 N/m^2 lower in proportion to disease affected patient RBC. However, by increasing the amplitude higher than 5 mm, negative results where contact pressure increased up to 104 N/m^2 were achieved. The monitored values of increased displacement up to 50 mm did not show any reduction of maximum contact pressure between the erythrocyte and capillary walls. It has been observed that the displacement ranging from 13 mm to 22 mm decreases the maximum contact pressure value and are desirable during the vibrational oscillations at a 3 Hz frequency. Moreover, the displacement in the range from 0.6 mm to 2 mm in tandem with a 4 Hz frequency obtained a decrease of maximum contact pressure by 41.2 N/m^2.

The other form of RBC deformation has been observed as well. Sometimes, pathological disorders affects the form of RBC. In this case, the erythrocyte without indentation in the middle of the body has been analysed. The maximum contact pressure values were higher, even during the natural entrance without affecting it by external vibrations (Fig. 30). Further analysis has to be done in comparison of different forms of the RBC and influence of vibrational excitation.

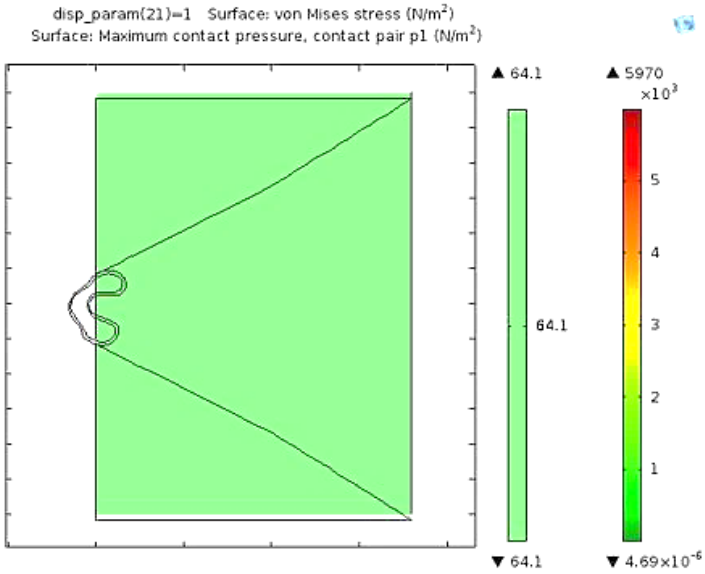

Fig. 29. Disease's affected patient RBC on vibrational exposure of 3 Hz with 20 mm displacement

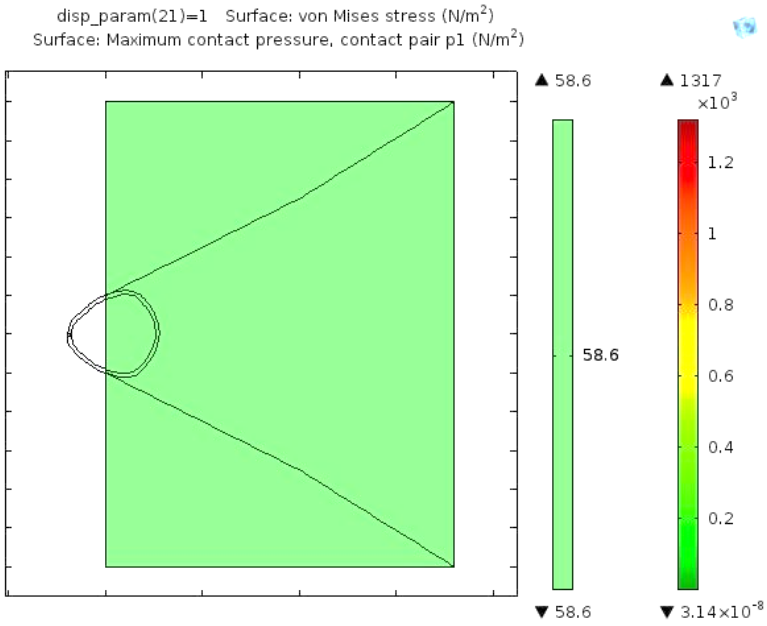

Fig. 30. Different form erythrocyte entering capillary without affecting by external vibrations

Similar results have been obtained on transforming the Hyperelastic material properties to the Linear Elastic. The values of the maximum contact pressure of stiffer

erythrocyte decreased in the range of 10 – 22 mm of displacement at the 3 Hz frequency. However, the decrease was significantly lower in all cases.

2.4. Section Conclusions

As it was noted before, the low-frequency vibrational excitations could be used for an improvement of human blood flow. However, there is a lack of numerical analysis studies made on investigating the cause of positive effect. Thus, meeting the objectives of research; the blood flow on the microchannel of capillary and erythrocyte's deformability analysis has been made by using the COMSOL Multiphysics software.

Designed models of micro channel and erythrocyte enables researchers to make an analysis of the external mechanical vibrations influence on blood flow velocity and deformability of the body structure. Furthermore, the deeper mechanical analysis of micro cells can be executed by investigating Eigenfrequencies and its dependence on various input parameters of the model.

The numerical simulations performed throughout the research may be grouped in a few case studies: i) Evaluation of fluid flow improvement in the micro channel due to vibrational excitation; ii) Evaluation of RBC's natural frequencies depending on changes of material properties of rigidity; iii) Evaluation of erythrocyte's deformability improvement by using external vibrational oscillations.

Main conclusions drawn from the numerical simulation results are the following:

- COMSOL Multiphysics modelling results of the blood flow through the results enables reliable use of computer models for further studies. Numerical analysis showed that low frequency (from 4 to 8 Hz) and higher amplitude (from 3.4 to 8 mm) of external vibrations could significantly increase blood flow. However higher frequencies combined with lower amplitudes did not give similar results. The beating phenomenon method could be used for creating the prescribed vibrations on a human's limbs.
- Three types of natural frequencies' analysis has been done for the erythrocyte's membrane: as a solid model without interaction with liquid; as a solid containing cytosol and as an immersed solid containing cytosol. The Eigenfrequencies' studies of immersed erythrocyte have shown that lower frequencies could be used in the case of deformability of morbid RBC. The frequencies of 4.02 Hz affect the outer areas of the cell, thus provides higher deformability of the membrane with enhanced rigidity. Further analysis should be done in case of clearly defining the erythrocyte's material properties.
- Healthy and disease affected erythrocyte's entrance to the capillary study has been conducted. The results showed that vibrational excitations of 3 Hz frequency, coupled with the displacement ranging from 13 to 22 mm, lowered the maximum contact pressure value by 28 % at the contact of the erythrocyte's and capillary's wall in the study of RBC with three times increased stiffness. The maximum contact

pressure increased when higher displacement than 22 mm occurred during the same frequency vibrational excitation. The lower displacement in a couple with 4 Hz frequency obtained a decrease of the maximum contact pressure by 54 %.

According to the results of the experiments, it was decided to develop a vibrating bracelet for experiments on a human's hand. Identified motor regimes will allow researchers to generate the correct vibrations when using them on a human's limbs. This would allow researchers to gather the physiological parameter changes. Next, it is planned to make an investigation of blood circulation with a leg vibrating machine.

The vibrating bracelet device and vibration training machine for legs are developed and will be used for further experiments with humans suffering from diabetes mellitus. Identification and computation methodology of rheological properties [72] of the human body surface tissue will be integrated to choose the proper frequency for every person. The results of the planned studies will enable researchers to identify the proper and optimal limb frequency of each person individually.

3. DEVELOPMENT OF BLOOD FLOW IMPROVEMENT ACTUATORS

An overview of the existing applications of vibrational technologies in the healthcare field have provided an understanding of the needs and manner to solve problems of blood flow disorders. Accessible means are designed for different problems but all have relations with issues of insufficient blood circulation. In most cases, the vibratory movement of higher than 20 Hz frequency is used. This is the most significant difference separating the suggested approach from the existing solutions. Side effects to long-term vibration exposure to the internal organs are well known. Considering this, it was decided to develop devices by using locally adopted technological solutions. With the importance in mind of sufficient blood flow, especially in limbs, the devices have been developed for these human body parts actuation.

The importance of safety issues has to be considered in the case of development of human body interacting devices. Low voltage electrical components have been selected, ensuring assessment of possible injury issues. The accessibility dimension for people with disabilities was estimated in the cases of Arthritis or Diabetes mellitus.

From the technical point of view, sufficient and directly transferred force were the main issues to solve. Low-frequency vibrational excitations by generating considerable displacement was the main aim. Furthermore, the vibrational actuation should be transmitted directly to the limb, avoiding any loses so the source components should be coupled motionlessly with the excited part of human body.

Size and weight of the developed actuators were also relevant. The importance of usability at home, as well as transportation, were extremely high. Transportation matters are crucial, because the treatment of circulatory disorders should be performed daily. Furthermore, the device control has to be simple, without the need of any specific knowledge. Safety issues should be considered, therefore the rotating and electrical parts have to be covered to eliminate human interaction.

The aim of previously conducted numerical research was to define the proper working range of vibrational exposure devices for a solution of specific problems of blood flow disorders. The extraction of concentrated axial vibrations through the interaction with specific parts of human body, which have various degrees of freedom, has been taken into consideration as the most important issue. The variability of weights of human body parts has been calculated and estimated in the case of providing sufficient vibrations. Improvement of the quality of life for people with diseases of circulatory disorders is the main purpose of the developed actuators.

3.1. Actuator for the human hands

Stimulation of blood circulation by external vibration should be from one to two minutes. As it was noted previously, the low frequencies are considered more efficient to improve blood flow than high frequencies. But the additional higher frequency component on the main low frequency is suitable in many cases. As capillaries are considered as the “second heart” the mechanical vibrations could be useful for the human limbs actuation and the intensification of the blood circulation in the human body. Sufficient force has to be generated in the case of vibrational excitation on

human limbs. To ensure low frequency vibrations and higher than 1 mm limb amplitude, the beating phenomenon has been considered as the most appropriate. Otherwise, high voltage and heavy motors have to be selected in the case of aspiration of low-frequencies.

The beating phenomenon [92] occurs when two harmonically oscillating pendulums (signals of their vibrations are shown in Fig. 31, a and b of slightly different frequencies are impressed on a body. They are a periodic variation in vibration at a frequency that is the difference between to two frequencies.

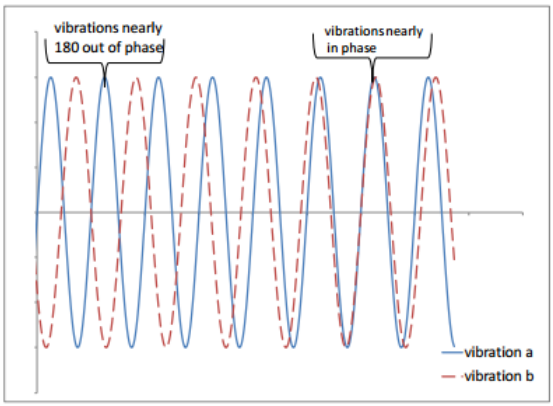

Fig. 31. Beating phenomenon occurrence [92]

The beating phenomenon enables the transfer of energy in to the system where low-frequency vibrations could be induced by coupling two high-frequency sources. The beating phenomenon is part of the classical theory of mechanical vibrations, but its beneficial facilities are not widely used in contemporary technologies. The equation of motion of the pendulums without damping can be acquired from the equation [93]:

$$\begin{bmatrix} 1 & \mu\alpha\mu \\ \alpha & 1 \end{bmatrix}\begin{bmatrix} \ddot{x_1} \\ \ddot{x_2} \end{bmatrix} + \begin{bmatrix} \omega_1^2 & 0 \\ 0 & \omega_2^2 \end{bmatrix}\begin{bmatrix} x_1 \\ x_2 \end{bmatrix} = \begin{bmatrix} 0 \\ 0 \end{bmatrix} \quad (3.1.1)$$

where, μ mass ratio,ω_1 – natural frequency of the structure and ω_2, - is the natural frequency of the damper, x_1 and x_2 – systems' displacements,

The modal frequencies of this system are given by:

$$\bar{\omega}_{1,2} = \sqrt{\frac{\omega_1^2 + \omega_2^2(1+\mu) \pm \Pi}{2(1+\mu-\alpha^2\mu)}} \quad (3.1.2)$$

where $\Pi = (\omega_1^2 - \omega_2^2(1+\mu))^2 + 4\omega_1^2\omega_2^2\alpha^2\mu$

The parameter α is responsible for the beat phenomenon.

If the primary and the secondary systems are damped, equation of motion applies:

$$\begin{bmatrix} 1 & \mu\alpha\mu \\ \alpha & 1 \end{bmatrix}\begin{bmatrix} \ddot{x_1} \\ \ddot{x_2} \end{bmatrix} + \begin{bmatrix} 2\omega_1\zeta_1 & 0 \\ 0 & \omega_2^2\zeta|\dot{x_2}|/4g \end{bmatrix}\begin{bmatrix} \dot{x_1} \\ \dot{x_2} \end{bmatrix} + \begin{bmatrix} \omega_1^2 & 0 \\ 0 & \omega_2^2 \end{bmatrix}\begin{bmatrix} x_1 \\ x_2 \end{bmatrix} = \begin{bmatrix} 0 \\ 0 \end{bmatrix} \quad (3.1.3)$$

where ζ is the head loss coefficient and g gravitational acceleration. This equation can be numerically integrated at different levels of the ζ coefficient. The

graphical interpretation of the differences of the beat response and head loss coefficient are shown on Figure (Fig. 32).

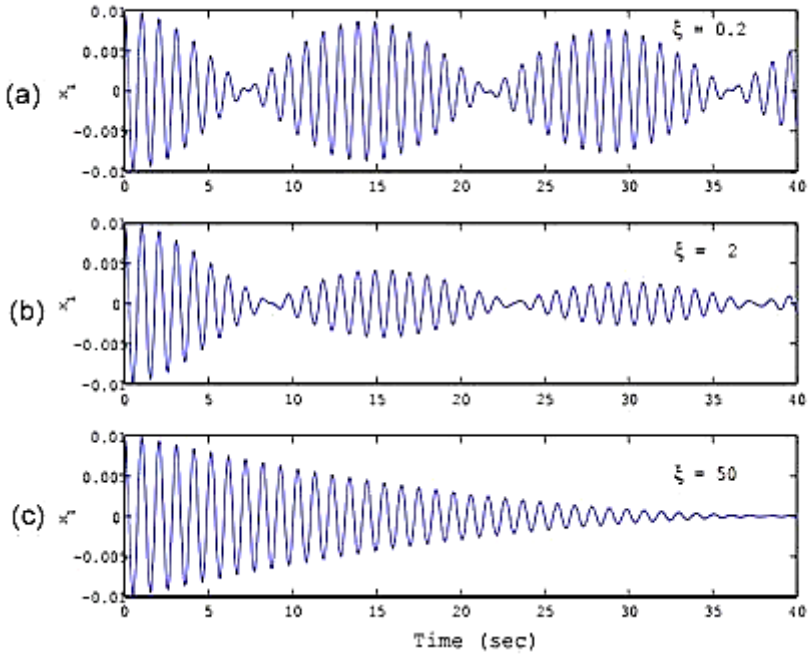

Fig. 32. Time histories of response for ξ= 0.2 (a), 2 (b) and 50 (c)

In the case of low-vibration exposure on the human limbs, the induction of the beating phenomenon has been chosen as the most suitable approach. To generate sufficient force to the limbs, the proper apparatus had to be chosen. In this case, the force induced while beating was calculated before selecting the electromechanical motors and designing unbalanced masses. It was considered that the average weight of handbreadth of the human hand is about 400g, therefore the sufficient generated force has to be at least twice as higher. As the proper vibrating motors with unbalanced masses were not found on the market, it was decided to choose an existing motor and to design the unbalanced mass. In the case, two vibrating motors for beating phenomenon and the calculated mechanical parameters were divided by two. Avoiding possible harm to the human body, high frequencies of the rotating unbalanced masses have not to exceed 100 Hz.

It was considered that a spring-mass system was constrained to move only in a vertical direction and excited by unbalanced rotating mass (Fig. 33). Here x is the displacement, m is the mass of the eccentric and r is the distance from the motor shaft to the centre of the eccentric mass (r is usually called eccentricity e), ω is the angular velocity, M is bulk mass of the whole system and F_0 is the constant load. Then the equation of motion is:

$$(M-m)\frac{d^2x}{dt^2}+c\frac{dx}{dt}+kx=F_0\sin(\omega t) \tag{3.1.4}$$

The generated force can be calculated from the simple equation below:

$$F=mr\omega^2 \tag{3.1.5}$$

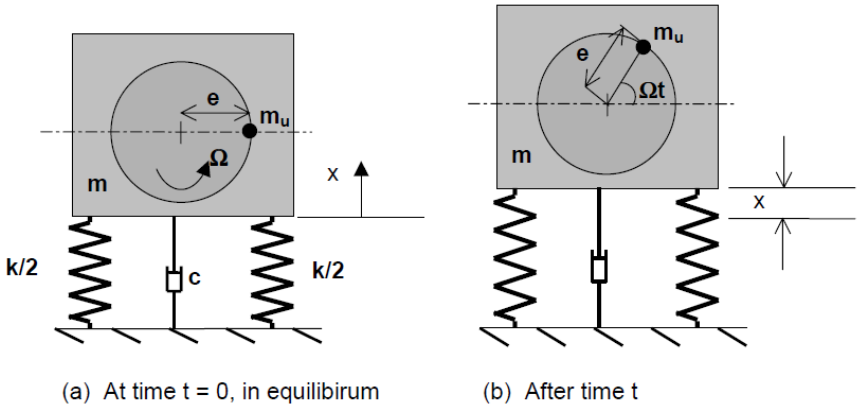

Fig. 33. Scheme of the motor with unbalanced mass system on the shaft [94]

It has been calculated that the angular speed of the motor should be equal or higher than 2000 rpm. The upper limit of this speed is desired up to 5700 rpm. In this range of operation, the force induced by the beating phenomenon can be ranged from 6 to 42 N.

According to the calculations, overall dimensions and electrical parameters, the JOHNSON 20703 electromechanical motors were chosen as most eligible. Below, the main parameters of this motor are given (Table 2).

Table 2. JOHNSON 20703 motor parameters

Name	Value
Voltage	3-13 V
Current	0.24 A
RPM	2989-5977
Rotor dimensions	13 x 2 mm
Motor dimensions (LxØ)	31 x 24 mm

For human handbreadth excitation the vibrating bracelet was developed for disable people as a tool for executing this exercise without any muscle effort. It could be useful for healthy people to simplify this exercise and enhance concentration on vibrational training in eliminating actuation of muscles. The main part of the vibrating bracelet consist of two small size, low voltage vibrating motors with unbalanced masses creating the beating phenomenon..

Beats were observed when two sine functions with near-equal frequencies were superimposed. When frequency ratio $r \approx 1$, the forced solution for two superimposed frequencies is approximately [92]:

$$x(t) = \frac{2F_0}{m}\frac{1}{\omega_n^2 - \omega^2}\sin(\frac{\omega - \omega_n}{2}t)\cos(\frac{\omega + \omega_n}{2}t) \quad (3.1.6)$$

Where ω frequency, t time, F_0 force amplitude, m – mass, $x(t)$ – mass displacement.

Therefore, no data was given according to the motor's RPM dependence on voltage. These parameters are crucial in the case of calculating the force created by the rotating unbalanced mass. Furthermore, the load of the unbalanced masses modifies the factory provided parameters. To identify these parameters a short experiment was made and RPM values have been registered at different voltages. The means were registered with photo tachometer / stroboscope Lutron DT-2259 [95].

The vibrational oscillations can be created by making unequal allocation of mass around an axis of the rotor. It is called a rotating unbalance when the centre of mass does not match the geometric axis. The moment caused by unbalance initiates a vibratory movement thus generating oscillations and displacement of the rotations' source. To initiate this phenomenon, two identical masses were made to be mounted on the rotors of the selected electromechanical motors. Unbalance mass was designed by using Solidworks software and was made from AISI 1020 steel. The aim of the beating phenomenon was to create a force higher than 7.85 N by using small sized and lightweight electromechanical motors. Therefore, masses were limited by the free area next to the second unbalanced mass. The main parameters of the unbalanced masses are given below (Table 3).

Table 3. Unbalance mass parameters

Parameter	Value
Bulk mass	14.86 g
Mass without unbalance	5.95 g
Unbalance mass	8.91 g
Whole diameter	7.5 mm
Diameter without unbalance	4.5 mm
Diameter by the middle of unbalance	6 mm

For the evaluation of eligibility, a special experimental set up was made whose structural scheme is presented in Fig. 34. Two motors were fixed together linearly on the cantilever without any possibility to move relatively to each others direction, even at high level vibrations. The motors were screwed on the glass-cloth laminate (HGW) cantilever. The cantilever's fixing holes were drilled at different lengths (50 mm and 100 mm) to observe alterations of vibrations regarding the cantilever length. Motors were screwed at the end of this cantilever in a position to generate a vertical force. Primary experiments were made without using any damping element. Later on, a damping box package of water and air was created for further experiments to eliminate any possibility of cantilever resonance (Fig. 35). Inductive sensor IFM IG6084 was used to measure the cantilever's frequency and displacement. The data was registered

by using the Oscilloscope Picoscope 3424 and the PC software 'PicoScope 6'. Motors and vibrations measuring sensors were fed by three power suppliers.

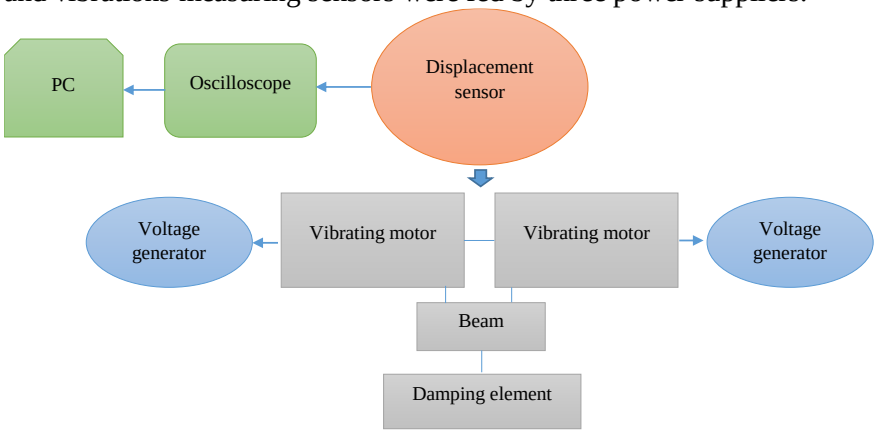

Fig. 34. Structural scheme of the vibrating platform and measuring elements

Fig. 35. Vibrating motors (3) on the cantilever (2) with damping element (1) and displacement sensor (4) on the top

The rotor's RPM alterations on the supplied voltage was investigated. The experiment was conducted by starting the motor's rotations at 4 V with registered 1370 rpm. The value of RPM has been registered at every 0.5 V. Angular speed was increased by approximately 200 rpm. At the peak value of 16.5 V, the motor's rotor had reached nearly the highest mean that is noted in the datasheet – 5960 rpm (Fig. 36). The collected data enabled researchers to make calculations of the generated force during the beating phenomenon. These parameters are essential for the evaluation and selection process of the availability of the electromechanical motors.

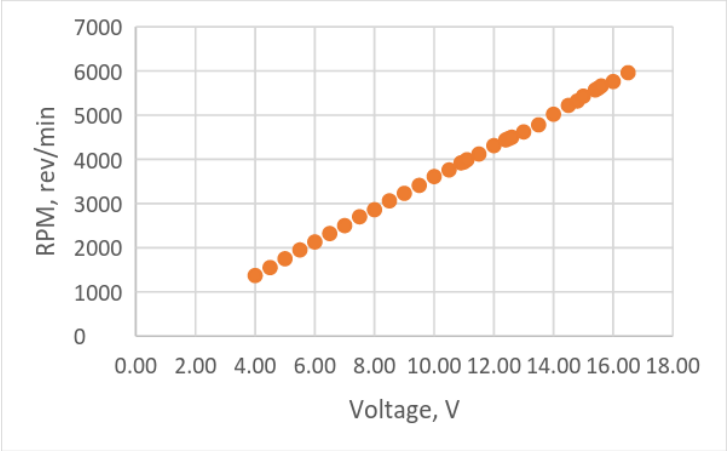

Fig. 36. Electrical motors RPM dependence on voltage

Next, an experiment with one motor fixed on the cantilever was made with the purpose of investigating its generated force. The gathered data on different voltage values disclosed that the vibrating frequencies remain stable independently from the supplied voltage and RPM values. The value of 25 Hz was calculated by using a shorter cantilever (50 mm length) at a voltage range from 4 to 6.5 V (Fig. 37). In the case of using a damping element and when the system is out of resonance, one motor was not able to generate sufficient force that would be high enough to cause cantilever vibrations. The values of the measured vibrational frequencies' were different with the longer cantilever (100 mm length), but they were not analysed deeply because of the presence of resonance. Therefore the usage of one motor is insufficient for wrists excitation purposes.

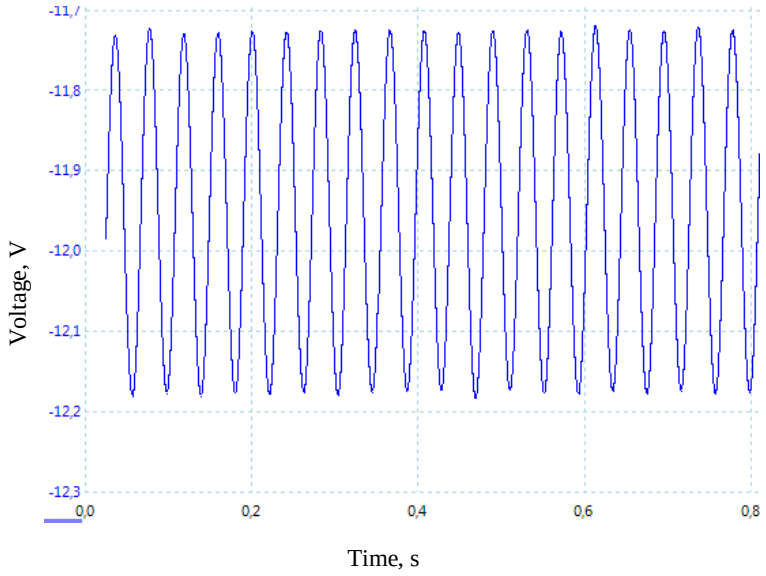

Fig. 37. One motor vibrations without beat phenomenon at 24 Hz frequency

After the completion of experiments with one motor, another motor was fixed on the top of the cantilever. The most appropriate results were collected during experiments with two motors and using higher than 10 V voltage values (Fig. 38). Supplied lower voltage values were insufficient to exceed the cantilever's resonance. The cantilever without the damping element was actuated in the range of displacement of 13 mm on the beating phenomenon. The oscillations frequency from 2 to 10 Hz was obtained. The beating phenomenon is clearly noticeable from the curves below (Fig. 38). This phenomenon occurred after the vibrating motors have generated enough force to surpass the cantilever resonance.

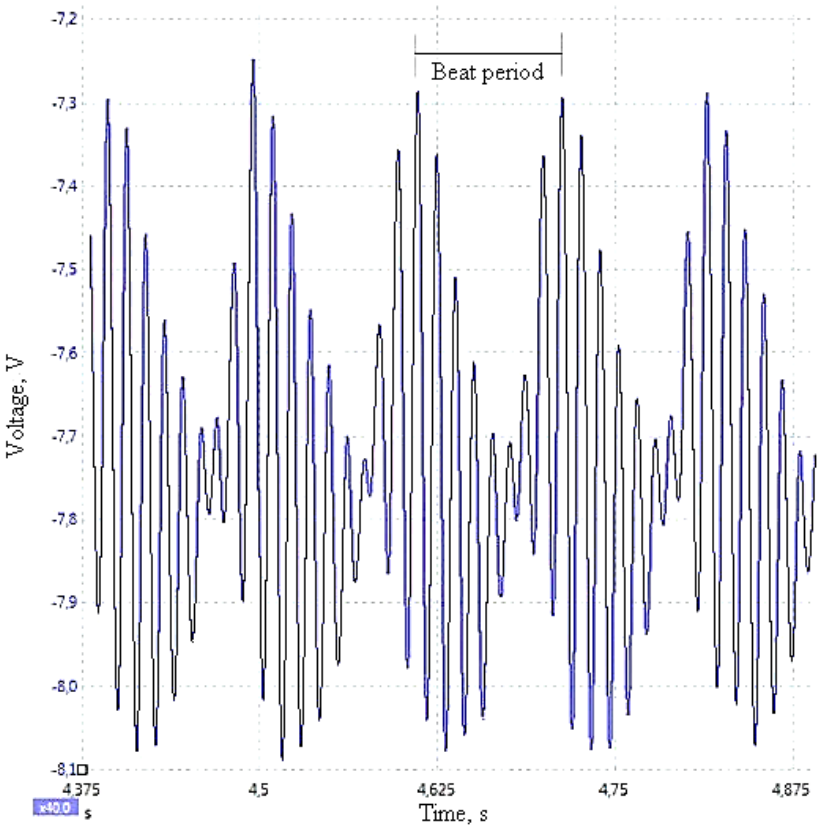

a)

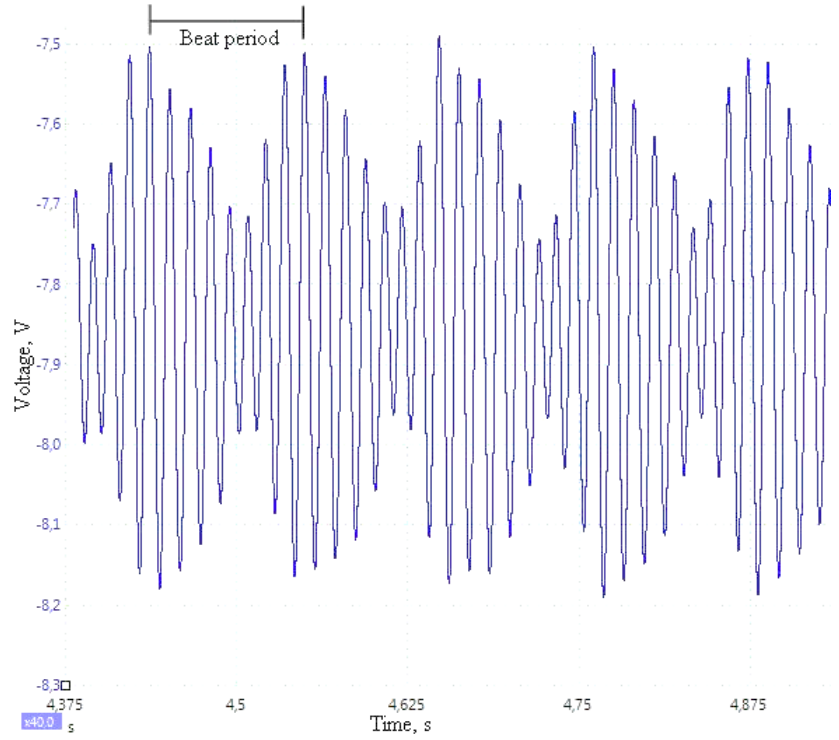
Beat period
-7,5
-7,6
-7,7
-7,8
-7,9
-8,0
-8,1
-8,2
-8,3
Voltage, V
4,375
4,5
4,625
4,75
4,875
x40,0
s
Time, s

b)

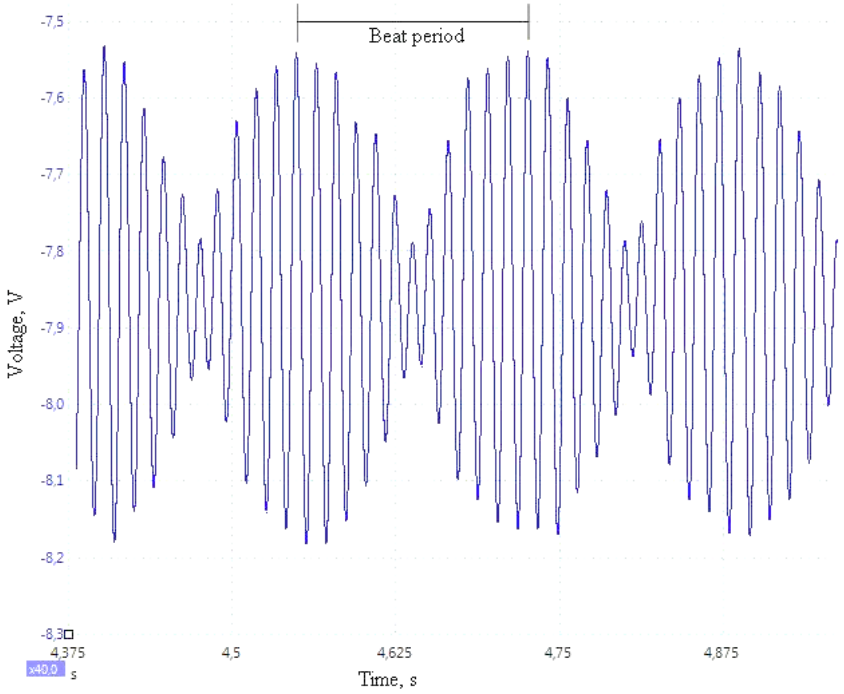
Beat period
-7,5
-7,6
-7,7
-7,8
-7,9
-8,0
-8,1
-8,2
-8,3
Voltage, V
4,375
4,5
4,625
4,75
4,875
x40,0
s
Time, s

c)

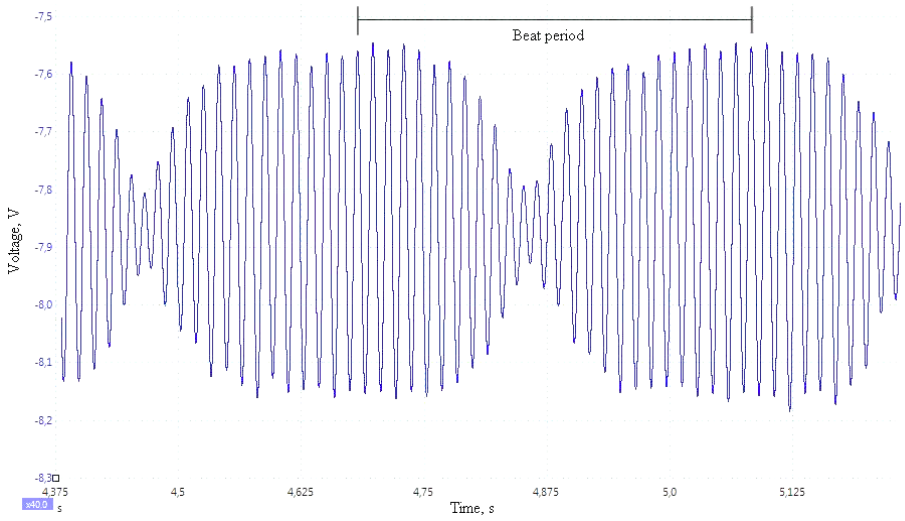

d)

Fig. 38. Two motors vibrations without damping: a) at 10 Hz (14.5 V – 11 V); b) at 8 Hz (12.5 V – 10 V); c) 6 Hz (12 V – 10 V); d) 2 Hz (11.5 V – 10 V).

However, it has to be taken into consideration that the human wrist is made from various connections, joints and tissues, which causes damping. Especially if wrist is held raised and has no fulcrum except the shoulder joint. Therefore, it is necessary to investigate the cantilever's frequencies by using a damping element. It is essential to find a working regime that would allow the device to generate oscillations independently on the wrists position or weight.

Further experiments with a damping element have shown that electromechanical motors with unbalanced masses generate sufficient force to overcome the damping force and the system was not allowed to enter in to the resonance stage (Fig. 39). All observations were obtained only when the beating phenomenon occurred. During the measurements on the beating phenomenon, the amplitude of the cantilever's movement reached 5 mm. This value is even higher compared to the existing solutions. Investigations of the influence on displacements' and frequencies' has to be done subsequently. However, these results have confirmed the assumptions that the designed cantilever platform could be used for further experiments without the necessity of using human body parts.

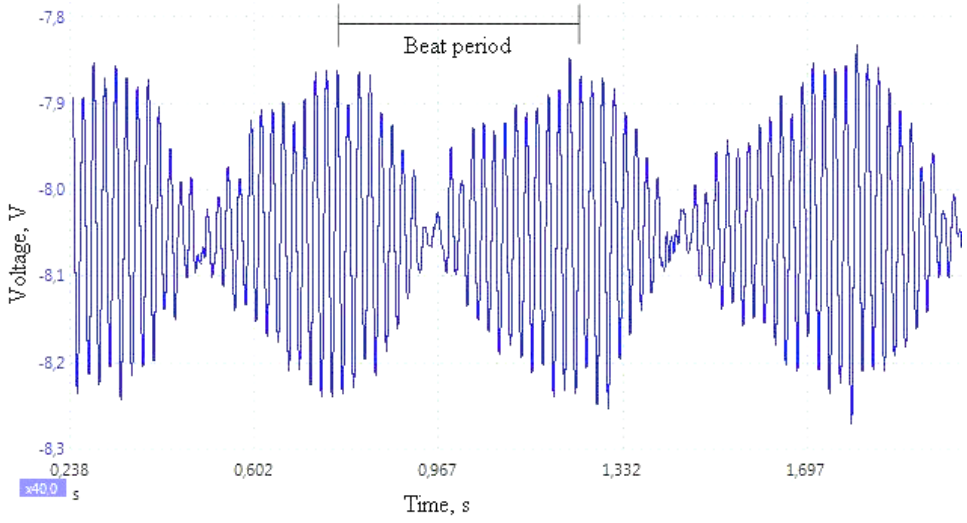
Beat period
-7,8
-7,9
-8,0
-8,1
-8,2
-8,3
Voltage, V
0,238
0,602
0,967
1,332
1,697
x40.0
s
Time, s

a)

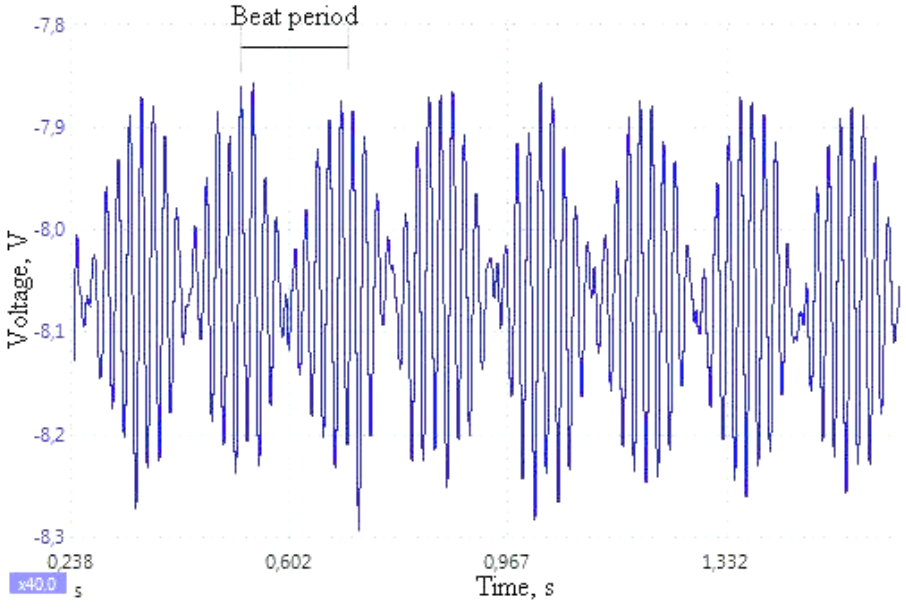
Beat period
-7,8
-7,9
-8,0
-8,1
-8,2
-8,3
Voltage, V
0,238
0,602
0,967
1,332
x40.0
s
Time, s

b)

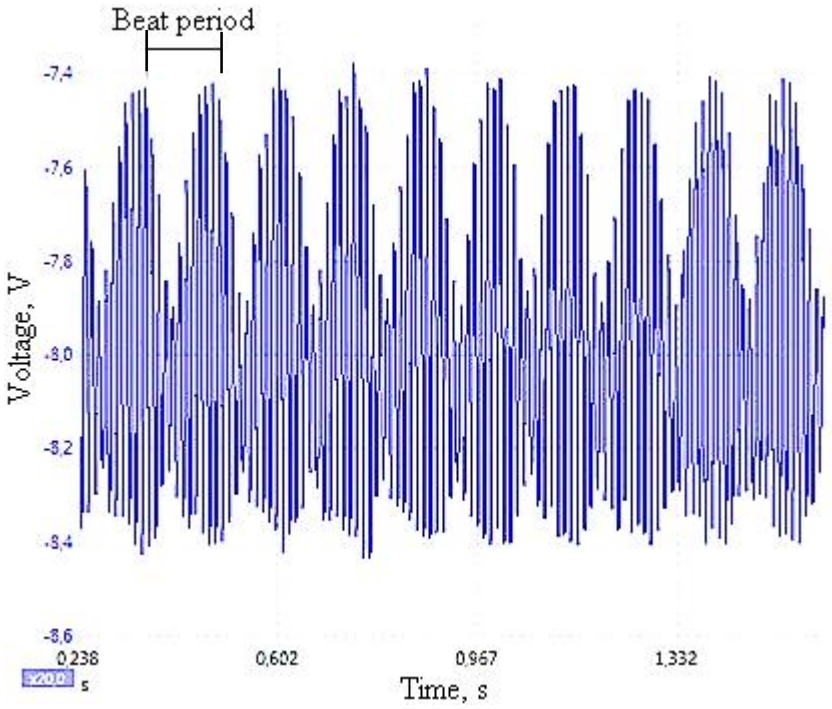

c)

Fig. 39. Two motors vibrations with damping: a) at 2 Hz (8V – 8 V); b) at 6 Hz (9.5 V – 8.5 V); c) at 8 Hz (14.8 V – 14.8 V)

Furthermore, the exciting force calculations have been conducted for each voltage combination in studies when the damping element was used. The values were divided into three groups according to the higher frequency value that could be used without harm to a human's internal organs or separate body parts [96]. The first group of values were up to 50 Hz, second – from 51 Hz to 80 Hz and third, from 81 Hz to 100 Hz. The calculated range of vertically generated force for the first group is from 3.31 N to 11.54 N by using two vibrating motors. The force values for the second group started from 12.32 N and increased to 28.08 N. The third group values were distributed in the range from 26.29 N to 41.48 N. Values from the first, safest group are high enough to generate vibrational oscillations on a human's wrist. The means were defined as sufficient to select the motors for the development of a vibrating bracelet prototype. This is a new approach of implementation of low frequency vibrational methodology with the purpose of stimulating blood circulation in human wrists. Similar technology of using two electromechanical motors has been claimed in previously described patent US 4570616 A [59]. The main difference of the application of the beating phenomenon in these cases is that the patented object consists of connected unbalanced disks, unlike the suggested approach. Furthermore, the proposed methodology enables the shift between different frequency values without the need of changing the unbalanced masses. At the end, the patented device was designed specifically for massage purposes.

The prototype of a vibrating bracelet device has been designed with the purpose of transferring the vibrational force perpendicularly to the palm and fingers of a human hand. The position of the vibrational actuator has been selected to minimize biomechanical damping elements (for example, wrist joint) and induce maximum oscillations to the palm and fingers. The virtual model of the prototype is shown at Fig. 40. The bracelet comprises of two vibrating motors with inwardly rotating motors relative to one another. Consequently this approach enables the device to induce vertical vibrational movement at the Y axis as it is shown at Fig. 40.

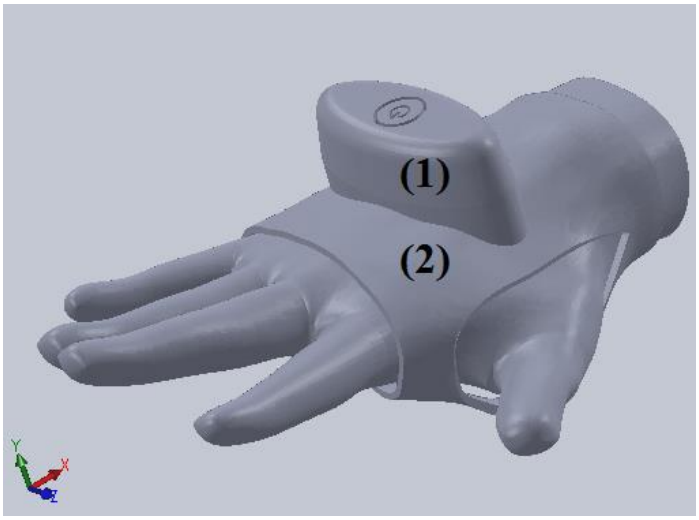

Fig. 40. Virtual model of vibrational bracelet prototype fixed on the human handbreadth: (1) – vibration actuator and control panel; (2) – human skin interacting soft material

The terms of reference of the vibrating bracelet control panel has been prepared according to the needs and application purposes. The aim of testing the device prototypes development for medical trials was the main reason.

The control panel has been designed to control each motor individually with a step of 0.1 V and displaying the voltage on the screen. The voltage can be changed by pushing a button up or down. For experimental purposes, manually tuned voltage enables the motors to work continuously. A button for the prescribed working time intervals has been implemented. The purpose of this button is to set the motors to work for a defined time of 30, 60 and 90 seconds and continuing until 300 seconds with 30 second intervals, respectively with one push. The motors and control panel are fed by a li ion battery and can work continuously for at least 60 minutes. Charging can be done via a standard micro USB connector. Red and green LED indications define the battery capacity, charging process, turning on and off of the motor's prescribed time regimes. The terms of reference of the control panel have been designed with the purpose of the adoption to the different parameters' motors, thus the replacement of motors will not require changing the control panel. The electrical scheme has been designed with the possibility to integrate a Bluetooth module for data transmission. Selected microprocessor MSP430F2272IRHAT with 16MHz CPU

speed and 32KB program memory size would be sufficient for more sophisticated calculations. This enables to refinement of the control panel if there will be a need.

Preliminary tests disclosed the need of pressing the vibrating motors by hand to eliminate leaping by the induced force. During the preliminary tests, this issue was solved by using plastic straps as shown on the left image of Fig. 41. According to this problem, the case of the bracelet has been designed (Fig. 41 right image) with the SolidWorks software. The case prototype, comprising three separate parts, was printed with a 3D printer. The main box with a 1 mm thickness wall and two covers (top and bottom) comprises of a plastic printed case. The vibrating motors are placed in the bottom part of the case, which is pressed to the hand by using the Velcro strap that passes through the specially designed rectangular hole. A non-elastic strap enables the force to be more fluently transmitted. The upper part of the case consist of a control panel and a cover. The battery, with a capacity of 500 mAh, is placed in the bottom part of the case.

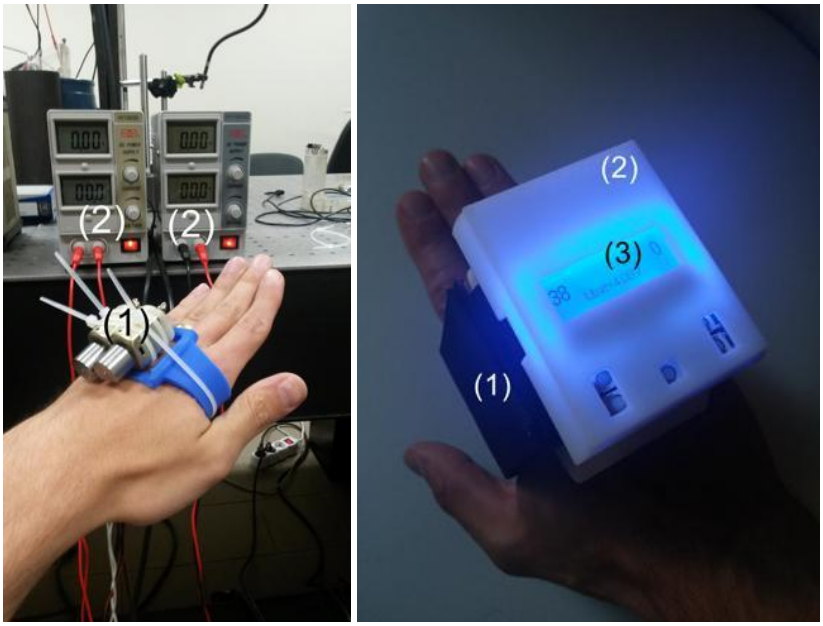

Fig. 41. Vibrating bracelet prototype development (left – primary prototype where vibrating motors (1) were fed by stationary voltage suppliers (2); right – autonomously working 3D printed (2) prototype comprising control panel (3), vibrating motors, battery and adjustable strap (1))

The vibrating bracelet fulfils all the previously defined needs. The autonomous energy supply, control panel and adjustable strap enables research and clinical trials to be made. Furthermore, after the identification of the patients' needs, the case size can be reduced to about 20 – 50 % of volume.

3.2. Human legs actuator

The demand for treatment of blood circulatory disorders in legs is considerable, especially in Diabetes mellitus patients. Considering the legs' weight, different

components have to be used to obtain the same frequencies and at least the same displacements as provided by the prototype of the vibrating bracelet. Therefore, more powerful electromechanical motors have to be selected. A new constructional approach of leg vibration exposure has also to be designed.

For this reason, glass epoxy material has been considered as the most appropriate to transmit vibrational oscillations because of its flexibility and high cycle fatigue properties. The plate's length of 485 mm and width of 400 mm were chosen because of comfortability and ergonomic reasons. It was decided to make a constructional solution with an option of changing the longitudinal position of the plate where the legs have to be located. Thus the machine must be comfortable for a persons of any height. Four fixing points are located at both sides of the end part of plate. Therefore, the plate is considered as a cantilever, where one end is fixed and the other end has displacement freedom at the Y-axis. A cross tube has been attached to reduce the plate's shear deformations. Considering a human's legs position, the electromechanical motors were screwed at the free end of the cantilever plate. The mount construction has been designed for the reason of fixing two motors motionlessly. The plate's fixing points enable users to reduce the unacceptable shear deformations and provide concentrated vertical vibrations at the local axis of the plate to achieve the maximum effect. The plate was coated by a thin foam to make it more comfortable.

In most cases, existing ready-made vibration motors are specified and adopted for various systems and it would be hard to find a suitable motor for the defined research. For this reason, unbalanced mass was designed by using SolidWorks software with parameters given in Table 4. Two identical steel imbalances were manufactured to be mounted on the rotors axis of the electromechanical motors to induce vibrations during the rotational movement, thus generating a vertical direction (perpendicular) force to the glass epoxy cantilever plate.

Table 4. Unbalanced mass parameters

Parameter	Value
Bulk mass	616,8 g
Mass without unbalance	212,92 g
Unbalance mass	403,88 g
Diameter	66 mm
Diameter without imbalance	36 mm

DOGA D.C. electromechanical motors were selected because of the suitable dynamic properties. Both motors (Table 5, Fig. 42) with mounted unbalanced masses were used to induce the beating phenomenon and higher amplitude oscillations compared to one vibration motor. Each motor's angular speed parameter was controlled by a shifting voltage on the power supply. Two rotating imbalances with slightly different frequencies (supplied voltage values) induce the beating phenomenon.

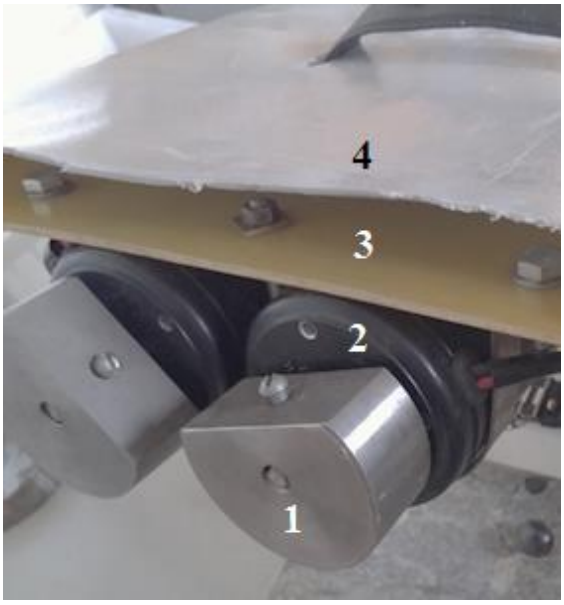

Fig. 42. DOGA D.C. electromechanical motors with unbalanced masses (1 – imbalance; 2 – motor; 3 – glass epoxy plate; 4 – foam cover)

It is known that the beats occur when two frequencies are close together. The frequency of the beating phenomenon can be controlled by raising or lowering each motor's supplied voltage. Transfer of energy takes place in the coupled system which could induce vibration in the primary system instead of suppressing them. The coupled equations of motion without damping in both systems can be obtained from equation 1, by setting the damping in each system equal to zero.

Table 5. DOGA D.C. motor parameters

Parameter	Value
Bulk mass	2,6 kg
Nominal voltage	24 V
Nominal Torque	0,75 Nm
Nominal speed	1000 rpm
Nominal current	5,5 V

One of the main tasks of the leg vibrational actuator (Fig. 46) is to solve blood circulation disorders for people with disabilities. The facility of changing the slope of the plate's position enables the accessibility and variability of usage in different environments for the different state of patients. The first prototype version has been designed with a facility to change the angle manually, but it is foreseen to automate this process. Furthermore, it is well known that raised legs increases blood flow and reduces poor circulation the in human body.

Leg mass calculations have to be done before the investigation of the cantilever plate natural frequency. The data was collected according to the findings of Plagenhoef et al. (1983) studies [97]. The total legs weight is equal to 16.68 % of a

total males' weight and 18.43 % of a total females' weight. Identification of leg mass in dependence of different body weight was accomplished and presented in Table 6. These values are necessary for the material selection process of the vibrating plate and for Eigenfrequency analysis with Comsol Multiphysics software.

Table 6. Leg mass identification

Body weight	Leg mass
55 kg (female)	20.273 kg
60 kg (female)	22.116 kg
65 kg (female)	23.959 kg
70 kg (female)	25.802 kg
75 kg (male)	25.02 kg
80 kg (male)	26.688 kg
85 kg (male)	28.356 kg
90 kg (male)	30.024 kg
95 kg (male)	31.692 kg
100 kg (male)	33.36 kg

Similar principles of vibrational exposure as in the vibrating bracelet have been considered in the use of developing the legs actuator. Thus, Comsol Multiphysics software with the structural mechanics module has been used for the calculations of the cantilever type vibrating plate. The Structural Mechanics Module was tailor-made to model and simulate applications and designs in the fields of structural and solid mechanics. The module is dedicated to the analysis of mechanical structures that are subjected to static or dynamic loads. The Eigenfrequency analysis was made for the natural frequencies of both unloaded and loaded structures.

A computational model of the cantilever plate has been used to assess its natural frequencies and response to the applied load. The cantilever plate, according to the engineering mechanics, is a component that is designed to support transverse loads that act perpendicularly to the longitudinal axis of the cantilever. The bending load is supported by the cantilever only, without external bracing. It is assumed that the cantilever has a longitudinal plane of symmetry and is fixed at only one end. Glass epoxy plate of the legs actuators 2D calculations has been performed.

A rectangular shape solid model of 0.485 m length and 0.004 m thick was designed. The length has been selected according to the ergonomic parameters of the human calf. Glass epoxy material properties with a density of 2000 kg/m3, Young's modulus of 17 KPa and Poisson's ratio of 0.32 was assigned to the model (Fig. 43). Resonance frequency could be used if higher displacement values will be required. The model was fixed at the left end and the motors' weight load was set on the right end with vertical direction and on the top of the human legs weight imitating load. Loads of leg mass of 25.02 kg and the motors bulk mass of 6.43 kg were added to the cantilever model at relevant places on the vibrational actuator.

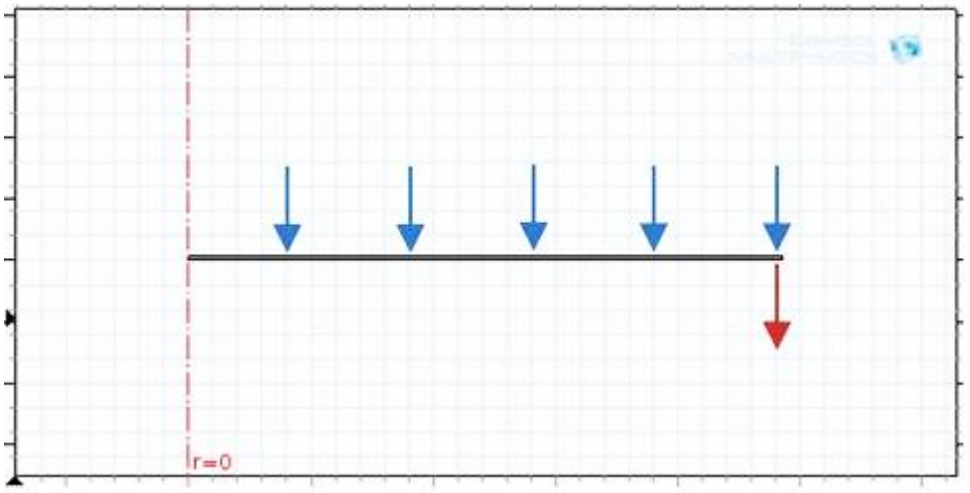

Fig. 43. Glass epoxy cantilever plate model with legs mass load (blue arrows) and motors mass load (red arrow), fixed edge is indicated by dotted red line

The designed model could be easily adjustable considering variations of input parameters such as length, width or load material. The model is simplified and requires minimal time resources for making large amounts of calculations. This model will be used for further studies for the purpose of identifying Eigenfrequency values of different heights of vibrating glass epoxy cantilever plates. A 3D model was not admissible due to the low efficiency of the use of time for calculations.

The Eigenfrequency analysis of the epoxy glass cantilever plate was accomplished with Comsol multiphysics software. Primary calculations were without adding leg mass and after then tapping in the legs mass of 75 kg weight male (equal to the tested person). The Eigenfrequency of the glass epoxy cantilever without leg mass load was equal to 9.05 Hz (Fig. 44). After adding leg mass of 25.02 kg and the motors bulk mass of 6.43 kg, the Eigenfrequency value decreased to 3.28 Hz (Fig. 45).

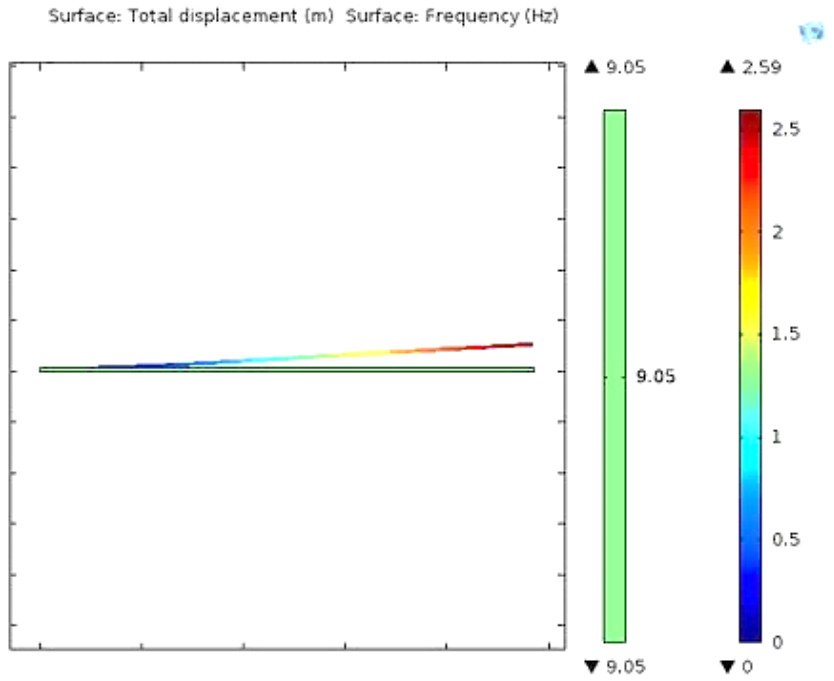

Fig. 44. Eigenfrequency value of the main vibration mode without load

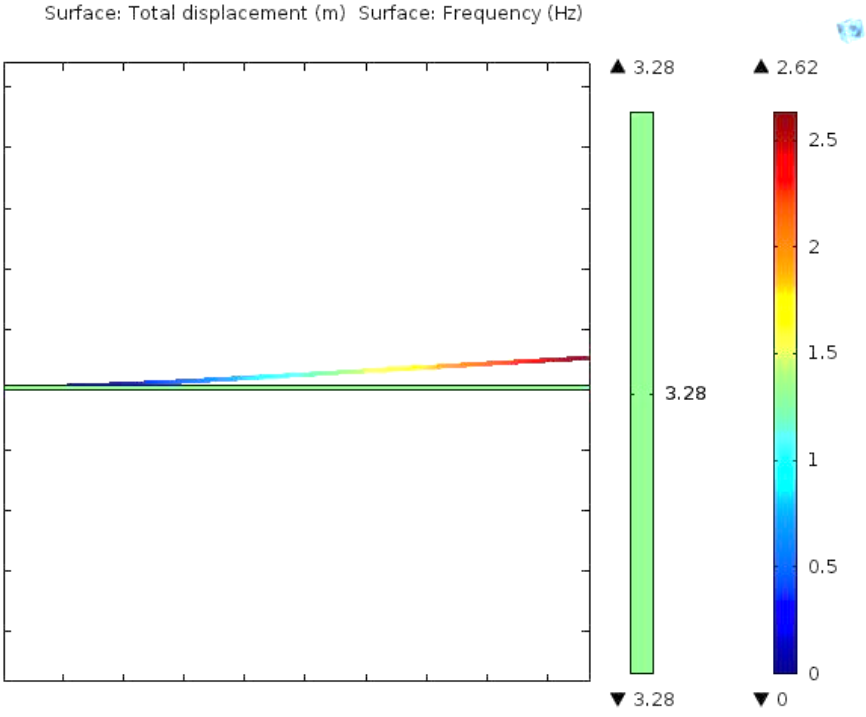

Fig. 45. Eigenfrequency value of the main vibration mode with load

Further calculations with the aim to identify frequency range of different weights' of male and female were made by changing the legs' mass load on the cantilever plate are reflected in Table 7. Frequency values from 3.47 Hz to 3.25 Hz for females at 55 kg to 70 kg weight range and frequency range from 3.28 Hz to 3.02 Hz for males at 75 kg to 100 kg range were noted and are given in Table 7.

Table 7. Eigenfrequency value differ depending on body mass and gender**.**

Body mass (kg)	Gender	Eigenfrequency (Hz)
55	Female	3.47
60	Female	3.39
65	Female	3.32
70	Female	3.25
75	Male	3.28
80	Male	3.22
85	Male	3.17
90	Male	3.11
95	Male	3.06
100	Male	3.02

The leg vibrational actuator was developed with the aim to eliminate the negative effects of standing human vibrations that are described in various studies and recommendation papers. For example, in ISO 2631-1 guidelines on Mechanical vibration and shock – "Evaluation of human exposure to whole-body vibration" is written, which considers that long-term high-intensity whole-body vibration indicates an increased health risk to the lumbar spine. It is noted that this may be due to the biodynamic behaviour of the spine: horizontal displacement and torsion of the segments of the vertebral column. Furthermore, whole-body vibration exercise may worsen certain endogenous pathologic disturbances of the spine. The approach of local exposure at the developed legs' actuator eliminates the negative vibrational excitation effects that are caused by the standing position. Further studies are planned for the measurements of physiological parameters after affecting a human by the prescribed protocol of vibrations by using the prototype of a legs' actuator.

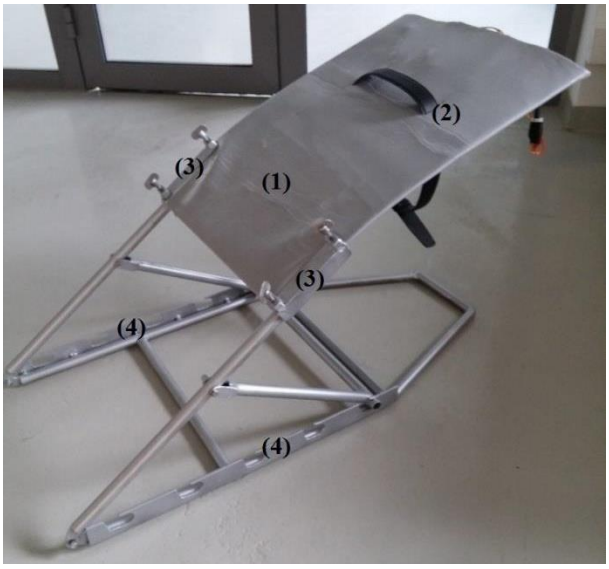

Fig. 46. Leg's actuator (1 – glass epoxy vibrating cantilever type plate; 2 – legs fixing belt; 3 – plate's fixing points, 4 – slope selection holes

The need to fix the legs on the plate has been obtained considering the movement disorders for people with disabilities. A belt has been attached for this purpose, but in this case the need of a second contributory person exists. Therefore, in a newly designed construction it is foreseen to replace this persons' function by an easily maintained construction.

The construction strength calculations have been made with SolidWorks Simulation software. The additional frame of a trapezia shape has been added in the front of the construction to ensure stability and keep a vertical velocity vector inside the build. An initial prototype has been made from stainless steel tubes and it is foreseen to update this construction by manufacturing it from aluminium. This will make the machine lighter and more easily transportable.

The constructional solutions of the assembled parts provide an ability to test it in various environments. Testing of human interaction with a prototype may present suggestions of constructional changes, therefore the main purpose of the designed prototype was to provide a device for a suggested approach.

The same control panel as the vibrating bracelet is used for the legs actuator. In this case, the main difference will be the voltage source. The actuator will be supplied from a power socket, because the motors' voltage is too high for the use of a compact and lightweight portable power source.

The visualised usage of the coupled vibrational actuators consisting of the actuating bracelet and legs actuator are presented in Fig. 47. The vibrating devices are recommended to be used on raised limbs to gain the maximum effect. In Fig. 47 the legs actuator is placed on a special table but it could be used by placing it on the floor or just on a bed. The devices can be used separately or together, dependent on the purpose or type of disease. Prototypes are designed to be used separately because there are no communication modules integrated in any of them. This function is foreseen in

further steps of development. Generally these devices may be used for different purposes and different diseases.

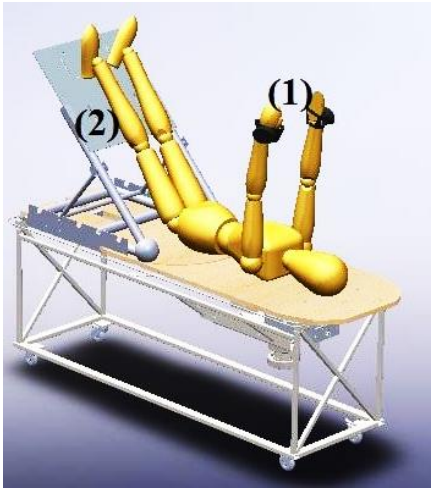

Fig. 47. Vibrational therapy system comprising vibrating bracelet (1) and legs actuator (2)

3.3. Section conclusions

Products on the market are using different vibrational frequencies (mostly higher than 30 Hz) and different amplitudes (up to 5 mm) of the oscillations, therefore the purpose of its applicability is different. The majority of vibrational therapy devices are made for athletes for the purpose of enhancing muscle performance, bone density or just a warm-up before any physical activity. For this reason, a decision was taken to design and manufacture the prototypes by focusing on blood flow disorders and improvement possibilities. Therefore, the devices of low-frequency and higher vibration amplitude have been designed. The beating phenomenon has been induced to create a sufficient force and oscillations frequency ratio. Comprehensive conclusions of this section are listed below:

- Experimental stand of glass epoxy cantilever comprising of vibrational actuators has been designed for experimental investigations. The working regimes of a sufficient force and low-frequency vibrations has been defined during the studies. A vibrating bracelet has been designed as an experimental tool to investigate blood flow improvement by using different vibrational frequencies. An autonomous device, comprising the vibrating motors, control panel and adjustable strap was developed for clinical trials. The prototype is mainly intended for arthritis patients because the pain occurrence is mostly in the hands.
- Vibrating machine for legs has been developed with a purpose of making investigations of blood flow improvement in legs, by changing the working frequencies, slope and human body position. The prototype was created considering the needs of people with disabilities and diabetics. Furthermore, constructional changes are foreseen in the case of improving accessibility and comfort level.

- Numerical calculations considering the vibrating plate as a cantilever have been conducted. The natural frequencies without the leg's weight load were equal at 9.05 Hz and after assessing a 75 kg male's legs weight 3.28 Hz. This value is close to the determined frequency range from the earlier experiments where the highest impact of cardiovascular parameters and liquid (blood) property changes were obtained.
- Eigenfrequency values of 3.47 Hz to 3.25 Hz for females (weight: 55 – 70 kg) and 3.28 Hz – 3.02 Hz (weight: 75 – 100 kg) for males were calculated for a cantilever of a glass epoxy material. These values prescribe the working regimes and supplied voltage means depending on human weight and will be implemented in the device control algorithm.

4. EXPERIMENTAL INVESTIGATIONS OF BLOOD FLOW IMPROVEMENT OF LIMBS' VIBRATIONAL EXCITATION

The following section defines the experimental investigations of the vibrational excitation influence on blood flow parameters. The main aim of these studies was to identify the most influential vibrational frequency and amplitude range. The experimental setup of an imitational blood circulation system consisting of the peristaltic pump, artificial blood vessel, pressure sensor and vibrational actuator has been designed. The aim of this study was to identify the influence of the vibrational excitation within the range of frequencies of 0.5 – 30 Hz to the fluid pressure parameters and to identify the most influencing values. This was followed by deeper analysis of the processes in fluid during the vibrational bouts being investigated by using the micro-particle image velocimetry method. The analysis of fluid velocity vectors' and abstraction of different velocities' streaming lines inside the channel has been conducted.

Considering the process when external vibrations are affecting human body, the body tissue could be assumed as a damping system. Thus, the presumption of possible frequencies' difference between the source (vibrational actuator) and receipt (micro blood vessels) needed to be investigated. The analysis of the human body tissue response on the vibrational influence has been done with the purpose of identifying the differences of frequencies between the source and finger marker in the range of 1 – 10 Hz vibrational bouts. Furthermore, validity studies were conducted by monitoring cardiovascular parameters and temperature changes in limbs before and after vibrational excitation. The studies were carried out with the designed prototypes of vibrating bracelet and legs actuator. The effect on oscillating limbs was monitored by changing input parameters of electromechanical motors. Furthermore, the cardiovascular parameters (ECG, heart rate, respiration rate) have been analysed against the effect of vibrational exposure. These studies were necessary to validate the developed prototypes and to define proper working regimes for further investigations on disease affected patients with circulatory disorders.

4.1. Experimental blood flow imitational stand and pressure monitoring technique

Investigation of blood flow pressure response on the vibrational excitation was performed with an assembled experimental setup, consisting of a peristaltic pump and fluid filled medical tubes that were fixed by a vibrating beam (Fig. 48, Fig. 49). The aim of this experiment was to identify the vibrations' influence on fluid pressure and to determine the proper working regimes for the designed prototypes. Moreover, this study provides an understanding of how the external vibrations influence a human's blood vessels. The medical peristaltic pump has been used to imitate the blood's exhaust from the heart. Furthermore, in later studies, plastic tubes were replaced by an artificial blood vessel (Table 8) that was connected with the output tube of the pump. The artificial blood vessel's part was mounted on the vibrational actuator comprising of two electromechanical motors to initiate the beating phenomenon. The vessel was surrounded by foam to imitate human body tissue. A displacement sensor

has been attached at the top of the actuator. Pressure changes were registered by the pressure sensor during the generation of different frequencies.

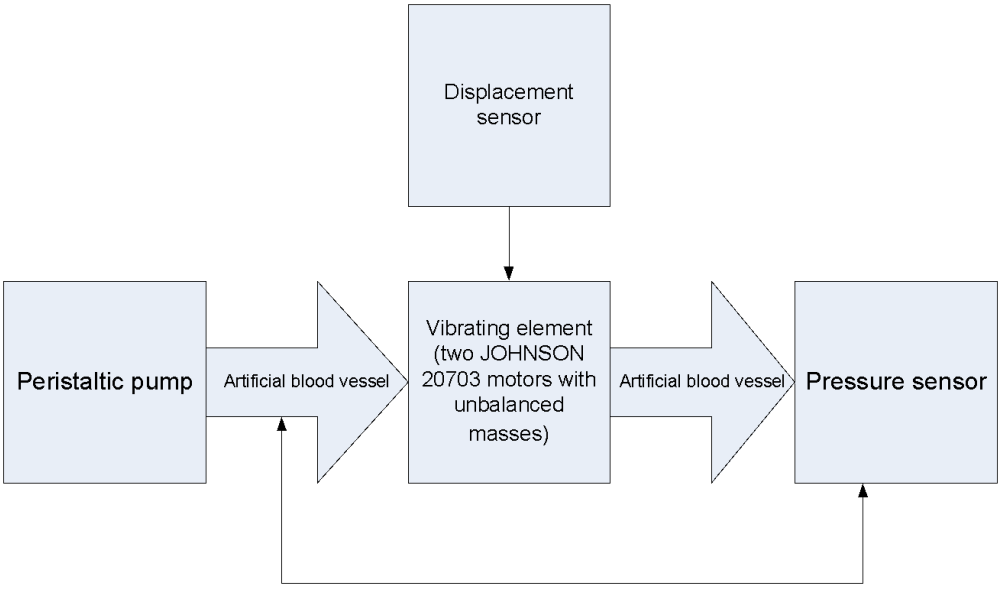

Fig. 48. Principal scheme of the experimental setup

Motor and vibration measuring sensors were fed by three laboratory power suppliers. Inductive displacement sensor IFM IG6084 was used to measure the beam's vibrations. All data was registered by the Oscilloscope Picoscope 3424 and was stored and analysed by using the PC software PicoScope 6. Motors characteristics (revolutions per minute) have been registered with a photo tachometer / stroboscope Lutron DT-2259. Therefore, the measurement of the motors' RPM on different voltage values by using the damping element was conducted during this experiment. RPM values were measured in regimes of tachometry and stroboscope to get validated data. First of all, the experiment was conducted without the damping element. Next, the experiment was repeated by adding the damping element consisting of air and water packages. The damper has been placed at the bottom of a vibrating beam with the actuator. The damper was designed with the purpose of eliminating the resonance frequencies of the beam and to reproduce similar characteristics such as human body tissue rheological characteristics. The inlet and outlet tubes were immersed in the fluid tanks. The fluid pressure parameter was monitored by the developed pressure sensor. The pressure sensor (Fig. 50) comprising of pressure gauge Mpx5010gp, voltage stabiliser 7805 TO220 (2) and compensator 2200uF was created for this experiment (Fig. 50). The pressure gauge was selected because of the accuracy (4.413 mV/mm H_2O) and range of pressure monitoring (0 – 10 kPa). Output signals of the pressure sensor were gathered by an oscilloscope. The sensor was connected by a trident tube that was placed beyond the vibrating beam.

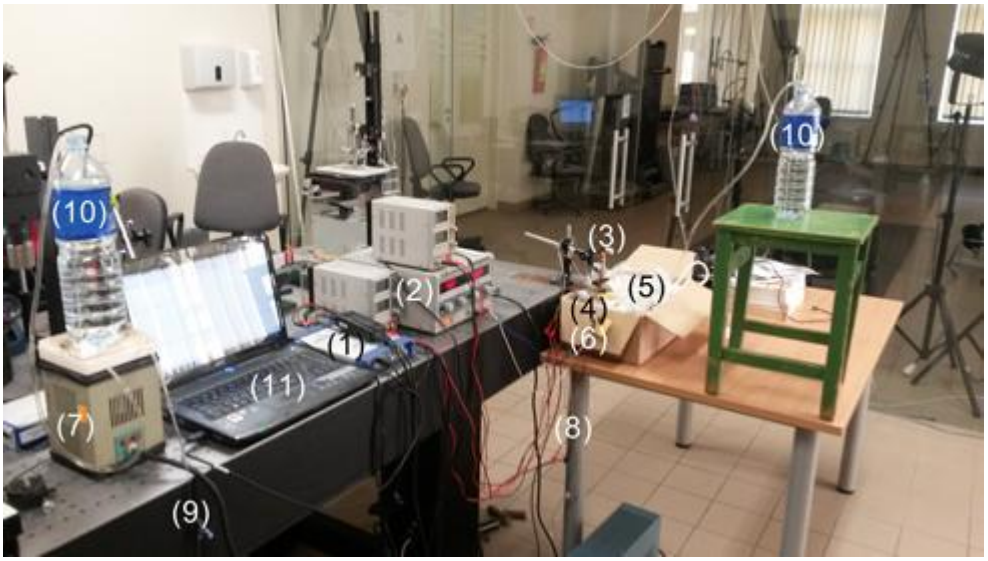

Fig. 49. Experimental setup: 1 – oscilloscope; 2 – DC supply; 3 – inductive sensor; 4 – vibrating motors; 5 – damping element; 6 – pressure sensor; 7 – peristaltic pump; 8 – artificial blood vessel (Table 2); 9 – medical tubes; 10 – water tanks; 11 – PC with Picoscope software

Table 8. Physical and mechanical properties of the artificial blood vessel made from expanded polytetrafluoroethylene [98]

Physical properties	**Metric**	**Mechanical Properties**	**Metric**
Density	0.700 - 2.30 g/cm^3	Ball Indentation Hardness	27.0 - 37.0 MPa
Apparent Bulk Density	0.360 - 0.950 g/ cm^3	Tensile Strength, Ultimate	10.0 - 45.0 MPa
Water Absorption	0.000 - 0.100 %	Tensile Strength, Yield	0.862 - 41.4 MPa
pH	9.5	Modulus of Elasticity	0.392 - 2.25 GPa
Viscosity	19.0 - 25.0 cP	Flexural Modulus	0.490 - 3.36 GPa
	1.00e+13 - 1.00e+15 cP	Flexural Yield Strength	14.0 - 27.6 MPa
	Temperature 340 - 380 °C	Compressive Yield Strength	1.50 - 23.4 MPa

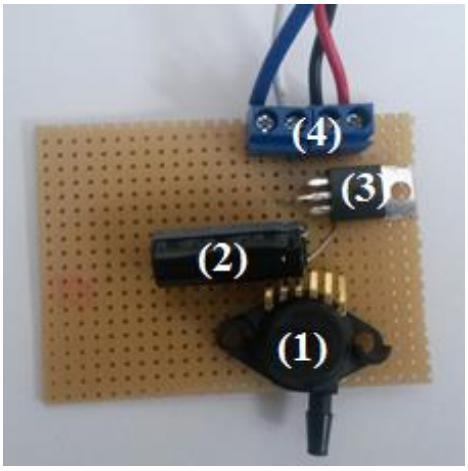

Fig. 50. Designed pressure sensor (1 – pressure gauge Mpx5010gp; 2 – capacitor 2200uF; 3 - positive-voltage regulator 7805 TO220)

At the beginning, an experiment with one motor has been conducted by altering the voltage value. The supplied voltage ranged from 3 V to 16 V with 0.1 V step and without using any damping element. The next experiments with two motors were performed. The voltage for each motor had been altered in the same range, starting form 3 V to 16 V with 0.1 V step. Then, the damping element was added with a purpose to eliminate the natural beam's frequencies. Motors were supplied by the same range of voltage as in earlier experiments. The same experiments were repeated after substituting the medical plastic tube with an artificial blood vessel. Pressure alterations were registered at the beginning of the experiment and during it, together with the beam's displacement.

The fluid pressure in the fulfilled channel has been registered. The value of 4.5 kPa was recorded, which is close to the mean of pressure in human capillaries.

The peristaltic pump working regime of 1 Hz was set, which is equal to a heart rate of 60 beats per minute. The initial experiment was conducted with one motor. The highest pressure change of about 1 kPa was noted when the motor was supplied by 6 V and 11 V voltages respectively. The artificial blood vessel and damping element have been added for experimentation. Damped beam vibrations of 6 Hz frequency were noted when the motor was supplied by 5 V voltage. A pressure rise of 2 kPa was registered (Fig. 51).

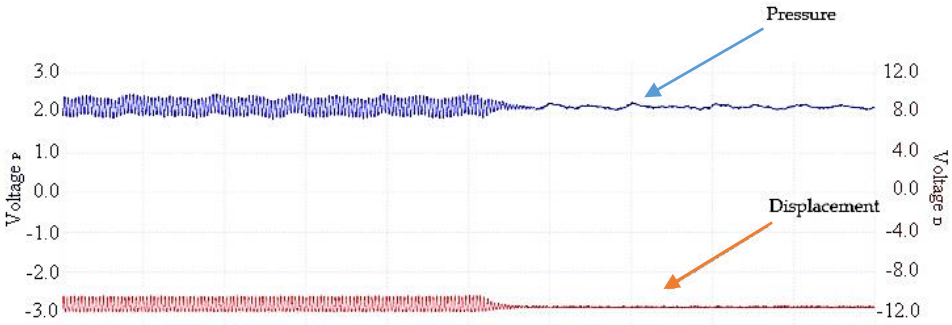

Fig. 51. Pressure rise of 2 kPa affecting artificial blood vessel by 6 Hz frequencies.

The beating phenomenon was induced by starting the second motor with unbalanced mass. The two motors were supplied by voltage of 5 V and 5.8 V respectively to generate the beating phenomenon (Fig. 52). The results of pressure and displacement measurements are represented in one line to show the dependency. In the graph below it is clearly visible that the fluid pressure is directly dependent on the beam's oscillations. An overlapped view of diagrams shows that reliance. The pressure rises during the vibrational excitation and decreases dramatically when displacement amplitude was close to zero. These results were similar when comparing the medical plastic tubes and the artificial blood vessel.

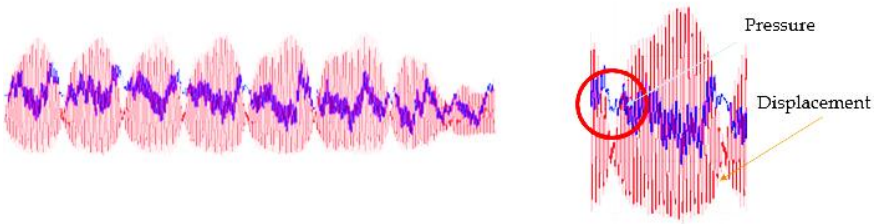

Fig. 52. Overlapped pressure and displacement graphs during the beating phenomenon.

The later experiments were conducted with an artificial blood vessel in the experimental setup instead of the medical plastic tube. Moreover, higher pressure rise was noted in the case of two motors. In comparison, the highest rise of pressure mean, using one motor that was supplied by 9 V, gained a 3 kPa increase in value. Furthermore, two motors supplied by 5.1 V and 4.9 V respectively, generated a rise of 8 kPa (Fig. 53). The processed results showed that the pressure changes have increased in parallel with the oscillating beam's displacement amplitudes. It was also observed that at higher frequencies than 10 Hz, pressure change amplitude becomes lower and the momentum value changes become more frequent. The most influential frequencies of the beating phenomenon were noted in the diapason from 2 to 5 Hz. As it was observed during the study, the displacement amplitudes ranging from 4 to 20 mm are the most desirables. The values are coherent with the results of numerical calculations.

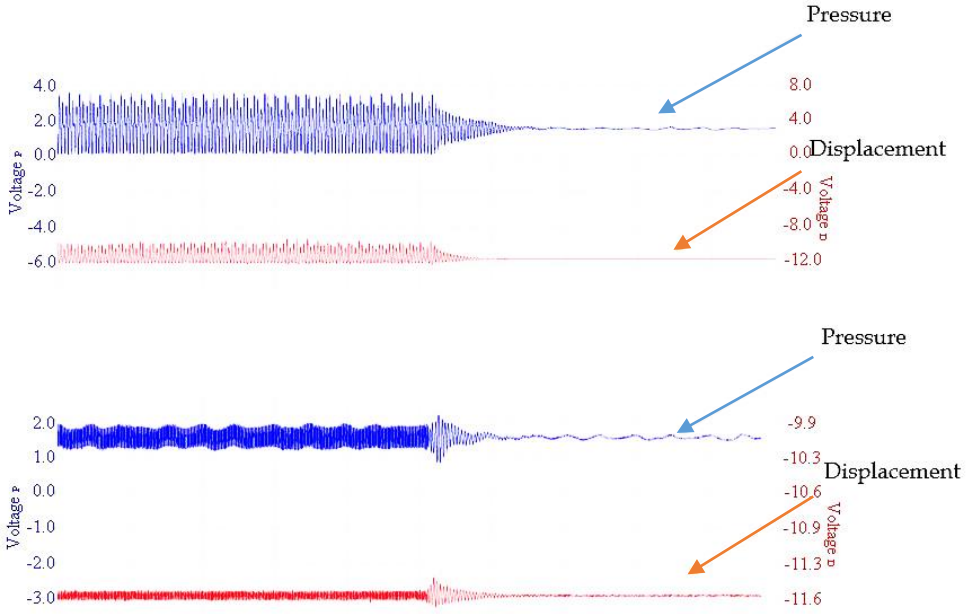

Fig. 53. Results of using artificial blood vessel: two motors' induced beating phenomenon and 8 kPa pressure rise (upper graph); one motor vibrations and 3 kPa pressure rise (lower graph).

The results of pressure monitoring provide only the momentum alterations but longer term pressure increase was not monitored. The peristaltic pump exhausts the same amount of volume of fluid, therefore it was unable to monitor the fluid volume alteration per time unit. However, the significant increase of fluid pressure enables researchers to make an assumption that low-frequency vibrations could be used with the purpose of improvement of blood flow in human limbs.

4.2. Experimental setup to monitor blood flow velocity changes during the vibrational excitation by using µPIV system

Experimental results of previous studies have showed demand for deeper analysis of fluid parameter changes during the vibrational bouts. Observation of the fluid velocity distribution stream lines and vectors' field was made by monitoring the movement of particles in fluid. The previously described experimental stand consistent of peristaltic pump, vibrational actuator and artificial blood vessel has been coupled with a µPIV system. Papers [22, 43, 44, 45, 46, 47] of fluid velocity analysis methods on vibrational excitation were analysed to select the most appropriate one.

Experiments of the flows in microchannels were made at the Lithuanian Energy Institute. A unique experimental setup (Fig. 54) consists of a µPIV system vibrational excitation and measurement equipment part. µPIV system (Fig. 55) consists of Nd: YAG laser (Dantec Dynamics), laser control system LPU 450 (Dantec Dynamics), 2048 x 2048 pixels FlowSense EO CCD camera (Dantec Dynamics) that was fixed on an inverted Leica DM ILM microscope (Leica Microsystems). The prescribed fluid flow was generated by a syringe pump (Aladdin AL4000, World Precision

Instruments) with connected medical blood tubing lines. The tubing line length starting from the syringe pump to measurement microscope was 1.5 meter long. About 30 cm away from the syringe pump, the tubing line was placed in a material imitating human tissue that was fixed by an oscillating epoxy glass cloth laminate beam. A special electromechanical actuator consisting of two small size, low voltage and high RPM electric motors (JOHNSON 20703) each with attached unbalanced masses of 14.86 g was used for generating the beating phenomenon and proper frequencies. These motors were screwed to the epoxy glass cloth laminate. As it was defined on an earlier study of the author, the electric motors could generate a force on beating phenomenon up to 41.48 N depending on the supplied voltage. Oscillations and movement amplitude of the beam were measured by an inductive displacement sensor IFM IG6084 that was stationary fixed right above the beam. The output signal was collected by an oscilloscope Picoscope 3424 and processed by the corresponding software on the PC. The measurements of the fluid parameters were made after a minute of the vibrational effect of every frequency value and amplitude. The input voltage of the motor was chosen considering the real-time generating frequency response. The voltage values, ranging from 2 V to 5.5 V for one motor and from 6.0 V and 6.1 V to 8.0 V and 11.1 V with 0.1 V step for two motors accordingly were selected to induce the beating phenomenon. The monitoring point was 1 meter of channel away from the vibrational actuator.

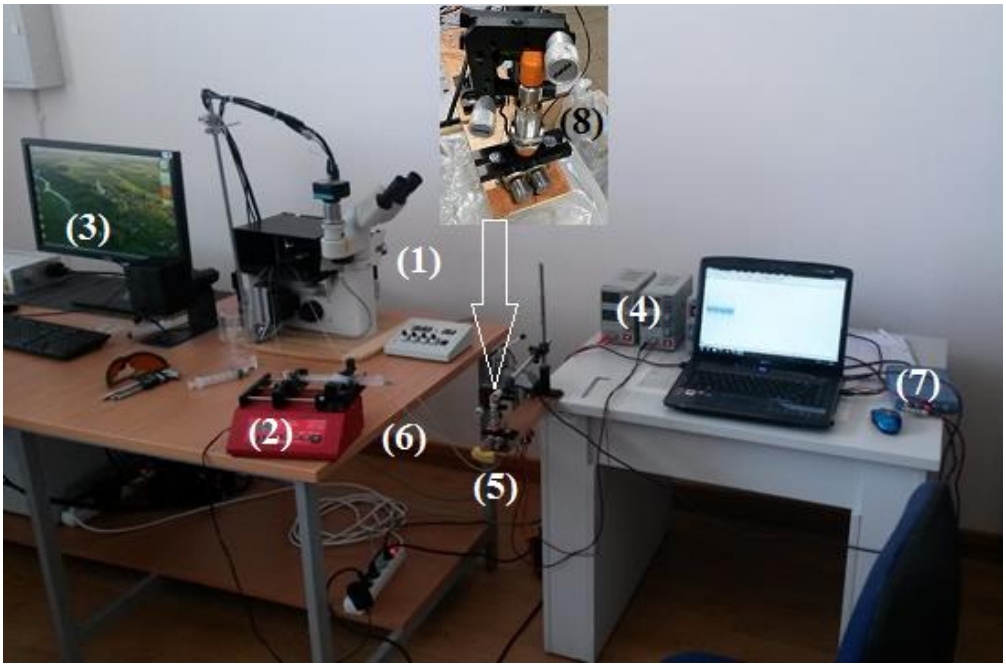

Fig. 54. Experimental setup: 1 – Leica DM ILM microscope; 2 – syringe pump; 3 – YAG laser; 4 – DC power supply; 5 – vibrating beam with two electric motors and attached unbalanced masses; 6 – medical tubes; 7 – oscilloscope Picoscope 3424; 8 – inductive displacement sensor IFM IG6084.

The scheme of the μPIV system separately is presented in Fig. 55.

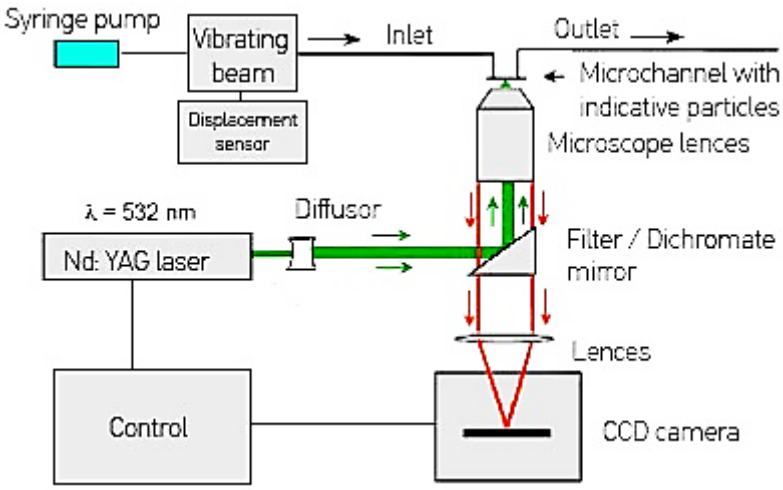

Fig. 55. Schematic drawing of μPIV system.

The microchannel used for experiments was made from special vascular graft, produced by the USA GORE Company. Here, GORE hybrid vascular graft is made of an expanded polytetrafluoroethylene (ePTFE) vascular prosthesis that has a section reinforced with nitinol. The nitinol reinforced section is partially constrained to allow easy insertion and deployment into the human body. The GORE hybrid vascular graft has a continuous lumen with a CARMEDA BioActive surface consisting of a stable covalently bonded, reduced molecular weight heparin of porcine origin.

The solution, having similar technical specifications as real blood, was used as a fluid. The velocity of the fluid flow is measured by applying spatial flow lightning and registering the movement of the indicating particles. The velocity vectors' field of the particles were determined by μPIV measurements. Knowing the time interval between taking pictures Δt and the displacement of the particles Δx, the velocity could be calculated by the equation (4.2.1):

$$v = \frac{\Delta x}{\Delta t} \qquad (4.2.1)$$

The fluorescent particles of 1.0 μm (3.94 × 10-5 in) diameter were used for the measurements. The density of the particles in space was close to fluid density and the size was chosen to avoid Brown flow influence, as well as getting a strong enough fluorescent signal.

The principal scheme of image analysis is shown below (Fig. 56) where the image intensity function in the fast Fourier transform and cross-correlation was established. The image intensity function was performed by inverse Fourier transform and the result was displayed by the velocity vector field and the velocity components.

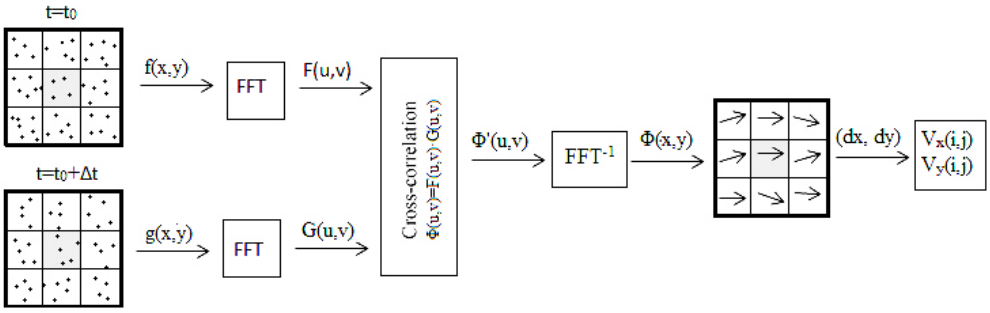

Fig. 56. Principal scheme of μPIV correlation establishment.

The displacement was calculated for all particles. The calculations were made by the cross-correlation method [99 - 103] using the fast Fourier transform method.

Calculating the Φ value,

$$\Phi(x,y) = \sum_{x=1}^{p}\sum_{y=1}^{q} f(x,y)\cdot g(x+m, y+n) \qquad (4.2.2)$$

where p and q – net window dimensions in x and y directions, $f(x,y)$ and $g(x,y)$ – the image intensity functions on the first and the second frames, m and n – the displacement coordination, $\Phi(x,y)$ – the correlation function between two windows of the net (p x q size) with mutual displacement (x,y),

The entire range of shear creates a cross-correlation plane, which features the largest value indicate of the displacement of the particles [102].

Analysis of the μPIV experimental results revealed that signs of turbulent flow has been detected on the vibrating microchannel (Fig. 57, Fig. 58). Spectrograms at Fig. 58 reflects that phenomenon the most. The velocity changes of the luminescence particles and the momentum opposite flow direction were noted (Fig. 57). On the separate time moment (on 4.3 Hz frequency) the velocity increases up to 2.7 mm/s, while the average velocity without vibrations was 0.65 mm/s. In the cases of 4.9 Hz, 5 Hz, 5.7 Hz, the beating frequencies' average velocity reaches or increases up to 0.8 mm/s. The average velocity of 0.7 mm/s was observed in most cases when the fluid was affected by the external vibrations. Short impulses of upstream velocity up to 1.5 mm/s were noted during the oscillating frequencies of 5 Hz, 5.3 Hz, 5.4 Hz and 5.8 Hz. Analysing the vector maps at each time moment separately, it can be observed that the real flow direction (from right to left Fig. 57 (a))) maps are much more frequent than maps with the upstream speed vectors (Fig. 57 (d)). It is also clearly visible that downstream speed at each time moment is much greater than upstream. It can be concluded that the average velocity direction cannot be reversed, as it is shown in vectors maps (Fig. 57, d) of the microchannel. During these moments of time the pressure in the microchannel should be higher than normal, as it was defined in the previous study.

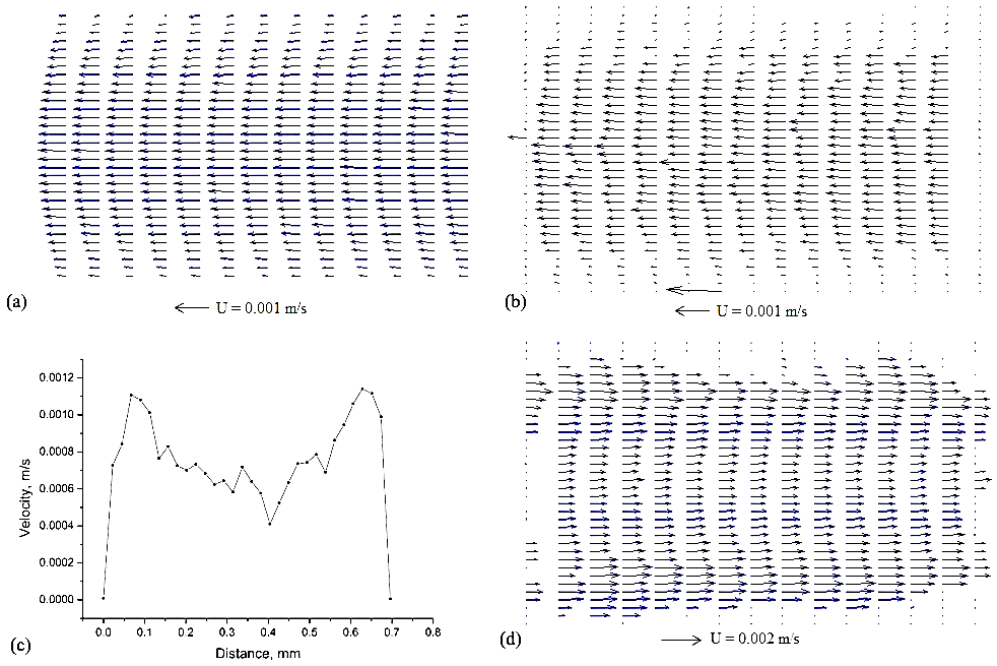

Fig. 57. (a) Velocity vectors‘ field without vibrations; (b) Velocity vectors‘ field during low amplitude vibrations (2.4 Hz, 0.98 mm); (c) Velocity profile and (d) vectors filed during high amplitude vibrations (4.3 Hz, 6 mm).

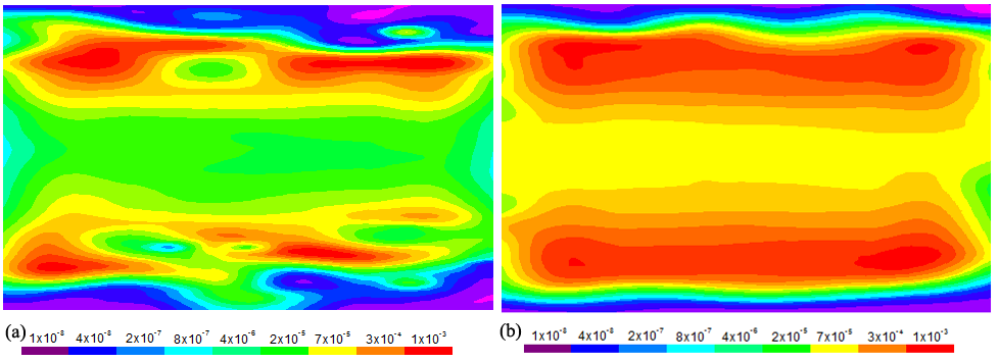

Fig. 58. (a) Fluid velocity spectrogram on 4.3 Hz frequency and 6 mm amplitude; (b) Fluid velocity spectrogram on 5.8 Hz frequency and 6 mm amplitude.

The μPIV experimental analysis showed a significant influence of vibrational bouts on the fluid velocity in the microchannel. Again, the low-frequency oscillations with higher amplitude of displacement provided the more significant findings. In most cases of vibrational exposure, the average increase of fluid velocity has been observed. These results proves the vibrational influence on fluid parameters and it could be assumed that properly selected vibrational expose to the human body could affect the blood flow. It was agreed that further analysis has to be done by using the developed

vibrating bracelet and legs actuator prototypes, and monitoring cardiovascular parameters coupled with temperature changes of limbs.

4.3. Finger tissue acceleration signal response analysis

Experimental investigations on human body tissue response at separate points of the body has been analysed in previous studies [72]. The results showed variation of the response frequency of monitored points that was caused by higher body mass indexes. Therefore the analysis of human finger tissue response has been conducted. The main aim of this study was to identify if there is a significant difference in the frequencies' values between the source and marker on a human finger of people with different body mass indexes. The comparison of the prescribed vibrational exposure values ranging from 1 to 10 Hz with 1 Hz step with the gathered data was conducted.

Human tissue acceleration signal analysis was performed at the Laboratory of Biomechanics of the Mechatronic Institute at Kaunas University of Technology. The purpose of this analysis was to identify the demand for a frequencies correction factor for modelling fluid flows. The experiment strictly follows the methodology for human body acceleration signal analysis, which suggests using a quantitative analysis method such as photogrammetry, or more specifically, cameras and markers [72]. Thus, the experiment was conducted using a ProReflex MCU 500 Type 170 241 camera (Fig. 59) with Qualisys Track Manager Software. The ProReflex MCU uses a 680 × 500 pixel CCD image sensor. The use of CCD technology results in very low-noise data compared to a higher resolution CMOS sensor, which has a considerably higher pixel noise level. By using a patented sub-pixel interpolation algorithm, the effective resolution of the ProReflex MCU is 20000 × 15000 subpixels in a normal setup, enabling the ProReflex MCU to discern motions as small as 50 microns. The prescribed oscillations were generated on the vibration stand Veb Robotron Type 11077 and the monitored human body part – the finger was placed on the top of this stand.

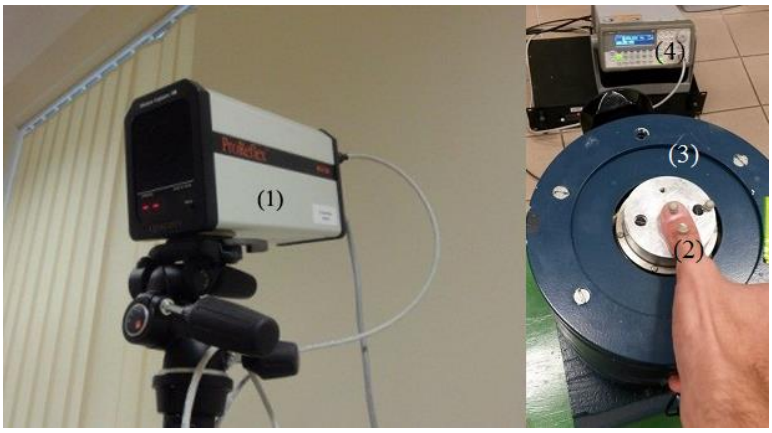

Fig. 59. Experimental setup: 1 – ProReflex MCU 500 Type 170 241 camera from Qualisys and the monitored finger with markers (2) on the vibration stand (3) (Veb Robotron Type 11077) and 4 – frequencies generator Tabor Electronics WW5064 50Ms/s.

Human tissue acceleration signal analysis was made by identifying the frequencies difference between prescribed values on the vibrational stand and tissue response with the purpose of obtaining undistorted results on the computer modelling and experimental setup. Two male persons (proper informed consent was obtained) with different body mass indexes, (BMI) of 22.0 (person I) and 28.9 (person II) were selected. Markers were fixed on the finger nail, thumb joint and vibration stand. The experiment was made by generating frequencies from 1 to 10 Hz oscillations with 1 Hz step for each person, registering markers' displacement with 100 Hz sample rate. The results were processed with Matlab software using a low pass filter of 0.5 Hz passband frequency. A 20 Hz stopband frequency had been applied.

The marker's displacement data gathered by the camera was filtered and the frequency difference ranges between the finger nail marker and the vibration stand were deeply analysed. During the 78 pulses of 2 Hz oscillations of vibrational stand, 1.975 Hz of finger's marker frequency were found for person I and a difference of 0.007 Hz for person II was calculated. The highest difference of 0.012 Hz was unregistered while scaling the analysed waves per 1 pulse value. The difference of 0.138 Hz for person II and 0.054 Hz for person I were noted on 4 Hz oscillations (Fig. 60). The difference of 0.135 Hz for person II and 0.036 Hz for person I were discovered on 5 Hz oscillations. The average difference of 82 pulses was equal to 0.001 Hz on 8 Hz vibrations, while the peak value was 0.025 Hz for person I. The highest differences of 0.209 Hz for person II and 0.134 Hz for person I were identified on the 9 Hz oscillating frequency.

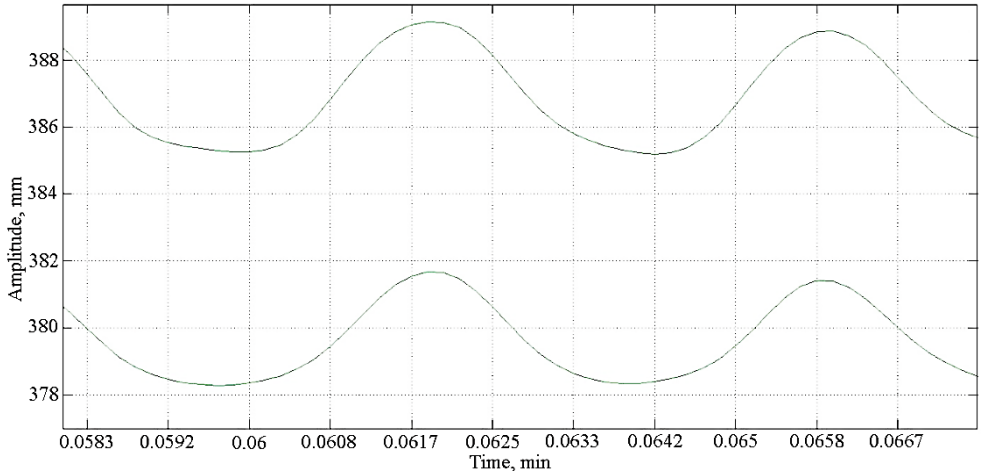

Fig. 60. 4 Hz oscillations of vibrational stand (lower curve). The highest frequency difference of 0.054 Hz for person's I finger (top curve).

The difference of values of the responding finger marker frequencies were not significant. Therefore no correction factor was necessary to add in to the selection of vibrational exposure of the limbs actuating device prototypes. During further experiments, the prescribed values of external frequencies were considered as equal value on the impact on the microvascular system.

4.4. Validity of vibrating bracelet and legs actuator

Experimental investigations of vibrational exposure on the human cardiovascular system by using the developed prototypes has been defined as a crucial validation process of the suggested approach. Therefore, various cardiovascular parameters were needed to be monitored before and after vibrational excitation. Furthermore, the thermal imaging monitoring method was obtained as the most appropriate in the evaluation process of blood flow disorders and improvement means. For this reason, thermal photos of hands and legs were taken before and after vibrational exposure.

First of all, the device with a tri-axial accelerometer [89] was used to identify the bandwidth of naturally vibrating limbs (hand). The accelerometer model LIS331DLH was selected to satisfy the needs for the measurement range and bandwidth. The accelerometer cannot operate on its own, so the previously developed device was used (Fig. 61).

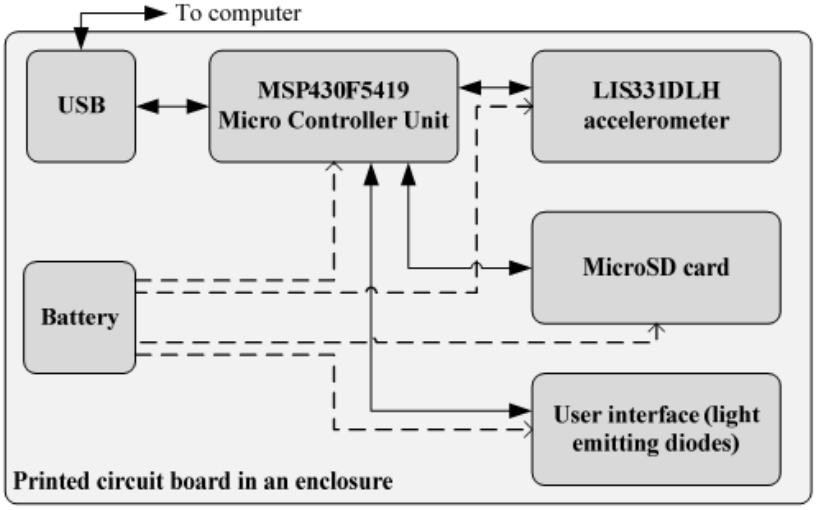

Fig. 61. Principal scheme of the acceleration measurement device.

The device contains a Micro Controller Unit (MCU) to hold all the logic, LIS331DLH MEMS [104] accelerometer to measure 3D accelerations, MicroSD card to save measured data samples, battery to power everything, some light emitting diodes (LEDs) to display the state the device is in and a USB connector so the data can be downloaded to a personal computer for further processing. The final acceleration range requirement was selected to be ±8g.

Naturally, the initiated limb frequencies during the suggested exercise of Katsuzo Nishi [20] were observed as high as 4 Hz. Therefore, the close values of frequencies have been argued as the most appropriate for a further study with patients.

First, blood pressure monitoring was performed before and after exercise to identify the effect of external vibrations on the human body. Blood pressure monitor Microlife BP A100 [105] was suggested by the clinicians, because of its high accuracy. Other physiological parameters were monitored with a Schiller MT-101 2-

channel Cardio Logger [106] device. The device monitors electrocardiogram (ECG) and heart rate from 4 points of body. Specified computer software was used for observation of collected signals.

Experiments of testing a human's body reaction on vibrational effect were conducted in the Centre of Mechatronc Science, Studies and Information at Kaunas University of Technology. The experimental setup is showed on Fig. 62. The vibration stand has been used to initiate the prescribed vibrations on a human hand. Displacement has been observed with the Keyence LK-G82 laser.

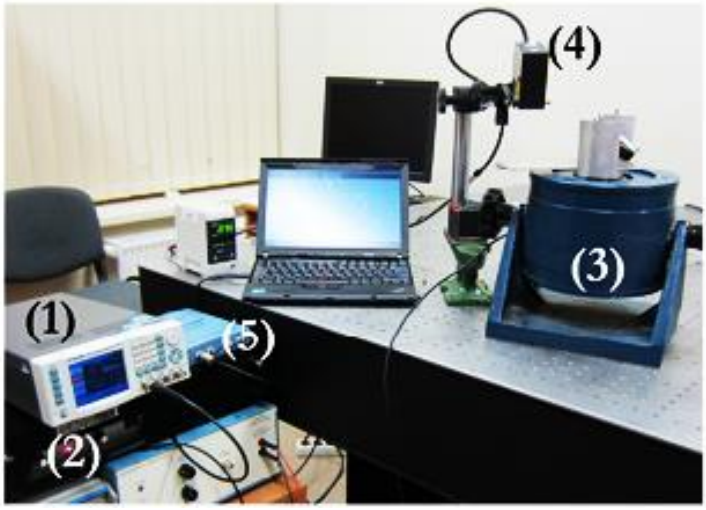

Fig. 62. Experimental setup: 1 – frequencies generator Tabor Electronics WW5064 50Ms/s; 2 – power amplifier VPA2100MN; 3 – vibrational stand Veb Robotron Type 11077 with developed device mounted on top; 4 – displacement measurement unit laser Keyence LK-G82 with controller Keyence LK-GD500; 5 – ADC Picoscope 3424.

Two types of experiments were conducted. Firstly, the experiments were made by changing the frequency (1^{st}: from 1 Hz to 40 Hz; 2^{nd}: from 1 Hz to 8 Hz; 3^{rd}: from 2 Hz to 12 Hz). The second type of experiments were made with constant frequency values of 3 and 4 Hz operating on different time periods. Frequency values used at the second type of experiments are close to the means that were observed as the most efficient. Experiments were repeated two times with two patients. The detailed description of each experiment is presented below:

- Right hand. Time: 120 s; Frequency: from 1 Hz to 40 Hz; Peak to peak amplitude: 300 mV;
- Right hand. Time: 120 s; Frequency: from 1 Hz to 8 Hz; Peak to peak amplitude: 500 mV;
- Right hand. Time: 600 s; Frequency: from 2 Hz to 12 Hz; Peak to peak amplitude: 1 V.
- Right hand. Time: 120 s; Frequency: 3 Hz; Peak amplitude: 1 V;
- Right hand. Time: 120 s; Frequency: 4 Hz; Peak amplitude: 1 V;
- Right hand. Time: 600 s; Frequency: 3 Hz; Peak amplitude: 1 V.

- Right hand. Time: 600 s; Frequency: 4 Hz; Peak amplitude: 1 V.

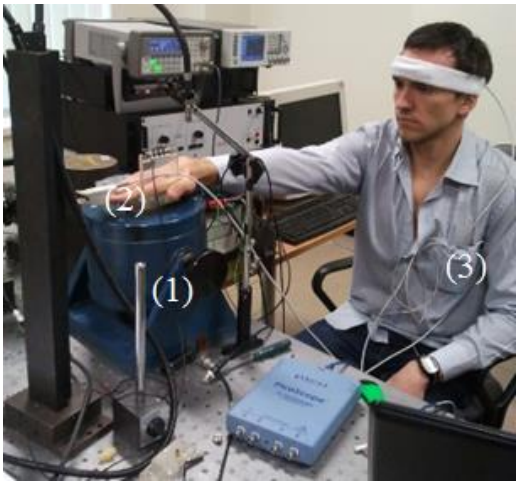

Fig. 63. Human's body reaction on vibrational effect experiment (1 – vibration stand; 2 – human hand with acceleration sensor; 3 – cardiologger device)

Blood pressure was measured before the vibrational excitation and two times after the experiment: 5 and 10 minutes later (Table 9). The significant change of diastolic blood pressure value was recorded.

Table 9. Blood pressure changes before and after experiment

Time period	Alteration of average systolic blood pressure (mm Hg)	Alteration of average diastolic blood pressure (mm Hg)
Before the experiment	-	-
5 min. after the experiment	-0.75 %	16.39 %
10 min. after the experiment	4.51 %	16.39 %

The experiment with vibrational oscillations of static frequency has shown different results (Table 10). The change of systolic pressure value was found right after the experiment. However, the average value of diastolic blood pressure has decreased. The alterations of blood pressure show the impact of vibrational excitation but a larger quantity of subjects were considered necessary in the case of proving correlation between values of vibrational frequencies and blood pressure.

Table 10. Blood pressure changes before and after the 10 min. experiment on vibrational stand**.**

Time period	Alteration of average systolic blood pressure (mm Hg)	Alteration of average diastolic blood pressure (mm Hg)
1 min. before the experiment	-	
Right before the experiment	9.34 %	-1.28 %
2 min. after the experiment	2.54 %	-7.69 %

The 10 minutes' duration peak to peak experiment has showed some significant changes on the respiration rate and ECG curves (Fig. 64, Fig. 65). The major amplitudes have been observed on the highest frequency values. The "uncomfortable feeling" of high frequency vibrations was outspoken by both patients. The higher frequencies values were eliminated from further studies.

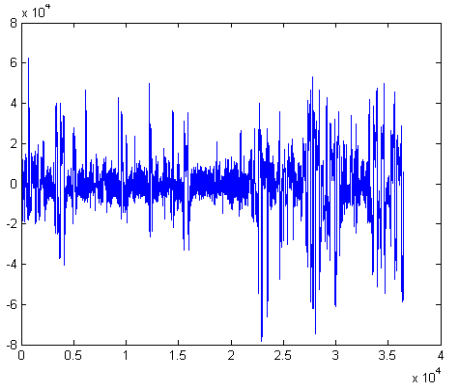

Fig. 64. Respiration frequency changes during the 10 min. peak to peak experiment with hand on vibrational stand.

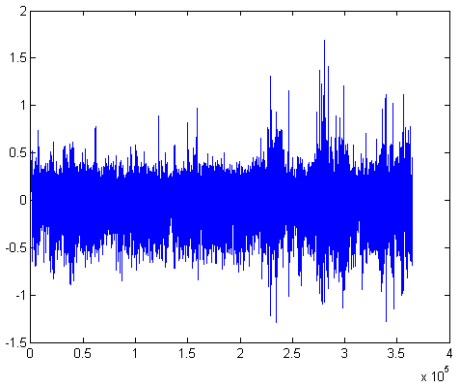

Fig. 65. ECG changes during the 10 min. peak to peak experiment with hand on vibrational stand.

Another separate investigation by registering heart rate has been performed. The subject's average and maximum mean of resting heart rate during the 5 minute time period before an experiment was registered. Then the heart rate was observed with a Polar HRM heart rate monitor at 2 minutes interval by holding the right hand raised. Values of the average and maximum heart rate were registered. Next, the heart rate measurement in the same position but with a vibrating bracelet was made. The beat frequencies of 3 Hz was induced for 2 minutes. The same physiological parameters defining blood output were registered. Tests were performed 5 times with a one day break between.

Heart rate measurements showed that the pulse decreases when the hand was affected by vibrations compared to measurements with the bracelet turned off. Average margin of measured average heart rate was 59.25 (without vibrations) comparing to 57 (with vibrations). The average maximum heart rate difference of 64.5 (without vibrations) and 61.25 (with vibrations) (Fig. 66). Furthermore, the following experiment's results showed a higher difference between vibrating bracelet and without vibrations. Average difference of average heart rate value was 71.5 (without vibrations) compared to 69 (with vibrations). Average maximum heart rate was 78 (without vibrations) compared to 74.25 (with vibrations) (Fig. 67).

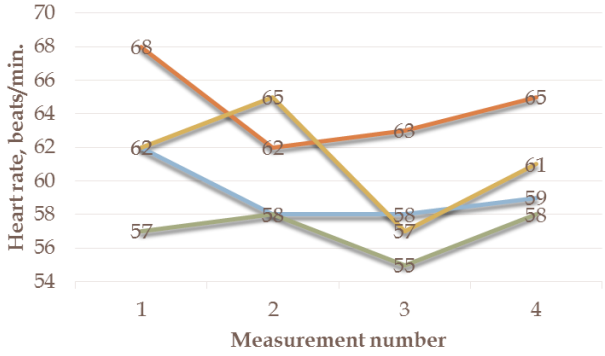

Fig. 66. First measurement of heart rate values (red line – MHR without vibrations; yellow line – MHR during vibrational exposure; blue line – AHR without vibrations; green line – AHR during vibrational exposure).

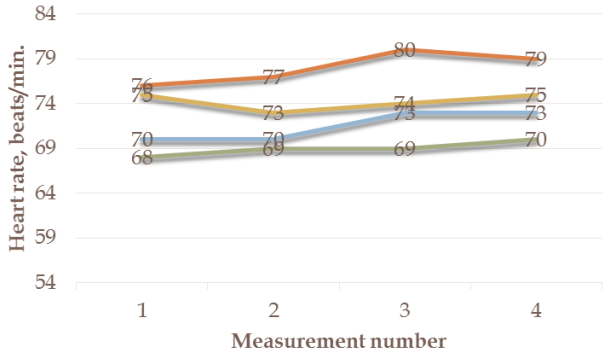

Fig. 67. Second measurement of heart rate values (red line – MHR without vibrations; yellow line – MHR during vibrational exposure; blue line – AHR without vibrations; green line – AHR during vibrational exposure).

A significant difference of heart rate value in the vibrational exposure effect has been noted. This can be explained by an assumption that increased blood flow with the effect of vibrational excitation reduces the need of the heart's effort to pump the blood. This shows that vibrational therapy could be used as a relaxation method for athletes after a physical load.

Temperature monitoring is one of the most common methods of identifying blood flow disorders or changes in separate parts of the human body. An investigation into monitoring temperature changes in the fingers were made after giving vibratory movement at the beating phenomenon frequencies ranging from 1 to 6 Hz with a step of 1 Hz. Each experiment was conducted for a time period of two minutes. The temperature measurement results were collected before and after the experiment. Temperature changes were registered with a FLIR t62101 thermal imaging camera. The images were captured on both sides of the hand, on three points of two fingers, before and after the experiment. The vibrational excitation has been induced with the prototype of the vibrating bracelet that was defined in the chapter before.

The highest increase of temperature was obtained after 4 and 4:30 minutes of vibrational exposure. The most significant alterations of 0.8°C (Fig. 68) were on the palm after a vibrational exposure of a 6 Hz frequency and 0.7°C raise on the other side of the hand after the vibrational excitation of 3 Hz were noted. Increases in temperature were obtained after all tests of vibrational excitation. Experiments were repeated ten more times and the results were very similar. In some cases, the temperature increase after the vibrational exposure was lower compared to the numbers monitored before, but it increased after a period of a few minutes. The remaining cases showed almost the same increase of temperature of 0.1 to 0.2° C raise after the exposure. Temperature increases of 0.3 to 0.5° C have been registered after a 5 minute period in all the remaining experiments of vibrational excitation. These results show that the beating phenomenon frequencies of coupled motors with unbalanced masses could be used for the improvement of blood flow in human limbs. The increase of temperature is significant in most cases and low-frequencies are appropriate with the purpose of improvement of blood flow in handbreadth.

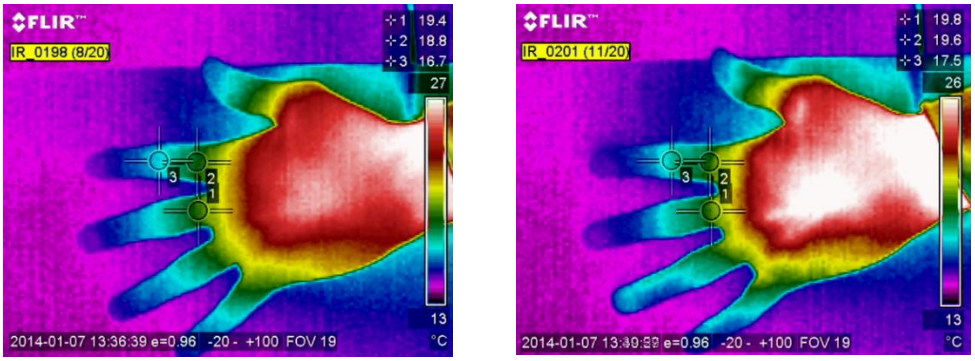

a) b)

Fig. 68. Handbreadth temperature measurement results at three points of palm: a) before the experiment; b) after the experiment.

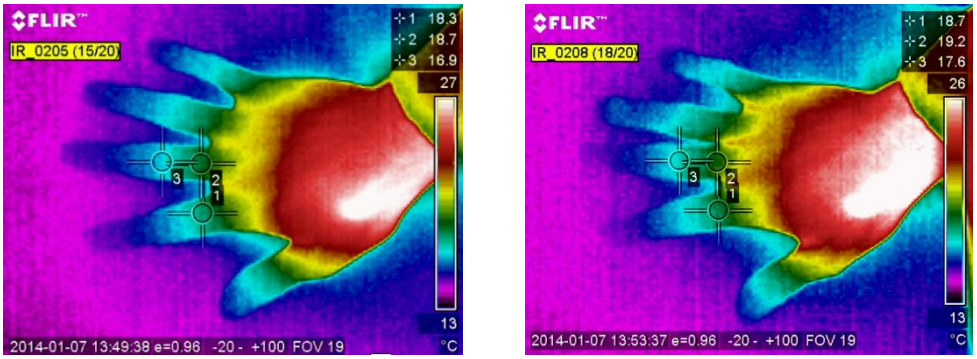

a) b)

Fig. 69. Temperature measurement results at three points of the outer part of handbreadth: a) before the experiment; b) after the experiment

The experiment by monitoring the leg temperature has been conducted too. Moreover, the vibrational frequencies of Glass epoxy plate were registered with the aim of validating the results of numerical modelling. The prototype of the legs actuator that was previously described in detail, was a main part of the experimental setup presented in Fig. 70. The prototype of the legs actuator (Fig. 70. (1)) was developed with the ability of changing the plate's inclination angle while the tested patient's legs are fixed. An angle of 45^{o} degree was selected for this experiment. The glass epoxy cantilever type plate was chosen as the vibrating part because of its high cyclic durability of the flexural strength. The plate was covered with foam for better comfort reason. The plate's length can be adjustable depending on the human's height or leg length. Motors were fixed motionlessly next to each other and adjusted to give an inward rotation to unbalanced masses, so creating a force in the vertical direction. Slightly different voltage values creates the beating phenomenon that enables it to induce sufficient force by using low voltage and small size motors for making vibrational movement of adequate displacement. Vibration data was gathered with a Robotron 00032 with a low frequency acceleration sensor KB12 and a resolution of 300 mV per 1 m/s^2, then processed with a Picoscope 3424 with Picoscope PC software. Motors were supplied by Digimess HY3020 power suppliers (1ch, 30V, 20A, adjustable).

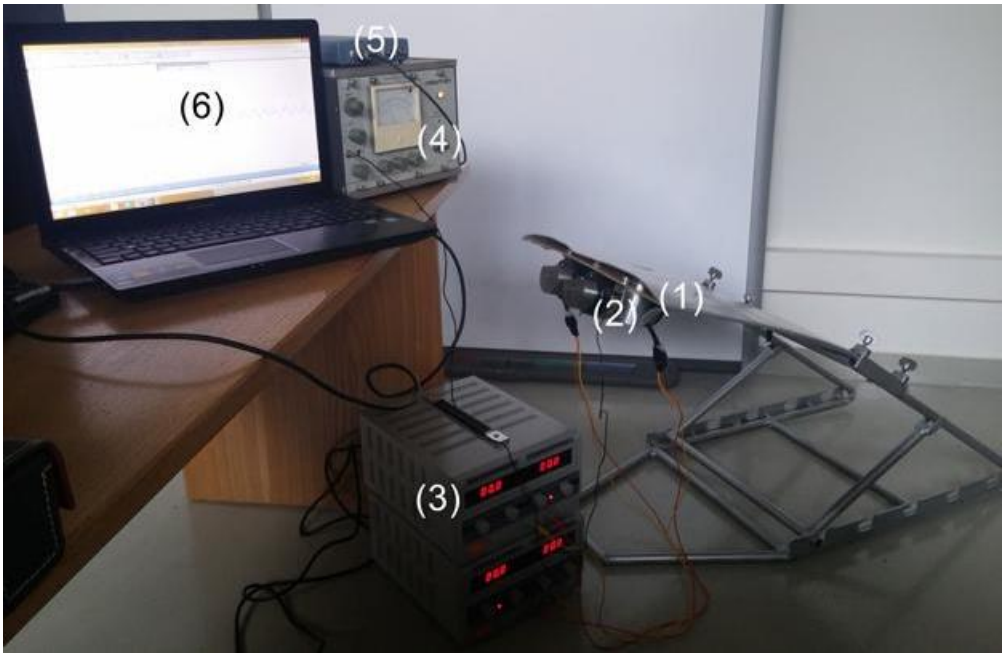

Fig. 70. Experimental setup for legs actuation: *1* - legs actuator with motors and unbalanced masses; *2* - acceleration sensor KB12; *3* - power suppliers (0-30V/20A, adjustable); *4* - Robotron 00032; *5* - Picoscope 3424; *6* - PC with Picoscope 6 software

Vibrational excitation influence is widely defined in previous studies and was mentioned in the first chapter. Various techniques of measurement can be used. In this

papers case, the high-sensitivity infrared thermal imaging camera FLIR-t62101 was used to identify the vibrational excitation influence on foot blood flow. Four points on the right foot (Hallux toe, Long toe, right point on the foot and left point on the foot) were considered to be monitored before and after experiments. Temperature differences were registered by making thermal images immediately after the exposure and capturing images 3 and 5 minutes later.

The experiments with the legs vibrating machine on identifying working frequencies were executed. The beating phenomenon was induced during vibrational excitation in order to establish higher force and low-frequencies. Considering the importance of higher displacement amplitudes as a more influential effect, frequency value has been chosen close to the Eigenfrequency value of Glass epoxy plate as a possible for each experimented leg mass. The experiment was conducted with a 75 kg weight patient with considered leg mass of 25.02 kg and motors bulk mass of 6.43 kg. The calculation of the leg mass has been made according to the previously described methodology of statistically defined percentage ratio from the body mass. Voltage values were chosen according to the results of the numerical study and tested person's vibrational excitation impact feeling. Beating phenomenon frequencies ranging from 0.5 Hz to 4.8 Hz were registered during the experiment (Fig. 71 - Fig. 76). Furthermore, the generated force values of vibrating motors have been calculated. These values are given in the figure captions of the graphs below.

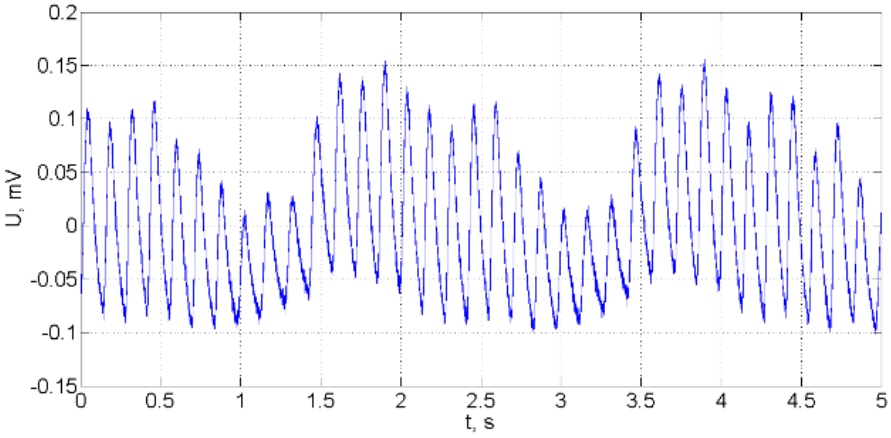

Fig. 71. Cantilever plate excitation voltage: 7.8 V – 7.4 V; beating frequency: 0.5 Hz; force to legs: 44.68 N

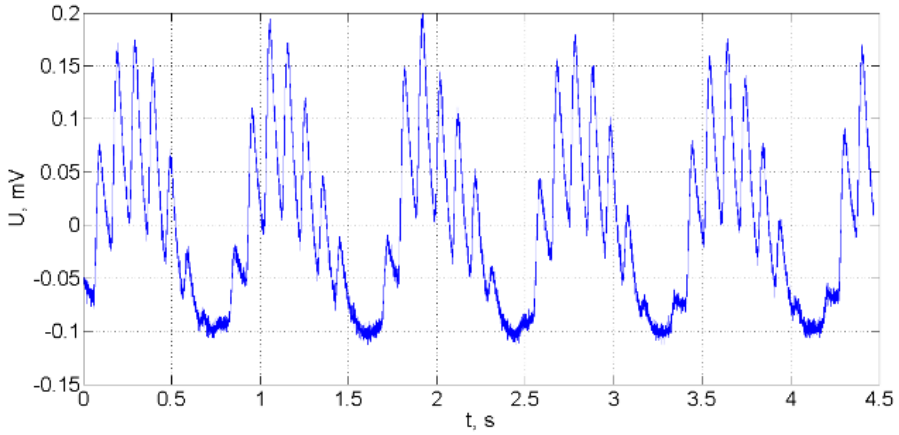

Fig. 72. Cantilever plate excitation voltage: 10.7 V – 9.6 V; beating frequency: 1.168 Hz; force to legs: 78.12 N

Low voltage causes low angular speed and a lower acting force. The resistance force of legs starts from approximately 200 N. Higher amplitudes of oscillations were obtained with the highest force values. The flexibility properties and calculated Eigenfrequency value of the vibrating plate enables research to induce sufficient vibrations with lower values of generated force. In the graphs at Fig. 71 and Fig. 72, glass epoxy plate's and feet oscillating frequencies are significantly smaller compared to Eigenfrequencies values that were calculated numerically. This means that the influence of blood flow stimulation should be minor. Therefore, higher voltage values were used for further investigations (Fig. 73 - Fig. 76) with the purpose to generate a higher force. Beating phenomenon has been induced by adjusting the input voltage of each motor. The beat phenomenon could be defined from all diagrams listed below. It should be noted that natural frequencies of the motors have not been felt by the tested patients.

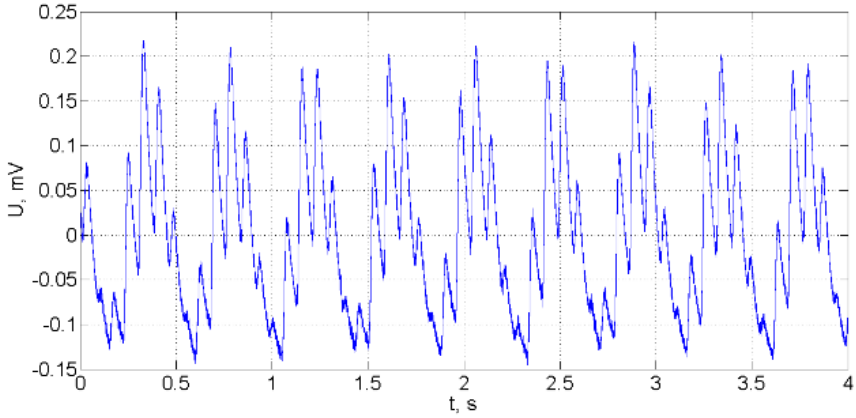

Fig. 73. Cantilever plate excitation voltage: 11.2 V – 13.8 V; beating frequency: 2.217 Hz; force to legs: 117.78 N

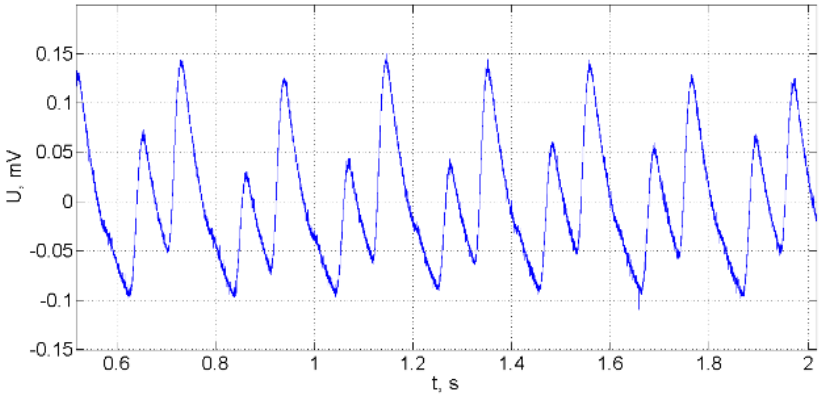

Fig. 74. Cantilever plate excitation voltage: 15.1 V – 10 V; beating frequency: 4.844 Hz; force to legs: 137.10 N

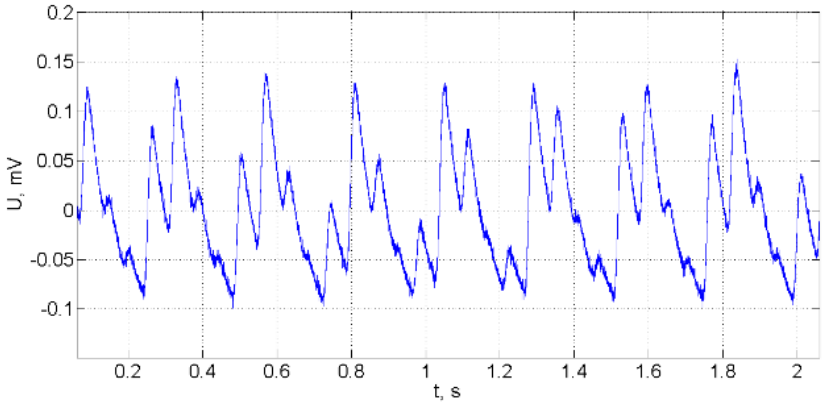

Fig. 75. Cantilever plate excitation voltage: 16.9 V – 12.4 V; beating frequency: 4.152 Hz; force to legs: 116.30 N

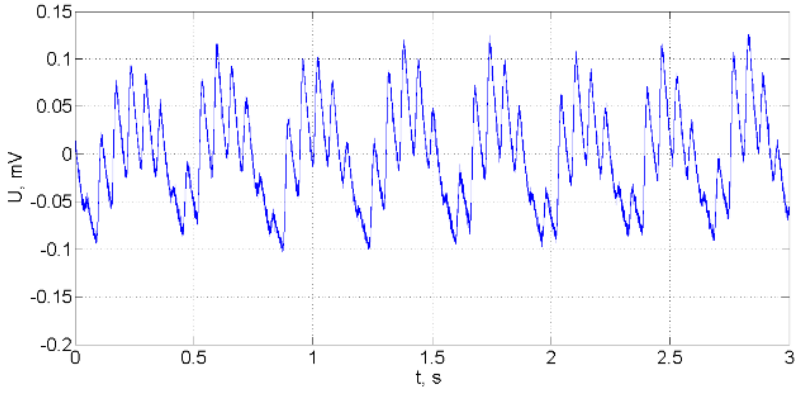

Fig. 76. Cantilever plate excitation voltage: 16.9 V – 13.9 V; beating frequency: 3.311 Hz; force to legs: 180.2 N.

The voltage values of 16.9 V and 13.9 V (Fig. 76) were chosen for further experiments to register the vibrational excitation influence on blood circulation at the foot. The frequency of 3.311 Hz was the closest value to Eigenfrequency, which was calculated with Comsol Multiphysics software. Motors with unbalanced masses working on this regime generate 180.2 N force. The force is enough for sufficient displacement and the greatest among the other values of beat frequencies (2.217 Hz, 4.844 Hz, 4.152 Hz,).

Temperature monitoring has been conducted on four points: two on different toes (Hallux and Long) and two points on the foot (one on the left and one on the right). The emissivity mean of 0.98 has been prescribed on the camera settings for monitoring human skin temperature. Temperature changes were recorded just after the exercise and after 3 and 5 minutes later. Peak temperature increase values were registered after resting 3 minutes after the vibrational excitation. A temperature rise

of 0.7° C on the Hallux toe (Fig. 77), 1° C on the Long toe (Fig. 78), 0.9° C on the right foot point (Fig. 79) and 1.5° C on the left foot point (Fig. 80) were captured.

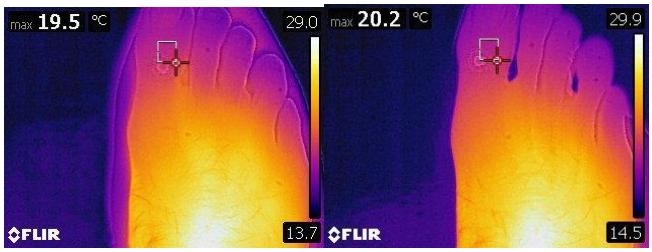

Fig. 77. Hallux toe temperature before (left) and after (right) legs actuation

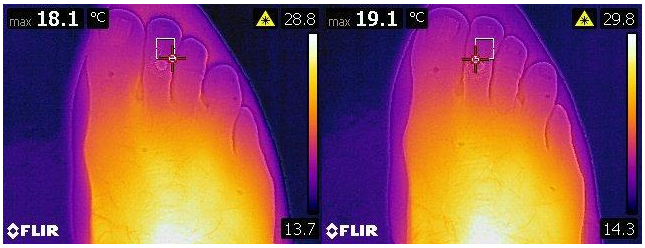

Fig. 78. Long toe temperature before (left) and after (right) legs actuation

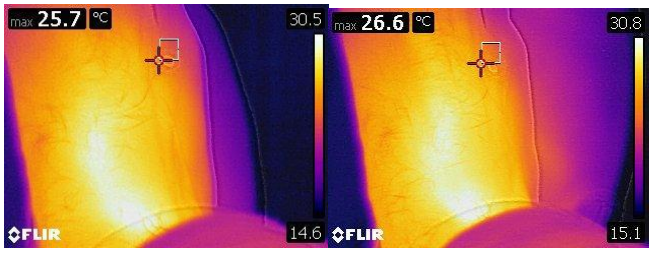

Fig. 79. Right foot point temperature before (left) and after (right) legs actuation

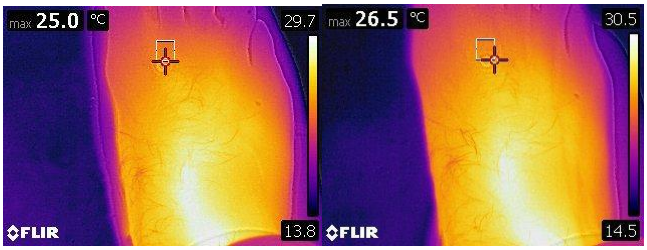

Fig. 80. Left foot point temperature before (a) and after (b) legs actuation

Furthermore, additional experiments were undertaken by monitoring temperatures by using a different measurement methodology. First, the temperature was monitored on three points of the Hallux toe, one point of the Long toe and two point on the right and left side of the foot. Second, the lowest temperature point of the foot has been monitored. The results were similar compared to the primary ones. The

captured values have been continuously increasing in the period of 5 minutes after the experiment. At the top point of the Hallux toe the temperature increased by 0.9° C after the first experiment and by 0.4° C after the second. In the middle point of the Hallux toe the captured increase was equal to 0.7° C and 0.4° C respectively. The lowest point's temperature of the same toe increased by 0.9° C at both measurements. The temperature of the Long toe increased by 0.8° C and 0.4° C respectively. Right and left points' of the foot became warmer at an average of 1° C. The results of the lowest value measurement have shown temperature increases of 0.4° C after 5 minutes after the experiment (Fig. 81).

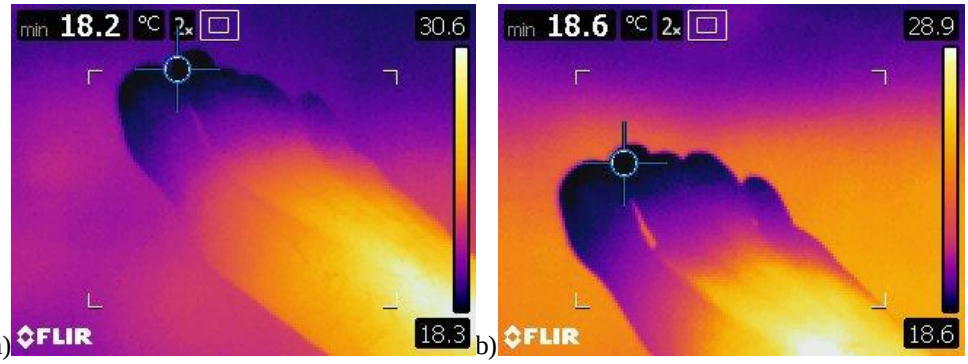

a) b)

Fig. 81. The lowest temperature point measurement: before (a) and after (b) the experiment

The alterations of temperature are significant, hence the assumption of increased blood flow can be proved. A gentile stitch feeling in the feet after the vibrational exposure was noted by the subject. Further investigations of using capillaroscopy methodology for monitoring a blood flow in capillaries is planned to be conducted. Capillaroscopy is the most common approach of examination of capillaries with a microscope. The use capillaroscopy means has been suggested by colleagues from the Lithuanian University of Medical Sciences.

4.5. Section conclusions

The main purpose of the experimental investigations was to verify the influence of low-frequency vibrational exposure on blood flow improvement. Physiological parameter monitoring has been conducted with and without the vibrational effect to the human body. The range of input parameters were suggested to make a local analysis of the affected parts of the body. Thus, the investigations on the temperature changes in limbs has been performed. The results of each experiment is listed below:

- Investigation on blood flow pressure changes during the vibrational exposure has shown that the highest pressure increases were obtained at lower frequency values and higher movement amplitude. However, the impact of vibrational exposure decreases after exceeding the value of 10 Hz. According to the results, 2 – 5 Hz frequencies and 4 – 20 mm amplitudes have been considered as the most influential on vibrational exposure.
- μPIV experimental stand has been assembled with the purpose of monitoring fluid stream lines during the vibrational excitation. COMSOL

Multiphysics modelling and experimental results were very comparable. This enables the reliable use of a computer model for further studies. Experimental results show that low frequency (from 4 to 8 Hz) and higher amplitude (from 3.4 to 8 mm) external vibrations could significantly increase blood flow. Vibrational excitation of 2.4 Hz frequency shows changes in velocity vectors and an increase in average blood flow. However higher frequencies combined with lower amplitudes did not give similar results. These results show that the beat phenomenon method could be used for creating the prescribed vibrations on a human's limbs.

- The investigation of human body tissue study showed no need to include a correction factor on frequency measurements. Therefore, prescribed values of external frequencies on further experiments were considered as equal value on the impact on the microvascular system.
- Cardiovascular parameter monitoring has been performed during the vibrational excitation on specific parts of the human body. The alterations of ECG and respiration rate was obtained, but it was considered that deeper analysis has to be done. Thus, the heart rate monitoring has been conducted. The significant difference of the average and maximum heart rate values were noted in comparison of using and not using the prototype of vibrating bracelet. The average heart rate value decreased by an average of 3.75 beats per minute during the vibrational bouts and the maximum value decreased by 2.5 beats per minute with the effect of vibrations on the hand.
- Investigation of temperature monitoring on hand has been conducted. The major increase of 0.8^{o}C on the palm after the vibrational exposure of frequency of 6 Hz and 0.7^{o}C increase on the other side of the hand after the vibrational excitation of 3 Hz were noted. Temperature increases of 0.3 to 0.5^{o} C have been registered after 4 – 5 minutes period in the case of all exercises of vibrational excitation.
- Experiment with the legs vibrating machine was conducted to identify the working regimes and necessary voltages for each motor to generate an Eigenfrequency value of 3.28 Hz for a 75 kg weight male. 16.9 V and 13.9 V supply voltage for each motor respectively generated beating vibrations of 3.311 Hz. Thermal analysis of the feet was executed at this frequency range.
- Vibrational effect assessing experiment was made on 3.311 Hz beating vibrations, registering temperature changes on four points of the foot. Temperature increases of 0.7 C on the Hallux toe, 1 C on the Long toe, 0.9 C on the right foot point and 1.5 C on the left foot point were registered. These values are very close to earlier experimental results of exciting the human hand and monitoring temperature changes.

CONCLUSIONS

1. Universal 2D and 3D numerical mathematical models of blood vessel, capillary and erythrocyte were developed to commit investigations on blood velocity alterations, deformability and flow through the micro-channel depending on the mechanical properties of the materials and different types of vibrational exposure, along with the Eigenfrequency analysis of immersed and fluid contained erythrocyte was conducted.
2. The results of the numerical studies of the vibrating microchannel have showed the highest impact on blood flow velocity at frequencies ranging from 4.3 to 8 Hz and with a displacement of 3.4 – 8 mm, while the significant reduction of the inlet maximum contact pressure between the RBC's and capillary's wall on vibrational exposure of 3 Hz with a displacement range of 13 – 22 mm and 4 – 4.5 Hz with a displacement range of 0.6 – 2 mm was obtained as the most influential.
3. Experimental studies of a simplified imitational blood circulatory system, consisting of the main parts of peristaltic pump, artificial blood vessel and vibrational actuator, disclosed a significant fluid pressure increase in the range of low-frequencies' beating phenomenon vibrational bouts of 2 – 5 Hz and 4 – 20 mm amplitudes, while the oscillations of higher frequencies than 10 Hz did not generated any significant changes.
4. Investigations by using an adapted experimental setup including the Micro-Particle Image Velocimetry (μPIV) equipment have indicated the adequacy of experimental and theoretical studies by obtaining an average increase in fluid velocity of 7.7 % during the vibrational bouts ranging from 2.4 Hz to 5.8 Hz and displacement range of 0.98 – 6 mm, herewith the momentum fluid velocity increase of 4.15 times and turbulent flow have been noted.
5. Prototypes of a vibrating bracelet and a vibrating machine for legs have been designed to induce the beating phenomenon with the purpose of giving low-frequency vibrational exposure and sufficient perpendicular force of at least 6 N to the handbreadth and 44 N to the legs by using small size components and relevant frequencies in coupled with a displacement range, according to the results of numerical studies.
6. Experimental studies with the designed prototypes have shown a significant increase in limb temperatures after the low-frequency vibrational excitation where the average increase of 0.3 – 0.5^{o} C of the hand, increases of 0.7^{o} C on the Hallux toe, 1^{o} C on the Long toe, 0.9^{o} C on the right foot point and 1.5^{o} C on the left foot point were registered after a 4 – 5 minute period. It also considered the potential influence of the relation between the numerically obtained natural frequency value of RBC of 4 Hz and the range of frequencies of external vibrations. Furthermore, the validity of the designed means of vibrational excitation was confirmed by registering the decrease of average (3.75 BPM) and maximum (2.5 BPM) values of heart rate after the vibrational exposure.

REFERENCES

1. World Health Organization. (2011). *Global Health and Aging*. Report. [Online]. [Cited: April 20 2013] Available at http://www.who.int/ageing/publications/global_health.pdf
2. Cipriani, C, D'Alonzo, M. ; Carrozza, M.C. (2012). A Miniature Vibrotactile Sensory Substitution Device for Multifingered Hand Prosthetics. *Biomedical Engineering*, Vol. 59, Issue 2, p. 400 – 408.
3. Vartholomeos, P., Papadopoulos, E. (2006). Analysis, design and control of a planar micro-robot driven by two centripetal-force actuators, *Robotics and Automation*. ICRA 2006. Proceedings 2006 IEEE International Conference on. ISSN 1050-4729, p. 649 – 654.
4. Lithuanian Ministry of Health, Health Information Centre of Institute of Hygiene. (2014). *Health Statistics of Lithuania 2013*. [Online] [Cited October 21 2014]. Available at http://sic.hi.lt/data/la2013.pdf
5. International Diabetes Federation. (2011). *Diabetes: The Global Burden.* [Online]. [Cited: July 02 2014]. Available at http://www.idf.org/sites/default/files/Media-Information-Pack.pdf
6. National Center for Chronic Disease Prevention and Health Promotion, Division of Diabetes Translation. *National Diabetes Statistics Report, 2014.* [Online] [Cited January 21 2015]. Available at http://www.cdc.gov/diabetes/pubs/statsreport14/national-diabetes-report-web.pdf
7. Hesham G. Mahran1, Omar Farouk Helal, Amir Abdel-Raouf El Fiky. (2013). Effect of Mechanical Vibration Therapy on Healing of Foot Ulcer in Diabetic Polyneuropathy Patients. *Journal of American Science*, 9(7), 76-87.
8. Centers for Disease Control (CDC), *National Institute of Arthritis and Musculoskeletal and Skin Diseases, and the Arthritis Foundation.* [Online]. [Cited: January 22 2015]. Available at http://www.niams.nih.gov
9. European Science Foundation. (2006). Report. [Online]. [Cited: July 05 2014]. Available at http://www.esf.org/fileadmin/Public_documents/Publications/spb%2026%20Rheumatic%20Diseases.pdf
10. World Health Organization. (2015). *World Health Statistics 2015*. . [Online]. [Cited: August 10 2015]. Available at http://apps.who.int/iris/bitstream/10665/170250/1/9789240694439_eng.pdf?ua=1
11. National Heart, Lung and Blood Institute. [Online]. [Cited August 10 2015]. Available at http://www.nhlbi.nih.gov/health/health-topics/topics/raynaud
12. Eileen M. Weinheimer-Haus, Stefan Judex, William J. Ennis, Timothy J. Koh. (2014). Low-Intensity Vibration Improves Angiogenesis and Wound Healing in Diabetic Mice. *PLoS One*, 9(3): e91355. doi: 10.1371/journal.pone.0091355
13. Gojiro Nakagami, Hiromi Sanada, Noriko Matsui, Atsuko Kitagawa, Hideki Yokogawa, Naomi Sekiya, Shigeru Ichioka, Junko Sugama, Masahiro Shibata. (2007). Effect of vibration on skin blood flow in an in vivo microcirculatory model, *BioScience Trends*, 1(3):161-166.
14. Monica Diez-Silva, Ming Dao, Jongyoon Han, Chwee-Teck Lim, and Subra Suresh. (2010). Shape and Biomechanical Characteristics of Human Red Blood Cells in Health and Disease, *MRS Bull*, 2010 May, 35(5): 382–388.

15. Nayak BS, Beharry VY, Armoogam S, Nancoo M, Ramadhin K, Ramesar K, et al. (2007). Determination of RBC membrane and serum lipid composition in Trinidadian type II diabetics with and without nephropathy, *Vasc. Health Risk Manag.*, 4:893-9. Back to cited text no. 2
16. Petropoulos IK, Margetis PI, Antonelou MH, Koliopoulos JX, Gartaganis SP, Margaritis LH, et al. (2007). Structural alterations of the erythrocyte membrane proteins in diabetic retinopathy, *Graefes Arch Clin Exp Ophthalmol*, 245:1179-88
17. Clinton D Brown, Halim S Ghali, Zhonghua Zhao, Lorraine L Thomas and Eli A Friedman. (2005). Association of reduced red blood cell deformability and diabetic nephropathy, *Kidney International*, 67, 295–300; doi:10.1111/j.1523-1755.2005.00082.x
18. Banerjee R, Nageshwari K, Puniyani RR. (1998). The diagnostic relevance of red cell rigidity, *Clin Hemorheol Microcirc*, 1998 Sep, 19(1):21-4.
19. Ailments, *Prevent Sickness Maintain Health Treat Nishi System* [Online] [Cited: January 10, 2012.] http://www.nishiusa.eurocontrol.biz/index.php?div_id=4&sub_id=13
20. Wikipedia. *Katsuzo Nishi – Wikipedia*, [Online] [Cited: March 30, 2013.]. Available at http://en.wikipedia.org/wiki/Katsuzō_Nishi.
21. Pries A. R., Secomb T. W., Gaehtgens P. (1999). Structural Autoregulation of Terminal Vascular Beds. *Hypertension*, 33: 153-161.
22. Arvydas Palevicius, Kazimieras Ragulskis, Algimantas Bubulis, Vytautas Ostasevicius, Minvydas Ragulskis. (2004). Development and operational optimization of micro spray system. *Proc. of SPIE*, Vol. 5390 p. 429-438
23. Cochrane DI, Sartor F, Winwood K, Stannard SR, Narici MV, et al. (2008). A comparison of the physiologic effects of acute whole-body vibration exercise in young and older people. *Archives of Physical Medicine and Rehabilitation*, 89: 815–821.
24. Stewart JM, Karman C, Montgomery LD, McLeod KJ. (2005). Plantar vibration improves leg fluid flow in perimenopausal women. American Journal of Physiology - Regulatory, *Integrative and Comparative Physiology*, 288: 623–629.
25. Otsuki T., Takanami Y., Aoi W., Kawai Y., Ichikawa H. & Yoshikawa T. (2008). Arterial stiffness acutely decreases after whole-body vibration in humans, *Acta Physiologica*, 194: 189-194.
26. Mester J., Kleinoder H. & Yue Z. (2006). Vibration training: benefits and risks. Journal of *Biomechanics*, 39(6): 1056-1065
27. Amy Mark, Maureen MacDonald, Mark Rakobowchuck, Christopher Gordon, Cameron Blimkie. (2002). Metabolic and cardiovascular responses during whole body vibration (WBV) exercise: a pilot study. Hamilton: Department of Kinesiology and Department of Radiology, McMaster University.
28. Yusuke Osawa, Yuko Oguma. (2011). Effects of whole body vibration on physiological responses to one bout of resistance training. *Journal of Exercise Physiology*, vol. 14, *Kanagawa:* ASEP, ISSN 1097-9751.
29. Antonios TF, Singer DR, Markandu ND, Mortimer PS, MacGregor GA. (1999). Structural skin capillary rarefaction in essential hypertension, *Hypertension*, a;33:998–1001.
30. Feihl F, Liaudet L, Waeber B, Levy BI. (2006). Hypertension: a disease of the microcirculation? *Hypertension*, 48:1012–1017.
31. Antonios TF. (2006). Microvascular rarefaction in hypertension–reversal or over-correction by treatment? *Am J Hypertens*, 19:484–485.

32. Levy BI, Ambrosio G, Pries AR, Struijker-Boudier HA. (2001). Microcirculation in hypertension: a new target for treatment? *Circulation*, 104:735–740.
33. Debbabi H, Uzan L, Mourad JJ, Safar M, Levy BI, Tibiriçà E. (2006). Increased skin capillary density in treated essential hypertensive patients. *Am J Hypertens*. 19(5): 477-83.
34. Cohn JN. Is it the blood pressure or the blood vessel? (2007). *Journal of the American Society of Hypertension*, 1:5–16.
35. Cheng C, Daskalakis C, Falkner B. (2008). Capillary rarefaction in treated and untreated hypertensive subjects, *Ther Adv Cardiovasc Dis*, Apr;2(2):79-88. doi: 10.1177/1753944708089696.
36. Herrero AJ., Martín J., Martín T., García-López D., Garatachea N., Jiménez B., Marín PJ. (2011). Whole-body vibration alters blood flow velocity and neuromuscular activity in Friedreich's ataxia, *Clin Physiol Funct Imaging*, 2011 Mar, 31(2):139-44.
37. Sañudo B., César-Castillo M, Tejero S, Cordero-Arriaza FJ, Oliva-Pascual-Vaca A, Figueroa A. (2013). Effects of vibration on legs blood flow after intense exercise and its influence on subsequent exercise performance, J Strengthc Condition Res Nat Strength Condition Assoc.
38. Noel Lythgo, Prisca Eser, Patricia de Groot and Mary Galea. (2008). Whole-body vibration dosage alters leg blood flow, *Scandinavian Society of Clinical Physiology and Nuclear Medicine*, 29, 1, 53–59.
39. Kerschan-Schindl K., Grampp S., Henk C., Resch H., Preisinger E., Fialka-Moser V. & Imhof H. (2001). Whole-body vibration exercise leads to alterations in muscle blood volume, *Clinical Physiology*, 21(3): 377-382. DOI: 10.1046/j.1365-2281.2001.00335.x.
40. Baum K., Votteler T. & Schiab J. (2007). Efficiency of vibration exercise for glycemic control in type 2 diabetes patients, *International Journal of Medical Sciences*, 31; 4(3): 159-163. DOI: 10.7150/ijms.4.159.
41. Maloney-Hinds C., Petrofsky J.S. & Zimmerman G. (2008). The effect of 30 hz vs. 50 hz passive vibration and duration of vibration on skin blood flow in the arm, *Medical Science Monitor*, 14(3): 112-116.
42. Lohman E.B., Petrofsky J.S., Maloney-Hinds C., Betts-Schwab H. & Thorpe D. (2007). The effect of whole body vibration on lower extremity skin blood flow in normal subjects, *Medical Science Monitor*, 13(2): 71-76.
43. Silva G., Leal N., Semiao V. (2009). Determiantion of microchannels geometric parameters using micro-PIV, *Chemical Engineering Research and Design*, 87: 298-306. DOI: 10.1016/j.cherd.2008.08.009.
44. Pucetti, G., Pulvirenti B., Morini G.-L. (2014). Experimental deermination of the 2D velocity laminar profile in glass microchannels using μPIV, *Energy Procedia*, Vol. 45, p. 538-547. DOI: 10.1016/j.egypro.2014.01.058.
45. Wang H., Wang Y. (2009). Measurement of water flow rate in microchannels based on the microfluidic particle image velocimetry, *Measurement*, 42: 119-126. DOI: 10.1016/j.measurement.2008.04.012.
46. Devasenathipathu S., Santiago J.G., Wereley S.T., Meinhart C.D, Takehara K. (2003). Particle imaging techiques for microfabricated fluidic systems, *Experiments in Fluids*, 34: 504-514. DOI: 10.1007/s00348-003-0588-y.
47. Tolouei E., Fouras A., Carberry J. (2009). In vitro micro PIV measurements of velocity profiles near a wall. *8th international symposium on particle image velocimetry* - PIV09. Melbourne, Victoria, Australia, August 25-28.

48. Completo C., Geraldes V., Semiao V. (2014). Rhaelogical and dynamical characterization of blood analogue flows in a slit, International *Journal of Heat and Fluid Flow*, 46: 17-28. DOI: 10.1016/j.ijheatfluidflow.2013.12.008.
49. Galileo Training | *Galileo vibrational training*. [Cited: 2013/09/05]. Available at http://www.galileo-training.com/.
50. Power plate fitness equipment | *Whole body workout*. [Cited: 2013/09/05]. Available at http://powerplate.mercola.com.
51. Vibramed | *Whole body vibration*. [Cited: 2013/09/05]. Available at http://www.vibramed.net/.
52. Rittweger J. (2010). Vibration as an exercise modality: how it may work, and what its potential might be, *European Journal of Applied Physiology*, 2010 Mar, 108(5):877–904. [PubMed]
53. Whole-Body Vibration Therapy for Osteoporosis [Internet]. Comparative Effectiveness Technical Briefs, No. 10. Wysocki A, Butler M, Shamliyan T, et al. Rockville (MD): Agency for Healthcare Research and Quality (US); 2011 Nov.
54. Brownmed | *Intellinetix*. [Cited: 2013/09/05]. Available at http://www.brownmed.com/.
55. Osim | *Massager*. [Cited: 2014/11/12]. Available at http://www.osim.com/UK/home.aspx.
56. OsterStyle | *Stim U Lax massager*. [Cited: 2014/11/12]. Available at http://www.osterstyle.com/accessories/oster-stim-u-lax-massager/076103-100-000.html#start=1.
57. Geko by FirstKind | *Circulation support*. Available at http://www.gekodevices.com/. [2014/10/10]
58. VibeTech | *Accessible Physical Therapy for Impaired Physical Mobility*. [Cited: 2014.09.15]. Available at http://www.vibetechglobal.com/.
59. Clairol Incorporated. Raymond W. Kunz, Gerald K. Pitcher. *Vibrator massager using beat frequency*, US patent 4570616 A, 1986. Available at: https://www.google.co.cr/patents/US4570616
60. Yury M. Podrazhansky, Mikhail N. Lyubich. *Method and apparatus for improving local blood and lymph circulation using low and high frequency vibration sweeps*, US patent 7909785 B2, 2002. Available at: https://www.google.co.cr/patents/US20040167446
61. Yuh-Yun Wang. *Foot sole massaging device*. US patent 5910123 A, 1999. Available at: http://www.google.co.cr/patents/US5910123
62. Andrew Kenneth Hoffmann, Carlo Menon. *Randomic vibration for treatment of blood flow disorders*, US patent 20090069728, 2009. Available at: https://www.google.co.cr/patents/US20090069728
63. Ibfk Gmbh. Jiro Katsuta. *Method for Improving Blood Circulation*. US patent 20080309132 A1, 2008. Available at: https://www.google.co.cr/patents/US20080309132
64. Vibrant Medical Limited. Ernest Peter Nelson, Anthony John Seaney. *Leg ulcer, lymphoedema and dvt vibratory treatment device*. Patent WO2002065973 A1. Available at: https://www.google.co.cr/patents/US7615018
65. Seidel H. (2005). On the relationship between whole-body vibration exposure and spinal health risk, *Ind Health*, 2005 Jul;43(3):361-77.
66. Kákosy T. (1989). Vibration disease, *Baillieres Clin Rheumatol*, 1989 Apr;3(1):25-50.

67. ISO | ISO Standards – ISO/TC 108 SC 4. *Human exposure to mechanical vibration and shock*. [Cited: 2013/06/12]. Available at http://www.iso.org/iso/iso_catalogue/catalogue_tc/catalogue_tc_browse.htm?commid=51514.
68. Wang H., Wang Y. (2009). Measurement of water flow rate in microchannels based on the microfluidic particle image velocimetry, *Measurement*, 42: 119-126. DOI: 10.1016/j.measurement.2008.04.012.
69. Auro Ashish Saha and Sushanta K. Mitra. (2008). Modeling and Simulation of Microscale Flows, *Modelling and Simulation*, InTech. DOI: 10.5772/5977.
70. Gene Hou, Jin Wang, and Anita Layton. (2012). Numerical Methods for Fluid-Structure Interaction — A Review, *Communications in Computational Physics*, 12, pp. 337-377.
71. Moore B., Jaglinski T., Stone D.S. and Lakes R.S. (2007). On the Bulk Modulus of Open Cell Foams, *Cellular Polymers*, 26(1): 1-10.
72. Benevicius V.; Gaidys R.; Ostasevicius V.; Marozas V. (2014). Identification of rheological properties of human body surface tissue, *Journal of Biomechaics*, 47 (6): 1368–1372. DOI: 10.1016/j.jbiomech.2014.01.050.
73. Huang Ji-Yun, Liu Shuang-Shuang, Wilcox Christopher S, Y Lai En, Han Feng. (2013). In Vivo Two-photon Fluorescence Microscopy Reveals Disturbed Cerebral Capillary Blood Flow and Increased Susceptibility to Ischemic Insults in Diabetic Mice, *Hypertension*, 62: A93.
74. Buys Antoinette V., Van Rooy Mia-Jean, Soma Prashilla, Van Papendorp Dirk, Lipinski Boguslaw and Pretorius Etheresia. (2013). Changes in red blood cell membrane structure in type 2 diabetes: a scanning electron and atomic force microscopy study, *Cardiovascular Diabetology*, 12:25.
75. Esmeraldo Martinez-Pardo, Salvador Romero-Srenas, and Pedro E. Alcaraz. (2012). Effects of different amplitudes (high vs.low) of whole-body vibration training in active adults, *Journal of Strength and Conditioning Research*, National Strength and Conditioning Association.
76. Weibel E.R. (1984). *The Pathway For Oxygen*. Harvard University Press.
77. Benjamin Mauroy. (2007). Following red blood cells in a pulmonary capillary. ESAIM Proceedings 11/2007; 23(1270-900X). DOI: 10.1051/proc:082304.
78. Polwaththe-Gallage, Hasitha-Nayanajith, Saha, Suvash C., & Gu, YuanTong. (2014). Formation of the three-dimensional geometry of the red blood cell membrane, *The ANZIAM Journal*, 55, pp. 80-95.
79. Tong Wang, Zhongwen Xing. (2010). Characterization of Blood Flow in Capillaries by Numerical Simulation, *Journal of Modern Physics*, 1, 349-356, doi:10.4236/jmp.2010.16049
80. Dominik Obrist, Bruno Weber, Alfred Buck and Patrick Jenny. (2010) Red blood cell distribution in simplified capillary networks, *Phil. Trans. R. Soc. A*, 368, doi: 10.1098/rsta.2010.0045
81. Lingyao Yu, Yi He, Arthur Chiou and Yunlong Sheng. (2011). Deformation of biconcave Red Blood Cell. *Proceedings of the 2011 COMSOL Conference in Boston*.
82. Lingyao Yu, Yunlong Sheng, and Arthur Chiou. (2013). Three-dimensional light-scattering and deformation of individual biconcave human blood cells in optical tweezers. *Optics Express*, Vol. 21, Issue 10, pp. 12174-12184 •doi: 10.1364/OE.21.012174

83. YongKeun Park, Catherine A. Best, Kamran Badizadegan, Ramachandra R. Dasari, Michael S. Feld, Tatiana Kuriabova, Mark L. Henle, Alex J. Levine, and Gabriel Popescua. (2010). Measurement of red blood cell mechanics during morphological changes, *PNAS*, 2010 vol. 107 no. 15 6731–6736, doi: 10.1073/pnas.0909533107
84. YongKeun Park, Catherine A. Best, Tatiana Kuriabova, Mark L. Henle, Michael S. Feld, Alex J. Levine, and Gabriel Popescu. (2010). Measurement of the nonlinear elasticity of red blood cell membranes, *Phys Rev E Stat Nonlin Soft Matter Phys*, 2011 May; 83(5 Pt 1): 051925.
85. Lenormand G., Henon S. Richert A., Simeon J. and Gallet F. (2001). Direct measurement of the area expansion and shear moduli of the human red blood cell membrane skeleton, *Biophysical J.*, vol. 81, pp.43-56.
86. Dulinska, I., M. Targosz, et al. (2006). Stiffness of normal and pathological erythrocytes studied by means of atomic force microscopy. *Journal of Biochemical and Biophysical Methods*, 66(1-3): 1-11.
87. Fung, Y. (1993). Biomechanics: mechanical properties of living tissues, *Springer-Verlag*, New York, 2nd edition.
88. Minamitani, H. Tsukada, K. ; Kawamura, T. ; Sekizuka, E. ; Oshio, C. (2000). Analysis of elasticity and deformability of erythrocytes using micro-channel flow system and atomic force microscope. *Microtechnologies in Medicine and Biology, 1st Annual International, Conference On*, 2000: 68 – 71. doi: 10.1109/MMB.2000.893743
89. Fornal M, Lekka M, Pyka-Fościak G, Lebed K, Grodzicki T, Wizner B, Styczeń J. (2006). Erythrocyte stiffness in diabetes mellitus studied with atomic force microscope, Clin *Hemorheol Microcirc*, 35(1-2):273-6.
90. Gregersen, M.I., C.A. Bryant, W.E. Hammerle, S. Usami, S. Chien. (1967). Flow Characteristics of Human Erythrocytes through Polycarbonate Sieves. *Science*, 157, No. 3786, 825-827.
91. Fabienne Pennec, Hikmat Achkar, David Peyrou, Robert Plana, Patrick Pons, et al. (2007). Verification of contact modelling with Comsol Multiphysics software, *Rapport LAAS* n°07604.
92. Yalla, S.K and Kareem, A. (2000). On the Beat Phenomenon in Coupled Systems. *Proceedings of the 8th ASCE Joint Specialty Conference on Probabilistic Mechanics and Structural Reliability*, Notre Dame, Indiana, July 24-26.
93. Yalla, S.K., Kareem, A., and Kantor, J.C. (1998). Semi-Active Control Strategies for Tuned Liquid Column Dampers to reduce Wind and Seismic Response of Structures. *Proceedings of Second World Conference on Structural Control*, Kyoto, John Wiley.
94. Meriam, J.L. and Kraige, L.G. *Engineering Mechanics Vol. 2, Dynamics, 2nd Edition* 1987 ISBN 0-471-84912-X (620.104 MER).
95. Lutron electronic enterprise co., ltd, [Cited: 2014/11/22]. Available at: http://www.lutron.com.tw .
96. Cardinale M., Wakeling J. (2005). Whole body vibration exercise: are vibrations good for you? *Br J Sports Med.*, 2005 Sep 39(9): 585-9.
97. Plagenhoef, S., Evans, F.G. and Abdelnour, T. (1983). Anatomical data for analyzing human motion, *Research Quarterly for Exercise and Sport*, 54, 169-178. http://dx.doi.org/10.1080/02701367.1983.10605290

98. Gore W. L. & Associates, Inc. 2002 – 2015. Arizona. *AP2400-EN124GORE Hybrid Vascular Graft.* [Cited 2015 Jan 15]. Available at http://www.goremedical.com/hybrid/technical/

99. Raffel M., Willert C.E., Wereley S.T., Kompenhans J. (2007). Particle Image Velocimetry. *A practical guide*, 2nd ed., 448 p.

100. Mielnik M. M., (2005). *Micro-PIV and its application to some Bio MEMS related microfluidic flows*, Trondheim: Department of Energy ad Process Engineering, Norwegian University of Science and Technology, Norway.

101. Yahya Mohammed. (2010). *Three dimensional finite-element modeling of blood flow in elastic vessels: effects of arterial geometry and elasticity on aneurysm growth and rupture*. Dissertation, Toronto: Ryerson University.

102. Hagsater M.S., (2008). *Development of micro-PIV techniques for aplication in micrfluidic systems*, Lyngby: DTU Nanotech, Department of Micro- ad Nanotechnology.

103. Pust O. (2000). PIV: Direct Cross-Correlation compared with FFT-based Cross-Correlation, In: *Proceedings of the 10th International Symposium on Applications of Laser Techniques to Fluid Mechanics*, Lisbon, Portugal.

104. STMicroelectronics, [Online] [Cited: March 5, 2013.] Available at http://www.st.com/jp/analog/product/218132.jsp.

105. Microlife, [Online] [Cited: May 2, 2013.] Available at http://www.microlife.com/products/hypertension/automatic/bp-a100/

106. Schiller America, [Online], [Cited: May 2, 2013.] Available at http://www.schillerservice.com

LIST OF PUBLICATIONS

Papers in ISI Web of Science journals with citation index

1. Benevičius, Vincas; Ostaševičius, Vytautas; Venslauskas, Mantas; Daukševičius, Rolanas; Gaidys, Rimvydas. Finite element model of MEMS accelerometer for accurate prediction of dynamic characteristics in biomechanical applications // Journal of Vibroengineering / Vibromechanika, Lithuanian Academy of Sciences, Kaunas University of Technology, Vilnius Gediminas Technical University. Vilnius : Vibromechanika. ISSN 1392-8716. 2011, Vol. 13, no. 4, p. 803-809. [Science Citation Index Expanded (Web of Science); INSPEC; Academic Search Complete; Central & Eastern European Academic Source (CEEAS); Computers & Applied Sciences Complete; Current Abstracts; TOC Premier]. [0,283]. [IF (E): 0,346 (2011)]
2. Venslauskas, Mantas; Ostaševičius, Vytautas; Jūrėnas, Vytautas. Development of vibrating bracelet for the actuation of the blood circulation at capillaries // Journal of Vibroengineering / Vibromechanika, Lithuanian Academy of Sciences, Kaunas University of Technology, Vilnius Gediminas Technical University. Kaunas : Vibroengineering. ISSN 1392-8716. 2014, Vol. 16, no. 3, p. 1535-1542. [Science Citation Index Expanded (Web of Science); INSPEC; Academic Search Complete; Central & Eastern European Academic Source (CEEAS); Computers & Applied Sciences Complete; Current Abstracts; TOC Premier]. [0,333]. [IF (E): 0,617 (2014)]
3. Venslauskas, Mantas; Ostaševičius, Vytautas; Jūrėnas, Vytautas. Novel training machine for stimulation of blood circulation in feet // Mechanika / Kauno technologijos universitetas, Lietuvos mokslų akademija, Vilniaus Gedimino technikos universitetas. Kaunas : KTU. ISSN 13921207. 2015, t. 21, nr. 3, p. 201206. DOI: 10.5755/j01.mech.21.3.11758. [Science Citation Index Expanded (Web of Science); INSPEC; Compendex; Academic Search Complete; FLUIDEX; Scopus; 0,333].

Papers in other journals referred in ISI databases (Proceedings and other)

1. Venslauskas, Mantas; Ostaševičius, Vytautas; Marozas, Vaidotas. Limb's vibrations exercise monitoring with MEMS accelerometer to identify influence of cardiovascular system // Vibroengineering PROCEDIA: international conference "'Vibroengineering- 2013", Druskininkai, Lithuania, 17-19 September 2013. Kaunas: Public Establishment "Vibroengineering". ISSN 2345-0533. 2013, Vol. 1, p. 48-52. [0,333]
2. Venslauskas, Mantas; Ostaševičius, Vytautas. Vibrating devices for stimulating blood circulation in limbs' capillaries // Proceedings of the 14th World Congress in Mechanism and Machine Science // 2015 (accepted for publishing).

SL344. 2015-11-11, 14 leidyb. apsk. l. Tiražas 10 egz. Užsakymas 408.
Išleido Kauno technologijos universitetas, K. Donelaičio g. 73, 44249 Kaunas
Spausdino leidyklos „Technologija“ spaustuvė, Studentų g. 54, 51424 Kaunas